13th October 2024
Revised versions 20th October 2024, 8th May 2025, 10th July 2025
Final version 15th July 2025 accepted by Europ. Phys. J. **A**

On Two Nucleons Near Unitarity with Perturbative Pions

Yu-Ping Teng[a,b1] *and* **Harald W. Grießhammer**[a2]

[a] *Institute for Nuclear Studies, Department of Physics, The George Washington University, Washington DC 20052, USA*

[b] *Department of Physics, University of Wisconsin-Milwaukee, Milwaukee WI 53211, USA*

Abstract

We explore the impact of perturbative pions on the Unitarity Expansion in the two-nucleon S-waves of Chiral Effective Field Theory at next-to-next-to leading order ($\mathrm{N^2LO}$). Pion exchange explicitly breaks the nontrivial fixed point's universality, *i.e.* invariance of S waves under both conformal and Wigner's combined SU(4) spin-isospin transformations. On the other hand, Unitarity explicitly breaks chiral symmetry. The two seem incompatible in their respective exact-symmetry limits. χEFT with Perturbative Pions in the Unitarity Expansion resolves the apparent conflict in the Unitarity Window (phase shifts $45^\circ \lesssim \delta(k) \lesssim 135^\circ$), *i.e.* around momenta $k \approx m_\pi$ most relevant for low-energy nuclear systems. Its only LO scale is the scattering momentum; NLO adds only scattering length, effective range and non-iterated one-pion exchange (OPE); and $\mathrm{N^2LO}$ only once-iterated OPE. Agreement in the $^1\mathrm{S}_0$ channel is very good. Apparently large discrepancies in the $^3\mathrm{S}_1$ channel even at $k \approx 100$ MeV are remedied by taking at $\mathrm{N^2LO}$ only the central part of OPE. In contradistinction to the tensor part, it is identical in the $^1\mathrm{S}_0$ and $^3\mathrm{S}_1$ channels. Both channels then match empirical phase shifts and pole parameters well within mutually consistent quantitative theory uncertainty estimates. Pionic effects are small, even for $k \gtrsim m_\pi$. Empirical breakdown scales are consistent with $\overline{\Lambda}_{\mathrm{NN}} = \frac{16\pi f_\pi^2}{g_A^2 M} \approx 300$ MeV, where iterated OPE is not suppressed. We therefore conjecture: Both conformal and Wigner symmetry in the Unitarity Expansion show *persistence*, *i.e.* the footprint of both combined dominates even for $k \gtrsim m_\pi$ and is more relevant than chiral symmetry, so that the tensor/Wigner-SU(4) symmetry-breaking part of OPE does not enter before $\mathrm{N^3LO}$. We also discuss the potential relevance of entanglement and possible resolution of a conflict with the strength of the tensor interaction in the large-N_C expansion.

Suggested Keywords: Chiral Perturbation Theory, Chiral Effective Field Theory, perturbative pions, Unitarity, Universality, scale/conformal invariance, Wigner-SU(4) spin-isospin symmetry, chiral symmetry, two-nucleon scattering, entanglement, Large-N_C.

[1] Email: yteng@uwm.edu
[2] Email: hgrie@gwu.edu (corresponding author)

1 Introduction

Why are the observables of few-nucleon systems dominated by anomalous scales? The deuteron is an exceptionally shallow bound state in the ${}^3\mathrm{S}_1$ channel of NN scattering, with a binding momentum of 45 MeV set by the inverse of the scattering length $a({}^3\mathrm{S}_1) \approx 5$ fm. Likewise the ${}^1\mathrm{S}_0$ channel has a virtual bound state at a binding momentum of -7 MeV from $a({}^1\mathrm{S}_0) \approx -24$ fm. These scales differ markedly from the natural low-momentum QCD scales of Nuclear Physics, the pion mass $m_\pi \approx 140$ MeV and $\frac{1}{m_\pi} \approx 1.4$ fm. The combined evidence of lattice computations and chiral extrapolations suggest that this fine tuning holds in QCD only in a small window around the physical value of the pion mass [1–3]; *cf.* [4].

Effective Field Theories (EFTs) of Nuclear Physics do not offer an explanation. They simply impose an ordering scheme whose leading-order (LO) iterates a NN interaction infinitely often. In the usually employed version of Chiral Effective Field Theory (χEFT), the one "with Nonperturbative Pions" (see *e.g.* [5, 6] for recent reviews), LO iterates one-pion exchange (OPE) and contact terms, tuned to reproduce the shallow bound states. Perfectly valid and consistent versions of χEFT exist in which LO is perturbative and the binding momentum (energy) of light nuclei is set by the scale m_π ($\frac{m_\pi^2}{M}$, with M the nucleon mass). But these are not realised in Nature.

And yet, one may recover the intrinsic momentum scales of S waves by expanding about scale zero, namely about Unitarity. This presentation explores how such an expansion emerges in χEFT, *i.e.* with pions, despite an apparent incompatibility with chiral symmetry, the cornerstone of χEFT, and finally argues that its highly symmetric limit is key for the wider question. The rest of the Introduction sets the stage: the Unitarity Expansion and its symmetries in NN systems; issues with pions as explicit degrees of freedom; the Conjecture we will infer from our results with perturbative pions; and the organisation of this article.

Let us first address the importance of Unitarity in general terms. The centre-of-mass two-body scattering amplitude at relative momentum k is

$$A(k) = \frac{4\pi}{M}\,\frac{1}{\mathrm{k}\cot\delta(k) - \mathrm{i}k} \quad . \tag{1.1}$$

The term "$-\mathrm{i}k$" ensures Unitarity of the S matrix, *i.e.* probability conservation. All information about the interaction is encoded in $\mathrm{k}\cot\delta(k)$. This invites two expansions.

In the **Born Corridor**, $|\mathrm{k}\cot\delta| \gtrsim |\mathrm{i}k|$, the phase shift is "small", $|\delta(k)| \lesssim 45°$, so contributions from interactions are small and can be treated perturbatively (Born approximation, no bound state). Their details enter at LO and are therefore crucial:

$$A(k)\Big|_{\mathrm{Born}} = \frac{4\pi}{M}\,\frac{1}{\mathrm{k}\cot\delta(k)}\left[1 + \frac{\mathrm{i}}{\cot\delta(k)} + \frac{\mathrm{i}^2}{\cot^2\delta(k)} + \mathcal{O}(\cot^{-3}\delta)\right] \quad . \tag{1.2}$$

This is the expansion about the "trivial/Gaußian" fixed point of zero interactions.

On the other hand, in the **Unitarity Window** $|\mathrm{k}\cot\delta| \lesssim |\mathrm{i}k|$ about the Unitarity Point $\cot\delta = 0$, the phase shift is "large", $45° \lesssim |\delta(k)| \lesssim 135°$. Albeit interactions are so strong that they must be treated non-perturbatively at leading order by resumming an infinite iteration, it is Unitarity which dominates the amplitude:

$$A(k)\Big|_{\rm Uni} = \frac{4\pi}{M}\,\frac{1}{-\mathrm{i}k}\left[1+\frac{\cot\delta(k)}{\mathrm{i}}+\frac{\cot^2\delta(k)}{\mathrm{i}^2}+\mathcal{O}(\cot^3\delta)\right] \quad . \tag{1.3}$$

This seems paradoxical, but the interactions are actually so strong that their details do not matter as much as the simple fact that they are very strong – so strong indeed that probability conservation limits their impact on observables. For example, the cross section is saturated, $\sigma = \frac{4\pi}{k^2}[1-|\mathcal{O}(\cot\delta)|]$. Moreover, an anomalously shallow bound state emerges naturally since the amplitude's pole is at zero, $k_{\rm pole} = 0 + \mathcal{O}(\cot\delta)$. Since the leading amplitude has no intrinsic scale, all dimensionless NN observables are zero or infinite at LO, while all dimensionful quantities (like the cross section) are homogeneous functions of k. Their exponents are set by dimensional analysis, and their dimensionless coefficients are independent of details of the interactions. This expansion in the Unitarity Window is hence one about the "Unitarity/non-trivial" fixed point of "maximally-strong" interactions, and Unitarity naturally implies Universality: Systems share the same behaviour, independent of interaction details at short distances. This applies when they are so close to the same Unitarity fixed point that differences between their interactions can be treated in perturbation. Universality classes differ by different sets of symmetries. That is important for imposing a dominant symmetry in sect. 4.1.

Universality, in turn, has been proposed as key to the emergence of simple, unifying patterns in complex systems like the nuclear chart [7–12]. Expanding about it quantitatively reproduces key observables like the binding of ^{4}He and its shallow first excitation. Such indications exist also for heavier systems and nuclear matter [13–18]; see [19, 20] for reviews.

The transition between Born Corridors and Unitarity Window is of course gradual rather than abrupt. One expects computations of observables still to be reliable to some degree as one intrudes into the other. The borders should therefore not be taken literally but are fuzzily located around phase shifts of about 45° and 135° ($|\cot\delta|\approx 1$); see fig. 1.

This leads to the natural question: Is the Unitarity Window relevant in NN? According to Partial-Wave Analyses (PWAs) [21–24][1], only the ^{1}S$_0$ and ^{3}S$_1$ channels contain anomalously shallow (real/virtual) bound states. Only their phase shifts are clearly inside it at momenta relevant for low-energy properties of systems of nucleons, namely $k \lesssim 300$ MeV (lab energies $\lesssim 200$ MeV). From fig. 1, that happens for 35 MeV $\lesssim k \lesssim$ 200 MeV. The estimate is conservative, and the boundaries are again to be understood as fuzzy.

In none of the other channels does the magnitude of the phase shift exceed even 25° ($|\cot\delta|\approx 2$) for $k \lesssim 300$ MeV. The ERE mandates that $k\cot\delta_l(k\to 0)\propto k^{-2l} \xrightarrow{k\to 0} \infty$ is at low momenta well outside the Unitarity Window in partial waves with orbital angular momentum[2] $l \geq 1$. The NN system knows no physical mechanism to overcome that at higher energies and push phase shifts into the Unitarity Window. ^{3}S$_1$ is part of a coupled

[1]While we use the Nijmegen PWA, uncertainties are minuscule in these channels. The ^{1}S$_0$ and ^{3}SD$_1$ phase shifts and mixing angles reported by the Granada group differ by less that 0.6° up to $k = 350$ MeV.

[2]A more careful K-matrix analysis of partial-wave mixing does not change this conclusion [77].

channel, but the magnitudes of ^{3}SD$_1$ mixing angle and ^{3}D$_1$ phase shift do not exceed 25° and may be amenable to treatment in perturbation. The ^{3}P$_{0,2}$, ^{3,1}P$_1$ and ^{3,1}D$_2$ channels hardly reach 25° ($|\cot\delta|\gtrsim 2$), either. The degree to which they must be treated nonperturbatively is evolving [25–27], and we are for the purpose of this presentation agnostic about the issue. All others have even smaller phase shifts ($|\delta(k)|\lesssim 10°$, $|\cot\delta|\gtrsim 5$) and can easily be described in perturbation [28–31]. Therefore, $l\geq 1$ partial waves are not considered here – not because they would not be important, but simply because the premises of the Unitarity Expansion do not apply. Unless explicitly mentioned, statements, results or conclusions in this article hold only for such a theory of NN S waves, in the régime where it applies.

Unitarity is so attractive because its two-nucleon state is highly symmetric. At the fixed point, nonrelativistic field theories are automatically not only scale-invariant but invariant under the larger Schrödinger group of nonrelativistic conformal transformations [32, 33]. The "Un-nuclear Physics" [34] this inspired is however not our focus. In systems of two spin-$\frac{1}{2}$ particles, ^{1}S$_0$ and ^{3}S$_1$ amplitudes are identical at Unitarity, so that the symmetry group is augmented by invariance under Wigner's combined SU(4) spin-isospin transformations [35–37]. Different scattering-length and effective-range corrections are included perturbatively; see [38, 39] for numerical evidence in phenomenological NN potentials. The tightest-bound light nuclei, ^{4}He, ^{12}C and ^{16}O, are all near-perfect spin-isospin singlets; *cf.* Similarity Renormalisation Group studies in ref. [40, 41]. Recently, Li Muli *et al.* [42] saw it dominate the β-decay of light nuclei. In QCD's large-N_C expansion, the leading non-tensor part of the NN interaction is automatically Wigner-SU(4) symmetric in even partial waves [43, 44]; *cf.* [45, 46] for a concise summary. [Sect. 4.4 returns to the interplay with large-N_C.]

While it would be an anthropomorphism to surmise that Nature prefers expansions about configurations with very high degrees of symmetry, theorists certainly do: Since Noether's theorem [47] relating continuous symmetries to conserved quantities, employing symmetry

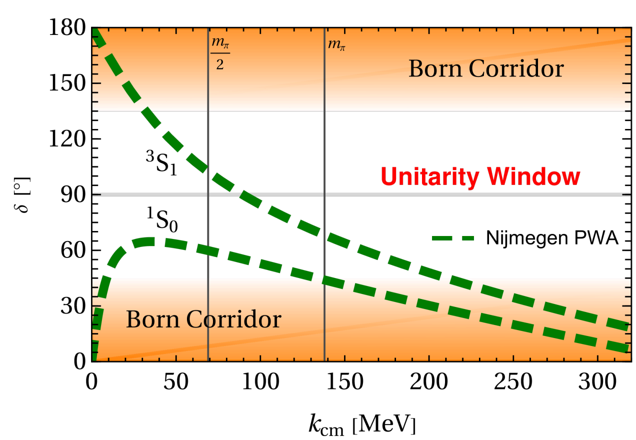

Figure 1: (Colour on-line) Born Corridor (shaded) and Unitarity Window (clear) of NN ^{1}S$_0$ and ^{3}S$_1$ phase shifts in the Nijmegen PWA [21]. Marked are also the scales of the first and second non-analyticity in k$\cot\delta(k)$, from the branch points $k=\pm\mathrm{i}\frac{m_\pi}{2}$ and $\pm\mathrm{i}m_\pi$ of non- and once-iterated OPE.

principles to construct systematic theories have become a cornerstone of modern Physics. As $\frac{1}{a(^1\mathrm{S}_0)} \neq \frac{1}{a(^3\mathrm{S}_1)}$ and neither is zero, both conformal invariance and Wigner-SU(4) symmetry are weakly broken in Nature for $|\mathrm{k}\cot\delta| < 1$. Therefore, a **Unitarity Expansion** about the nontrivial renormalisation-group fixed point with the symmetry group discussed above should be useful [30, 31, 48, 49].

In the language of Information Theory, it is the high degree of symmetry at Unitarity which may imply that the existence of anomalous scattering lengths is important, while their values are demoted to be less consequential, on par with other information (like effective ranges). The result is a compression of informational content by identifying relevant and filtering out irrelevant information.

Wigner-SU(4) symmetry plays also a prominent rôle in "Pionless EFT" (EFT($\not\pi$)). Its 3N Counter Term (CT) needed to renormalise LO is automatically spin-isospin invariant, with its Low-Energy-Coefficient (LEC) fixed by a 3N datum [50]. Other examples include classifying parity-violating and conserving 3N interactions [51–54]; and binding patterns in nuclear systems [55–60], like the ^{12}C ground and Hoyle states [61].

However, the first non-analyticity of $\mathrm{k}\cot\delta$ marks the formal breakdown scale of EFT($\not\pi$), *i.e.* its mathematical radius of convergence. It comes from the left-hand branch point $k = \pm \mathrm{i}\frac{m_\pi}{2}$ of NN OPE, the longest-range nonlocal exchange interaction. The associated scale $k \sim \frac{m_\pi}{2}$ lies well inside the Unitarity Window, as fig. 1 shows. It also appears to be right around where both partial waves are close to perfect Unitarity, $\delta = 90°$. And yet, EFT($\not\pi$) is of all EFTs the only one for which the Unitarity Expansion has thus far been explored [8, 9, 11–13, 18, 19]. That it appears to converge much better in practical applications, is well-known. For example, a recent combination of Bayesian order-by-order convergence analyses of np and nd scattering put its breakdown scale with 68% degree of belief at $[0.8; 1.2]\ m_\pi$ [62, 63]. Even that makes it cover barely more than half of the Unitarity Window. Such tension makes one ask how the Unitarity Expansion emerges with pionic degrees of freedom, *i.e.* in χEFT which should extend to higher momenta and automatically embed the non-analyticities [64].

However, the question is not simply how big the window is in which the Unitarity Expansion of χEFT is relevant, *i.e.* both converges and describes data efficiently. More fundamental is *how* the key aspects of Unitarity and Universality emerge with pions. In χEFT, conformal and Wigner-SU(4) invariance are not manifest in the chiral Lagrangean but hidden. They are not imposed when one constructs the EFT [65], in contradistinction to chiral, Lorentz and other symmetries. Rather, they are accidentally "discovered" when parameters are determined by data. They are *emergent phenomena*. Certainly, neither is manifest in OPE [$\vec{e}_q$: unit vector of momentum transfer $\vec{q}$; $\vec{\sigma}_i, \vec{\tau}_i$: nucleon i's spin, isospin]:

$$\begin{aligned} V_{\mathrm{OPE}} &= -\frac{g_A^2}{12 f_\pi^2}\,\frac{\vec{q}^{\,2}}{\vec{q}^{\,2}+m_\pi^2}\Big[(\vec{\sigma}_1\cdot\vec{\sigma}_2) + [3\,(\vec{\sigma}_1\cdot\vec{e}_q)\,(\vec{\sigma}_2\cdot\vec{e}_q) - (\vec{\sigma}_1\cdot\vec{\sigma}_2)]\Big]\,(\vec{\tau}_1\cdot\vec{\tau}_2) \\ &=: (\vec{\sigma}_1\cdot\vec{\sigma}_2)\,(\vec{\tau}_1\cdot\vec{\tau}_2)\,V_C + [3\,(\vec{\sigma}_1\cdot\vec{e}_q)\,(\vec{\sigma}_2\cdot\vec{e}_q) - (\vec{\sigma}_1\cdot\vec{\sigma}_2)]\,(\vec{\tau}_1\cdot\vec{\tau}_2)\,V_T \quad . \end{aligned} \tag{1.4}$$

The pion decay constant f_π and m_π break scale (and hence conformal) invariance explicitly because they carry mass dimensions, and the spin-isospin structure of the tensor part, V_T, induces S $\leftrightarrow$ D and D $\to$ D transitions. These are only possible in ^{3}S$_1$, and not in ^{1}S$_0$ where V_T is of course identically zero. Such ^{3}SD$_1$ mixing therefore manifestly breaks the Wigner-SU(4) symmetry between the S waves. In a possibly slight abuse of language, this is what we call "Wigner-SU(4) symmetry breaking"; see also sect. 2.3.2.

On the other hand, the spin-isospin structure of the central part, V_C, is identical in these channels, $(\vec{\sigma}_1 \cdot \vec{\sigma}_2)(\vec{\tau}_1 \cdot \vec{\tau}_2) = -3$, and can in a similarly slight abuse of language be called "Wigner-invariant" (projected onto the ^{1}S$_0$-^{3}S$_1$ system). It is also the *only* contribution in the ^{1}S$_0$ channel, where the tensor piece is of course identically zero. Thus, only amplitudes without V_T contributions are unchanged under Wigner-SU(4) transformations in the subspace of the ^{1}S$_0$-^{3}S$_1$ channels; *cf.* more formal discussion in sect. 2.3.2. Consequently, it is not self-understood how explicit pionic degrees of freedom are reconciled with the symmetries of the Unitarity Expansion which they appear to break rather strongly, while concurrently extending the range to the whole Unitarity Window, including $k \gtrsim m_\pi$.

The Unitarity Expansion with pions sets thus up as a apparent clash of fundamental but apparently incompatible symmetries. On the one side is the Unitarity Expansion whose weakly broken conformal and Wigner-SU(4) symmetries treat the ^{1}S$_0$ and ^{3}S$_1$ channels as fundamentally identical, and do therefore not allow ^{3}SD$_1$ mixing. On the other side, the weakly broken chiral symmetry of the Goldstone mechanism dictates the form of the OPE of eq. (1.4), ^{3}S$_1$ mixing, and that the ^{3}S$_1$ and ^{1}S$_0$ channels are fundamentally different as the tensor interaction in one is absent in the other, but *prima facie* explicitly breaks Conformal and Wigner-SU(4) symmetry rather strongly. All these symmetries are approximate, but neither scenario accommodates the idealisation from which the other starts. Each symmetry appears to be "hidden" and thus "accidental" from the perspective of the other.

It makes thus sense to investigate in detail how to reconcile the two approaches, so that both become manifest in observables. To our knowledge, that has not yet been attempted.

We therefore choose to investigate the transition from "pionless" to "pionic" EFT in χEFT "with Perturbative/KSW Pions", proposed by Kaplan, Savage and Wise [66, 67]. In it, LO consists still only of iterated, momentum-independent contact interactions. Together with corrections to these, OPE without iteration enters at next-to-leading order (NLO), and once-iterated OPE at N^{2}LO. Twice-iterated OPE as well as correlated two-pion exchange is relegated to higher orders. At its breakdown scale $\overline{\Lambda}_{\rm NN}$, OPE becomes non-perturbative [66–68], and its dimensionless expansion parameter at typical momenta $p_{\rm typ} \sim k, m_\pi$ is

$$Q = \frac{p_{\rm typ}}{\overline{\Lambda}_{\rm NN}} \;\;, \text{ with } \overline{\Lambda}_{\rm NN} = \frac{16\pi f_\pi^2}{g_A^2 M} \approx 300 \text{ MeV} \;\;. \tag{1.5}$$

Birse [30] pointed out that this scale depends on the total angular momentum of the partial wave, but we reiterated that we are only interested in S waves. From here on, we rephrase factors in OPE in terms of this scale, *e.g.* $\frac{g_A^2}{12 f_\pi^2} = \frac{4\pi}{3M\,\overline{\Lambda}_{\rm NN}}$ in eq. (1.4). While numerically $\overline{\Lambda}_{\rm NN} \approx 2m_\pi$ in the real world, it is not explicitly dependent of m_π and hence remains close to that value in the chiral limit. Fleming, Mehen and Stewart (FMS) found [68, 69] that perturbative pions at N^{2}LO fit ^{3}S$_1$ phase shifts rather poorly for $k \gtrsim 140$ MeV, *i.e.* well below $\overline{\Lambda}_{\rm NN}$, and found order-by-order convergence elusive. And yet, this is the only χEFT generally accepted to be self-consistent and renormalisable order by order, with a well-understood power counting [29], and thus regularly employed for predictions in the absence of data, *e.g.* in beyond-the-standard-model processes [70–72]. Modifications of this perturbative-pion version with better S-wave convergence have also been explored [26, 73–75].

We thus propose the **χEFT with Perturbative Pions in the Unitarity Expansion (χEFT$(\mathrm{p}\pi)_{\mathrm{UE}}$)**. Its N^2LO amplitudes are based on the work by Rupak and Shoresh (RS) in the $^1\mathrm{S}_0$ channel [76] and by FMS in $^3\mathrm{SD}_1$ [68, 69]. We will argue that it has a wider range of both convergence and agreement with PWAs than EFT($\not\pi$), if the following holds:

> **Conjecture:** The symmetries of the Unitarity Limit are broken weakly in Nuclear Physics. Their footprint shows *persistence*, *i.e.* their impact dominates observables at momentum scales $p_{\mathrm{typ}} \sim m_\pi$ and beyond, and is there more relevant than chiral symmetry. In particular, the tensor/Wigner-SU(4) symmetry-breaking part of one-pion exchange in the NN $^3\mathrm{S}_1$ channel is super-perturbative, *i.e.* does not enter before N^3LO.

Co-author Teng's MSc thesis gave first results [77]. Recently, we discussed findings and Conjecture at the ECT* workshop *The Nuclear Interaction: Post-Modern Developments*, the *11th International Workshop on Chiral Dynamics (CD2024)*, programme *INT-24-3 Quantum Few- and Many-Body Systems in Universal Regimes* and workshop *INT-25-92W Chiral EFT: New Perspectives* [78–81]. Ref. [82] contains a digest and addenda.

This article is organised as follows. Appendices detail important aspects which for the sake of flow are only summarised in the main text. Section 2 is devoted to methodology, with details relegated to app. A. We briefly review the EFT($\not\pi$) amplitudes to N^2LO in the Unitarity Expansion (sect. 2.1), and our choice to extract phase shifts, pole positions and residues from the amplitudes via kcotδ (sect. 2.2), with details in apps. A.1 and A.2. Section 2.3 discusses the χEFT amplitudes with Perturbative Pions in the Unitarity Expansion at $\mathcal{O}(Q^1)$ (N^2LO; sects. 2.3.4 to 2.3.6); with app. A.3 on their $k \to 0$ limit. It reviews the power counting (sect. 2.3.1) and group theory of Wigner-SU(4) symmetry, and identifies OPE's transformation properties (sect. 2.3.2), followed by specifying renormalisation point and parameters (sect. 2.3.3). Section 3 on the results starts with the zero-momentum and pole properties. Our central results are sects. 3.2 on the $^1\mathrm{S}_0$ channel, and 3.3 on the $^3\mathrm{S}_1$ channel both with and without its Wigner-SU(4) breaking parts. A detailed accounting of the robustness of our results and theory uncertainties is relegated to apps. B.1 and B.2 but summarised in sect. 3.5: order-by-order convergence, expansion parameters inside the Unitarity Window, convergence to the PWA, complementing phase shift extractions, and variation of the fit point. After such fact-oriented investigations, sect. 4 turns to ideas inspired by them. It develops the Conjecture (sect. 4.1) and speculates about the impact of the nontrivial fixed point on chiral symmetry (sect. 4.2), as well as about the interplay of Wigner symmetry with quantum-mechanical entanglement (sect. 4.3), and with QCD's large-N_C limit (sect. 4.4). After the customary summary, sect. 5 outlines steps to test if the symmetries of the Unitarity Limit persist and dominate well into a momentum régime in which pions must be accounted for.

2 Amplitudes and Observables

2.1 Amplitudes in Pionless EFT

To set up χEFT(pπ)$_{\text{UE}}$, we first consider the Unitarity Expansion at very low energies. That is the régime of EFT($\not\pi$), which is at N^{2}LO identical to the Effective Rage Expansion (ERE) [83–86]. We will use it in sect. 3 to check how important pions actually are. In addition, some subtleties on extracting observables in app. A.1 become more transparent.

The function kcot$\delta(k)$ which parametrises the interaction part proceeds for the expansion about $k = 0$ in powers of k^2 for $k \lesssim \frac{m_\pi}{2}$, *i.e.* below non-analyticities from non-iterated OPE:

$$\text{kcot}\delta(k) = -\frac{1}{a} + \frac{r}{2}\,k^2 + \sum_{n=2}^{\infty} v_n\,k^{2n} \quad , \tag{2.1}$$

with a the scattering length, r the effective range, v_n the shape parameters[3]. From fig. 1, phase shifts are inside the Unitarity Window even at these low momenta, so we choose:

$$\text{kcot}\delta^{\not\pi}_{0,-1} = 0 \;\;,\;\; \text{kcot}\delta^{\not\pi}_{0,0} = -\frac{1}{a} + \frac{r}{2}\,k^2 \;\;,\;\; \text{kcot}\delta^{\not\pi}_{0,1} = 0 \;\;. \tag{2.2}$$

The first subscript denotes the S channel ($l = 0$); the second the order in the expansion parameter $Q_{\not\pi}$ of EFT($\not\pi$). Inserting into the Unitarity Expansion of eq. (1.3), one finds at $\mathcal{O}(Q^1_{\not\pi})$ (N^{2}LO):

$$A^{(\text{S})}_{-1\not\pi}(k) = \frac{4\pi\text{i}}{M}\,\frac{1}{k} \;\;,\;\; A^{(\text{S})}_{0\not\pi}(k) = -\frac{4\pi}{Mk}\left(\frac{1}{ka} - \frac{kr}{2}\right) \;\;,\;\; A^{(\text{S})}_{1\not\pi}(k) = \frac{[A^{(\text{S})}_{0\not\pi}(k)]^2}{A^{(\text{S})}_{-1\not\pi}(k)} \;\;. \tag{2.3}$$

Therefore, the Unitarity Expansion in EFT($\not\pi$) proceeds in powers of and applies for $Q \sim \frac{1}{ka}, \frac{rk}{2} \ll 1$. This also implies $\frac{r}{2a} \sim Q^2_{\not\pi} \ll 1$, *i.e.* r is of natural size for anomalously large a. It breaks down for momenta which are either small, $k \lesssim \frac{1}{a}$, or large, $k \gtrsim \frac{2}{r}$, relative to the ERE scales. The dimensionless expansion parameters at, for example, $k \approx \frac{m_\pi}{2}$ are $\frac{1}{ka(^1\text{S}_0)} \approx 0.1$, $\frac{kr(^1\text{S}_0)}{2} \approx 0.5$, $\frac{1}{ka(^3\text{S}_1)} \approx 0.5$ and $\frac{kr(^3\text{S}_1)}{2} \approx 0.3$. Since none of these are particularly small, convergence of observables must be assessed carefully; see sect. 3.5. The two NLO contributions are of relative size $|\frac{ar}{2}\,k^2| \approx 4$ for $k \approx \frac{m_\pi}{2}$ in $^1\text{S}_0$ and ≈ 0.6 in $^3\text{S}_1$. So we follow [8] to define the Unitarity Expansion such that $\mathcal{O}(Q^0_{\not\pi})$ (NLO) includes both the scattering length and effective range. At higher k, a could be considered N^{2}LO since r dominates, but we strive for an expansion applicable throughout the Unitarity Window.

No new Physics enters in EFT($\not\pi$) at N^{2}LO since the amplitude is entirely determined by the LO and NLO results. The first additional datum comes then from the shape parameter v_2 at $\mathcal{O}(Q^2_{\not\pi})$ (N^{3}LO), *i.e.* one order higher than considered here. Additional information from v_n enters at $\mathcal{O}(Q^{2n-2}_{\not\pi})$ (N^{2n-1}LO). No new information enters at odd powers of Q (N^{2n}LO). Since pionic effects enter at each order beyond LO, that changes in χEFT(pπ)$_{\text{UE}}$ whose power counting is described in sect. 2.3.1.

[3]Other conventions include $v_n = -P_n\,r^{2n-1}$ with dimensionless P_n and factors of 2, 4 and $n!$.

2.2 From Amplitudes to Phase Shifts and Pole Positions

We follow the canonical Stapp-Ypsilanti-Metropolis (SYM/"bar") phase-shift parametrisation [87], also used by the Nijmegen [21] and Granada [22–24] PWAs. Phase shifts and bound-state properties (S-matrix poles and residues) are then found by an order-by-order expansion of the amplitude in "strict" perturbation as defined in Mathematical Perturbation Theory [88–91]; see also [76, 92] and a technical summary [93]. This preserves all symmetries at each order independently, including S-matrix unitarity. We will mostly use the expansion of kcotδ, as this is the fundamental variable of the Unitarity Expansion. The path from amplitudes via kcot$\delta(k)$, eqs. (A.9-A.11), to phase shifts and pole parameters is described in apps. A.1 and app. A.2, respectively. There, we also comment on approach's advantage outside the Unitarity Window. We show in app. B.1.5 that inside the Unitarity Window, extraction variants are consistent within expected higher-order uncertainties.

2.3 Amplitudes in χEFT with Perturbative Pions about Unitarity

2.3.1 Power Counting

Guided by the discussion around eq. (1.5) in the Introduction and sect. 2.1, we count powers of Q in χEFT$(\mathrm{p}\pi)_{\mathrm{UE}}$ as follows. In an EFT with resummed LO in the 2-body system, LO must for consistency on general grounds be counted as $\mathcal{O}(Q^{-1})$; see *e.g.* [65, 94]. The Unitarity Window of the NN system with perturbative OPE dictates then $\frac{1}{|a|} \ll p_{\mathrm{typ}} \ll \overline{\Lambda}_{\mathrm{NN}}$. For simplicity, we equate the two dimensionless expansion parameters into

$$Q := \frac{p_{\mathrm{typ}} = (k, m_\pi)}{\overline{\Lambda}_{\mathrm{NN}}} \approx \frac{1}{a\, p_{\mathrm{typ}}} \to Q \quad , \tag{2.4}$$

since they are numerically close for $k \approx m_\pi$ and physical values of the NN scattering lengths. We also set $r \sim m_\pi^{-1}$, *i.e.* $\frac{kr}{2} \sim Q$. All this implies $\frac{1}{a\overline{\Lambda}_{\mathrm{NN}}} \sim \frac{r}{2a} \sim Q^2$ and $\frac{r\overline{\Lambda}_{\mathrm{NN}}}{2} \sim Q^0$. That is not inconsistent with the real-world numerical values. With this, LO is Unitarity; NLO ($\mathcal{O}(Q^0)$) adds non-iterated OPE, finite scattering length and nonzero effective range (*cf.* sect. 2.1); and N^{2}LO ($\mathcal{O}(Q^1)$) once-iterated OPE and corrections in a, r. Neither is zero.

2.3.2 Wigner-SU(4) Symmetry and Its Breaking in χEFT(pπ)$_{\mathrm{UE}}$

We first briefly review the group theory of Wigner-SU(4) spin-isospin transformations, following [45]. Its second Casimir operator $C_2^{\mathrm{Wigner}} := \frac{15+\sigma+\tau+\sigma\tau}{2}$ has eigenvalue 5 for super-sextuplets (l even), and 9 for super-decuplets (l odd) (defining $\sigma := \vec{\sigma}_1 \cdot \vec{\sigma}_2$ *etc.*). As it commutes with the orbital angular momentum operator, we decide to classify super-multiplets in addition by a superscript l for $\vec{l}^{\,2} = l(l+1)$.

The $^1\mathrm{S}_0$-$^3\mathrm{S}_1$ channels form an (antisymmetric) super-sextuplet Irrep $[\mathbf{6}_A]^{l=0}$ ($(S, I) = (0, 1) \vee (1, 0)$). In general, a super-sextuplet $[\mathbf{6}_A]^l$ applies to all partial waves with even orbital angular momentum l. The next is $[\mathbf{6}_A]^2$, the spin-singlet isospin-triplet $^1\mathrm{D}_2$ combined with the Wigner-symmetric components of the spin-triplet-isospin-singlets $^3\mathrm{D}_2$ and $^3\mathrm{DF}_3$, as well as $^3\mathrm{D}_1$ which mixes with the $^1\mathrm{S}_0$-$^3\mathrm{SD}_1$ Irrep; see below. Odd partial waves pair to (symmetric) super-decuplet Irreps $[\mathbf{10}_S]^l$, $(S,I)=(0,0)\vee(1,1)$. The lowest-l representation combines the spin-singlet-isospin-singlet $^1\mathrm{P}_1$ and the Wigner-symmetric components of the spin-triplet isospin-triplets $^3\mathrm{P}_0$-$^3\mathrm{P}_1$-$^3\mathrm{PF}_2$. [One could also classify Wigner-supermultiplets by total angular momentum j. In mixed channels like $^3\mathrm{SD}_1$, the supermultiplet axes are then slightly tilted off the $l=j\pm1$ state. However, PWAs show that NN phase-shift mixing angles are very small, $|\epsilon|<5^\circ$, *i.e.* pure $l=j\pm1$ states can be treated as $[\mathbf{W}]^l=[\mathbf{W}]^j$ at LO, with corrections in perturbation; *cf.* also [45, sect. V.C].]

The origin of Wigner-SU(4) breaking is thus twofold. The central operator $\vec{\sigma}_1\cdot\vec{\sigma}_2$ splits members of each super-multiplet $[\mathbf{W}]^l$ at fixed l by spin $S=0$ (eigenvalue -1) or 1 (eigenvalue 3), *e.g.* by different effective-range parameters a and r in the two channels. However, it does not mix super-multiplets with different l since it commutes with both C_2^{Wigner} and $\vec{l}^2$. On the other hand, OPE's tensor operator in eq. (1.4) does not commute with $\vec{l}^2$ (but of course with $\vec{j}^2$), yet it does commute with C_2^{Wigner}. It lifts therefore the degeneracy both within and between super-multiplets $[\mathbf{6}_A]^l$ and $[\mathbf{10}_S]^l$ for different l (where sextets do not mix with decuplets because parity and j must be conserved). This justifies the term "Wigner-breaking". It does not affect $S=0$ states, but mixes exclusively the $S=1$ state in the same super-multiplet with one in another super-multiplet with the same j but different $l=j\pm1$, like the $j=1$ states $^3\mathrm{S}_1$ in $[\mathbf{6}_A]^0$ and $^3\mathrm{D}_1$ in $[\mathbf{6}_A]^2$. The operator of OPE's central part, $V_C\propto\sigma\tau$, also commutes with the Casimir operator. It acts on all members of super-sextuplets like $^1\mathrm{S}_0$-$^3\mathrm{S}_1$ by returning the same state with eigenvalue -3 and is thus there proportional to the unit operator. That justifies the name "Wigner-SU(4) symmetric" contribution, albeit some may prefer "Wigner-SU(4) covariant". In a super-decuplet $[\mathbf{10}_S]^l$ like $^1\mathrm{P}_1$-$^3\mathrm{P}_{0,1,2}$, the latter is more appropriate since it returns different values: 9 for $S=I=0$ and 1 for $S=I=1$. The impact of Wigner-symmetry there is worth exploring [45]. As the Unitarity Expansion is inapplicable in all partial waves except for the $^1\mathrm{S}_0$-$^3\mathrm{S}_1$ super-sextet, we continue with the attributions "symmetric" and "breaking".

We now discuss at which order and how Wigner-breaking terms enter in $\chi\mathrm{EFT}(\mathrm{p}\pi)_{\mathrm{UE}}$. At NLO, OPE is inserted once. Symbolically, one projects V_{OPE} (with contact terms for renormalisation) onto the $^1\mathrm{S}_0$ and $^3\mathrm{S}_1$ channels:

$$\begin{aligned} A_0(^1\mathrm{S}_0) &= \langle ^1\mathrm{S}_0|V_C|^1\mathrm{S}_0\rangle =: A_0^{\mathrm{S}} \\ A_0(^3\mathrm{S}_1) &= \begin{pmatrix} |^3\mathrm{S}_1\rangle \\ 0 \end{pmatrix}^\dagger \begin{pmatrix} V_C & \sqrt{8}\,V_T \\ \sqrt{8}\,V_T & V_C-2V_T \end{pmatrix} \begin{pmatrix} |^3\mathrm{S}_1\rangle \\ 0 \end{pmatrix} = \langle ^3\mathrm{S}_1|V_C|^3\mathrm{S}_1\rangle = A_0^{\mathrm{S}} \end{aligned} \tag{2.5}$$

The LO amplitudes and states $|^1\mathrm{S}_0\rangle$ and $|^3\mathrm{S}_1\rangle$ are S-waves only and Wigner-SU(4) invariant, $\sigma\tau|^3\mathrm{S}_1\rangle=\sigma\tau|^1\mathrm{S}_0\rangle$. The pion part at NLO is therefore necessarily Wigner-SU(4) symmetric. OPE-induced differences between the partial waves only enter at N^{2}LO:

$$\begin{aligned} A_1(^1\mathrm{S}_0) &= \langle ^1\mathrm{S}_0|V_C G V_C|^1\mathrm{S}_0\rangle =: A_{1\mathrm{sym}}^{(\mathrm{S})} \\ A_1(^3\mathrm{S}_1) &= \begin{pmatrix} |^3\mathrm{S}_1\rangle \\ 0 \end{pmatrix}^\dagger \begin{pmatrix} V_C & \sqrt{8}\,V_T \\ \sqrt{8}\,V_T & V_C-2V_T \end{pmatrix} G \begin{pmatrix} V_C & \sqrt{8}\,V_T \\ \sqrt{8}\,V_T & V_C-2V_T \end{pmatrix} \begin{pmatrix} |^3\mathrm{S}_1\rangle \\ 0 \end{pmatrix} \\ &= A_1(^1\mathrm{S}_0) + \langle ^3\mathrm{S}_1|8V_T G V_T|^3\mathrm{S}_1\rangle =: A_{1\mathrm{sym}}^{(\mathrm{S})} + A_{1\mathrm{break}}^{(\mathrm{S})} \end{aligned} \tag{2.6}$$

NLO is $A_0^{\rm S}$; the symmetric (breaking) N^{2}LO part is $A_{\rm 1sym}^{\rm S}$ ($A_{\rm 1break}^{\rm S}$). The "free" LO two-nucleon propagator G is Wigner-symmetric at Unitarity. Wigner-breaking comes exclusively from once iterating OPE via V_T and induces a S $\to$ D $\to$ S intermediate state. A DD matrix element does not appear before twice-iterated OPE, *i.e.* N^{3}LO. Extension to other channels is straightforward [95]. It is natural to assume that the amount of breaking at higher orders grows exponentially with the number of V_T insertions.

We reiterate that this reasoning only applies to the pion-part of the interaction and the corresponding CTs which absorb regulator-dependence. In our case, their "finite parts" are set by the empirical scattering lengths and effective ranges. These break Wigner-SU(4) symmetry explicitly but weakly. For a meaningful distinction between Wigner-symmetric and breaking contributions, it must of course be renormalisation-group invariant. That is fulfilled by construction if the regulator preserves Wigner-SU(4) symmetry, like in dimensional regularisation with Power-Divergence Subtraction [66, 67] which we use.

2.3.3 Pathway and Parameters

The NN amplitudes in the ^{1}S$_0$ and coupled ^{3}SD$_1$ channels with perturbative (KSW) pions were derived for finite scattering length by Kaplan, Savage and Wise [66, 67] to NLO, and extended to N^{2}LO by RS (^{1}S$_0$) [76], and then by FMS (^{3}S$_1$, ^{1}S$_0$) [68, 69] (both ^{1}S$_0$ results agree). Figure 2 shows the contributions at each order. The last line includes those diagrams with SD-mixing interactions, all of which enter only at N^{2}LO as just discussed. Those which enter only in the phase shift of the ^{3}D$_1$ channel and of the SD mixing angle are discussed in an MSc thesis [77] and will be subject of a future publication [95]. In order to confirm correct coding, we reproduced the FMS results with their parameter values. This is nontrivial since some are highly sensitive to the exact numbers used[4].

We then expanded the amplitudes about Unitarity to find the LECs at its natural renor-

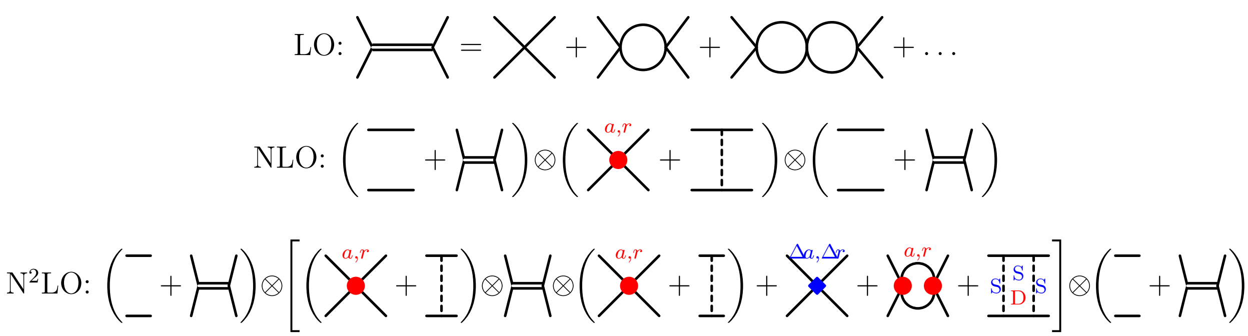

Figure 2: (Colour on-line) χEFT(pπ)$_{\rm UE}$ at LO (top); NLO (middle) with CTs (red circle) fixed to reproduce scattering length a and effective range r; N^{2}LO with CTs (blue diamonds) fixed so that a and r do not change from the NLO value. Last N^{2}LO term in square brackets: once-iterated OPE, with orbital angular momentum of the intermediate state as indicated.

[4]We are grateful for Iain Stewart's help in numerous conversations, both electronically and in person.

malisation point, $k_{\rm fit}=0$. Section 3.5 summarises discussions of different $k_{\rm fit}\neq 0$ in app. B.2.

FMS find their LO LECs (equivalent to our fixing a) from the pole positions, and their dimensionless NLO and N^{2}LO LECs ζ_1 to ζ_4 from weighted least-squares fits to the Nijmegen PWA which do not change the LO pole positions. We did confirm FMS' finding that further coefficients ζ_5,ζ_6 of higher-order contributions do not solve the poor convergence at N^{2}LO and discard them here from the start; *cf.* discussion in sect. 3.4.

For clarity, we regrouped the amplitudes into Wigner-SU(4) symmetric and breaking parts, each sorted by powers of the dimensionless ratio $\frac{k}{m_\pi}$. The results appear considerably shorter that those of FMS [68] for three reasons. First, they are rewritten using the ERE parameters a, r in favour of FMS' ζ_1 to ζ_4. Second, the Unitarity Expansion leads to a few simplifications. Third, we found some more economical ways to rewrite certain terms.

On a technical note, we do not differentiate between NN CTs which explicitly break chiral symmetry by quark (and hence pion) mass dependence. Staring at NLO, a NN LEC $D_2m_\pi^2$ enters [96] with the same operator structure as the CT whose LEC is determined by the scattering length. Here, we do not vary the pion mass, and the amplitudes we use are regulator-independent, so such effects cannot be disentangled.

We use the average nucleon and pion masses $M=938.91897$ MeV, $m_\pi:=\frac{2m_\pi^\pm+m_\pi^0}{3}=138.037$ MeV, the axial pion-nucleon coupling $g_A=1.267$, pion decay constant[5] $f_\pi=92.42$ MeV, and $197.327\ \text{fm}\,\text{MeV}=1$. The position of cuts and poles in amplitudes induced by pionic effects becomes manifest when one replaces $m_\pi^2\to m_\pi^2-\mathrm{i}\epsilon$ with $\epsilon\searrow 0$.

Generic scattering lengths and effective range are denoted by a and r and replaced by the $^1\mathrm{S}_0$ or $^3\mathrm{S}_1$ values as appropriate. We choose those reported by the Granada group [24]: $a(^1\mathrm{S}_0)=-23.735(6)$ fm, $r(^1\mathrm{S}_0)=2.673(9)$ fm; and $a(^3\mathrm{S}_1)=5.435(2)$ fm, $r(^3\mathrm{S}_1)=1.852(2)$ fm. The slightly different results and parameter values in the MSc thesis [77] used the Nijmegen group's 1995 analysis [21, 97]: $a(^1\mathrm{S}_0)=-23.714$ fm, $r(^1\mathrm{S}_0)=2.73$ fm; $a(^3\mathrm{S}_1)=5.420(1)$ fm, $r(^3\mathrm{S}_1)=1.753(2)$ fm. However, induced differences even at $k\approx 300$ MeV are smaller than 2.7° and hardly exceed the line widths.

2.3.4 Amplitude at $\mathcal{O}(Q^{-1})$ (Leading Order)

The LO contribution at Unitarity is identical in the $^3\mathrm{SD}_1$ and $^1\mathrm{S}_0$ channel and therefore obviously both conformally and Wigner-SU(4) invariant. Only the S-wave component is nonzero and of course identical to the pionless result of eq. (2.3):

$$A_{-1}^{(\mathrm{S})}(k)=\frac{4\pi\mathrm{i}}{M}\,\frac{1}{k}\quad. \tag{2.7}$$

2.3.5 Amplitude at $\mathcal{O}(Q^0)$ (Next-To-Leading Order)

Now, scattering length, effective range and pions enter:

$$A_0^{(\mathrm{S})}(k)=-\frac{4\pi}{M}\left[\frac{1}{k}\left(\frac{1}{ka}-\frac{kr}{2}\right)+\frac{1}{\overline{\Lambda}_{\mathrm{NN}}}\left(1-\frac{m_\pi^2}{4k^2}\,\ln[1+\frac{4k^2}{m_\pi^2}]\right)\right]\quad. \tag{2.8}$$

[5] KSW and FMS use $f=\sqrt{2}f_\pi$ [66–69].

This, including its OPE part, is indeed suppressed against LO in the Unitarity Window ($\frac{1}{ka}, \frac{k}{\overline{\Lambda}_{\rm NN}} < 1$), consistent with the power counting.

The first term is the NLO amplitude of the pionless version, eq. (2.3). Differences of scattering lengths and effective ranges induce the *only* Wigner-SU(4) breaking effects at this order. While the pionic potential of eq. (1.4) breaks conformal and Wigner symmetry, OPE at NLO naturally accommodates Wigner-SU(4) symmetry as its projections onto the $^1\mathrm{S}_0$ and $^3\mathrm{S}_1$ channels are identical, as anticipated in sect. 2.3.2. It is also the only non-analytic contribution, with just one branch point at $k = \pm \mathrm{i}\frac{m_\pi}{2}$.

As $k \to 0$, the non-pionic part is exactly the EFT($\not\pi$) result of eq. (2.3). Corrections come exclusively from pions and vanish in dimensionless units as $\frac{2k^3}{\overline{\Lambda}_{\rm NN} m_\pi^2}$; see eq. (A.25) in app. A.3. Thus, they contribute substantially only for $k \gtrsim 100$ MeV: Pion contributions violate scale invariance only weakly for low momenta, and not at all for zero momenta. This is expected since all scale-breaking at $k = 0$ is subsumed into the different scattering lengths and effective ranges in $^1\mathrm{S}_0$ and $^3\mathrm{S}_1$. The $\mathcal{O}(g_A^2)$ contribution in eq. (2.8) constitutes only the long-range part of OPE (without iteration), after CTs absorb divergences to reproduce the empirical a, r. The phrase "pion contribution" is understood in that sense: the pionic long-distance (non-analytic) part after renormalisation within the chosen renormalisation scheme (Power Divergence Subtraction in dimensional regularisation[66, 67]) and renormalisation condition ($k_{\rm fit} = 0$ with empirical a and r).

2.3.6 Amplitude at $\mathcal{O}(Q^1)$ (Next-To-Next-To-Leading Order)

No new low-energy scattering parameters enter. As argued in the Introduction and sect. 2.3.2, the Wigner-SU(4) symmetric part is identical to the contribution in the $^1\mathrm{S}_0$ channel:

$$A_1^{(^1\mathrm{S}_0)}(k) \equiv A_{1\mathrm{sym}}^{(\mathrm{S})}(k) = \frac{\left[A_0^{(\mathrm{S})}(k)\right]^2}{A_{-1}^{(\mathrm{S})}(k)} + \frac{8\pi}{M\,\overline{\Lambda}_{\rm NN}}\left\{\frac{4}{3am_\pi} - \frac{m_\pi}{k}\left(\frac{1}{ka} - \frac{kr}{2}\right) - \frac{M}{4\pi}A_0^{(\mathrm{S})}(k)\,\frac{m_\pi^2}{2k}\,\arctan[\frac{2k}{m_\pi}] - \frac{m_\pi}{\overline{\Lambda}_{\rm NN}}\left[\frac{1}{12} + \left(\frac{m_\pi^2}{4k^2} - \frac{1}{3}\right)\ln 2 - G_\pi(\frac{k}{m_\pi})\right]\right\} \quad (2.9)$$

The first term combines the N^{2}LO EFT($\not\pi$) amplitude of eq. (2.3) with insertions of the pionic NLO pieces; see eq. (2.8) and first term in square brackets in fig. 2. The second term is a correction from (non-iterated) OPE and CTs to keep a and r at N^{2}LO fixed to the NLO values (N^{2}LO diagrams labelled a, r and $\Delta a, \Delta r$ in fig. 2). The $\mathcal{O}(\overline{\Lambda}_{\rm NN}^{-2})$ contributions of the last line encode the long-range part of once-iterated OPE via S $\to$ S $\to$ S only (last N^{2}LO diagram in square brackets of fig. 2 and eq. (2.6)). The amplitude has a branch point from non-iterated OPE at $k = \pm\mathrm{i}\frac{m_\pi}{2}$, and in addition from once-iterated OPE at $k = \pm\mathrm{i}\, m_\pi$. The latter comes from the last term of the dimensionless function

$$G_\pi(x) := \frac{1}{8x^3}\left\{\arctan[2x]\ln[1+4x^2] - \mathrm{Im}\Big[\mathrm{Li}_2[\frac{2\mathrm{i}x+1}{2\mathrm{i}x-1}] + 2\mathrm{Li}_2[\frac{1}{2\mathrm{i}x-1}]\Big]\right\} \quad (2.10)$$

since Euler's Dilogarithm (Spence function) $\mathrm{Li}_2(z) = -\int\limits_0^z \mathrm{d}t\ \frac{\ln[1-t]}{t}$ has a branch point at $z=1$ [98, sect. 25.12(i)]. Furthermore, $G_\pi(x\to 0) = 1 - \frac{10x^2}{3} + \mathcal{O}(x^4)$ is finite as $k\to 0$, and monotonically falling towards its chiral limit $G_\pi(x\to\infty) = \frac{\pi}{8}\ \frac{\ln[2x]}{x^3} + \mathcal{O}(x^{-4})$.

The non-pionic ($(\overline{\Lambda}_{\mathrm{NN}})^0$) part reduces to the pionless version, eq. (2.3), *i.e.* a and r are unchanged from NLO. The pionic contribution to kcotδ vanishes faster than k^2, namely in dimensionless units as $\frac{4k^3}{\overline{\Lambda}_{\mathrm{NN}} m_\pi}(\frac{1}{am_\pi^2}, r)$ dominated by the size of $r \approx \frac{1}{m_\pi}$. With $a\,m_\pi \gg r\,m_\pi \approx 1$, the scale for once-iterated OPE is of the same magnitude, $\frac{k}{\overline{\Lambda}_{\mathrm{NN}}}\ \frac{k^2}{m_\pi^2}$. Both are hence again small for $k \lesssim m_\pi$. $A_0^{(\mathrm{S})}(k\to 0)$ is given in eq. (A.26) of app. A.3.

A Wigner-SU(4) breaking part enters in the $^3\mathrm{S}_1$ amplitude:

$$
\begin{aligned}
A_1^{(^3\mathrm{S}_1)}(k) =& A_{1\mathrm{sym}}^{(\mathrm{S})}(k) + A_{1\mathrm{break}}^{(\mathrm{S})}(k)\ \ , \qquad (2.11)\\
A_{1\mathrm{break}}^{(\mathrm{S})}(k) =& \frac{16\pi m_\pi}{M\,\overline{\Lambda}_{\mathrm{NN}}^2}\Bigg\{ \overbrace{\frac{571-352\ln 2}{210}}^{=1.5572...} - \left(1+\frac{3m_\pi^2}{2k^2}+\frac{9m_\pi^4}{16k^4}\right) G_\pi(\frac{k}{m_\pi}) \\
&+ \frac{2m_\pi^2}{5k^2}(\ln 4 - 1) + \frac{3m_\pi^4}{16k^4} - \frac{3}{2}\left[\left(\frac{k}{m_\pi}+\frac{m_\pi}{k}\right) - \left(\frac{m_\pi^3}{8k^3}+\frac{3m_\pi^5}{16k^5}\right)\right]\arctan[\frac{k}{m_\pi}] \\
&+ \frac{3}{16}\left(\frac{m_\pi^4}{k^4}+\frac{3m_\pi^6}{4k^6}\right)\ln[\frac{16(k^2+m_\pi^2)}{4k^2+m_\pi^2}]\Bigg\} - \frac{\left[A_0^{(\mathrm{SD})}(k)\right]^2}{A_{-1}^{(\mathrm{S})}}\ \ . \qquad (2.12)
\end{aligned}
$$

Since $A_{1\mathrm{break}}^{(\mathrm{S})}$ is $\mathcal{O}(\overline{\Lambda}_{\mathrm{NN}}^{-2})$, it comes exclusively from the transition S $\to$ D $\to$ S of once-iterated OPE; see fig. 2 and $\langle ^3\mathrm{S}_1|8V_T G V_T|^3\mathrm{S}_1\rangle$ of eq. (2.6). In curly brackets is the part which is not simply twice the non-iterated OPE between on-shell nucleons. It has branch points again at $k = \pm\mathrm{i}\frac{m_\pi}{2}$, $\pm\mathrm{i}\,m_\pi$, with the latter from $\arctan\frac{k}{m_\pi}$, $\ln[k^2+m_\pi^2]$ and G_π. The very last term is the on-shell piece, *i.e.* the NLO SD-mixing amplitude-squared:

$$
A_0^{(\mathrm{SD})}(k) = -\frac{\mathrm{i}\pi\sqrt{2}\,m_\pi^2}{M\,\overline{\Lambda}_{\mathrm{NN}}\,k^2}\left[\frac{3m_\pi}{2k} - \left(1+\frac{3m_\pi^2}{4k^2}\right)\arctan[\frac{2k}{m_\pi}]\right]\ \ . \qquad (2.13)
$$

However, that term cancels the same contribution in the phase shift, eq. (A.5), and in kcotδ, eq. (A.11), irrespective of whether $A_{-1}^{(\mathrm{S})}$ is at Unitarity or not. Since $A_0^{(\mathrm{SD})}(k=0)=0$, it does not contribute to shifting the pole, either; *cf.* eq. (A.19). The LO SD amplitude is zero; neither its N^{2}LO nor any DD amplitude enters for S waves at this order [77, 95].

According to eq. (A.27) of app. A.3, kcot$\delta(k\to 0)$ vanishes again as $\frac{k}{\overline{\Lambda}_{\mathrm{NN}}}\ \frac{k^2}{m_\pi^2}$ ($a\,m_\pi \gg r\,m_\pi \approx 1$), so that a and r are not shifted from the NLO values.

We see that all N^{2}LO OPE contributions are in the Unitarity Window suppressed by powers of $Q \sim \frac{1}{ka} \sim \frac{k, m_\pi}{\overline{\Lambda}_{\mathrm{NN}}} < 1$ against LO, and against both pionic and non-pionic NLO parts separately. This confirms Q and $\overline{\Lambda}_{\mathrm{NN}}$ of eq. (2.4) in S-waves for the Unitarity Expansion of χEFT with Perturbative Pions.

3 Results and Analysis

All observables include Bayesian truncation uncertainties at $\mathrm{N^2LO}$, estimated semi-quantitatively as 68% degree-of-belief (DoB) intervals via the "max" criterion [99, sect. 4.4] with reasonable priors following [100–102]. As posteriors are non-Gaußian, the width of 95% DoB intervals is about 2.7 times 68% DoB. These and other theory uncertainties are discussed in sect. 3.5, and apps. B.1, B.2. The centre-of-mass momentum k is the primary variable.

3.1 Zero-Momentum Limit and Pole Parameters

As $k \to 0$, NLO and $\mathrm{N^2LO}$ contribute to $\mathrm{kcot}\delta$ only via even powers of k, as required by analyticity below $k = |\pm\mathrm{i}\frac{m_\pi}{2}|$ [83–86]; see app. A.3. Since the renormalisation point is ERE at $k = 0$ with Unitarity, $\frac{1}{a} = 0$, LO is $\mathrm{kcot}\delta_{0,-1} = 0$. NLO is $\mathrm{kcot}\delta_{0,0} = \left(-\frac{1}{a} + \frac{r}{2}k^2\right) + \mathcal{O}(k^4)$; eq. (A.25). $\mathrm{N^2LO}$ vanishes, $\mathrm{kcot}\delta_{0,1} = 0 + \mathcal{O}(k^4)$; eqs. (A.26/A.27). Therefore, pole positions and residues in $\chi\mathrm{EFT}(\mathrm{p}\pi)_{\mathrm{UE}}$, table 1, are unchanged from ERE/EFT($\not\pi$), eqs. (A.23/A.24) in app. A.2. We use the Granada group's empirical values (with negligible uncertainties) [24]: in the $^3\mathrm{S}_1$ channel, derived from the deuteron's binding energy and asymptotic normalisation ($\gamma = \sqrt{MB_2}$, $Z = \frac{A_S^2}{2\gamma}$); fr the $^1\mathrm{S}_0$ channel, inferred from the scattering length, effective range and shape parameter as described in [103]. From app. B.1.4, the 68% DoB interval for theory truncation uncertainties is $\pm\frac{\mathrm{i}}{a}\frac{r^3}{2a^3}$ for the pole position and $\pm\frac{4r^3}{a^3}$ for its residue (times about 2.7 for 95% DoBs). Within these, comparison to the empirical values is favourable.

	$^1\mathrm{S}_0$		$^3\mathrm{S}_1$	
	$\mathrm{i}\gamma$ [MeV]	Z	$\mathrm{i}\gamma$ [MeV]	Z
NLO	$-\ 8.314\,\mathrm{i}$	0.887	$+36.3\,\mathrm{i}$	1.34
$\mathrm{N^2LO}$	$[-\ 7.898 \pm 0.006]\mathrm{i}$	$[0.906 \pm 0.006]$	$[+44.6 \pm 0.7]\mathrm{i}$	$[1.52 \pm 0.16]$
empirical	$[-\ 7.892 \pm 0.040]\mathrm{i}$	$[0.9034 \pm 0.0005]$	$[+45.7023 \pm 0.0001]\mathrm{i}$	$[1.6889 \pm 0.0031]$

Table 1: Pole position and residue in PWA and $\chi\mathrm{EFT}(\mathrm{p}\pi)_{\mathrm{UE}}$ at $\mathrm{N^2LO}$ (Bayesian uncertainties from app. B.1.4) and NLO (no errors).

3.2 The Spin Singlet, Isospin Triplet: $^1\mathrm{S}_0$ Phase Shifts

The pionic contribution to the $^1\mathrm{S}_0$ channel consists only of the Wigner-SU(4) invariant part. By inspection, its phase shift (top of fig. 3) converges well order-by-order until $k \to \overline{\Lambda}_{\mathrm{NN}} \approx$ 300 MeV approaches the putative breakdown scale. This point lies actually well outside the Unitarity Window (non-shaded area), but even there, the difference between $\mathrm{N^2LO}$ and PWA is only as large as the difference between NLO and $\mathrm{N^2LO}$. Remarkably, $\mathrm{N^2LO}$ is nearly indistinguishable from EFT($\not\pi$) at NLO=$\mathrm{N^2LO}$. [Recall that the $\mathrm{N^2LO}$ contribution of EFT($\not\pi$) is zero; see eqs. (2.2) and (A.14).] Thus, explicit pionic degrees of freedom appear to have a minuscule impact even close to or beyond the breakdown scale of EFT($\not\pi$), which is at least the scale of the first branch point $k \gtrsim \frac{m_\pi}{2}$. The bottom of fig. 3 also displays

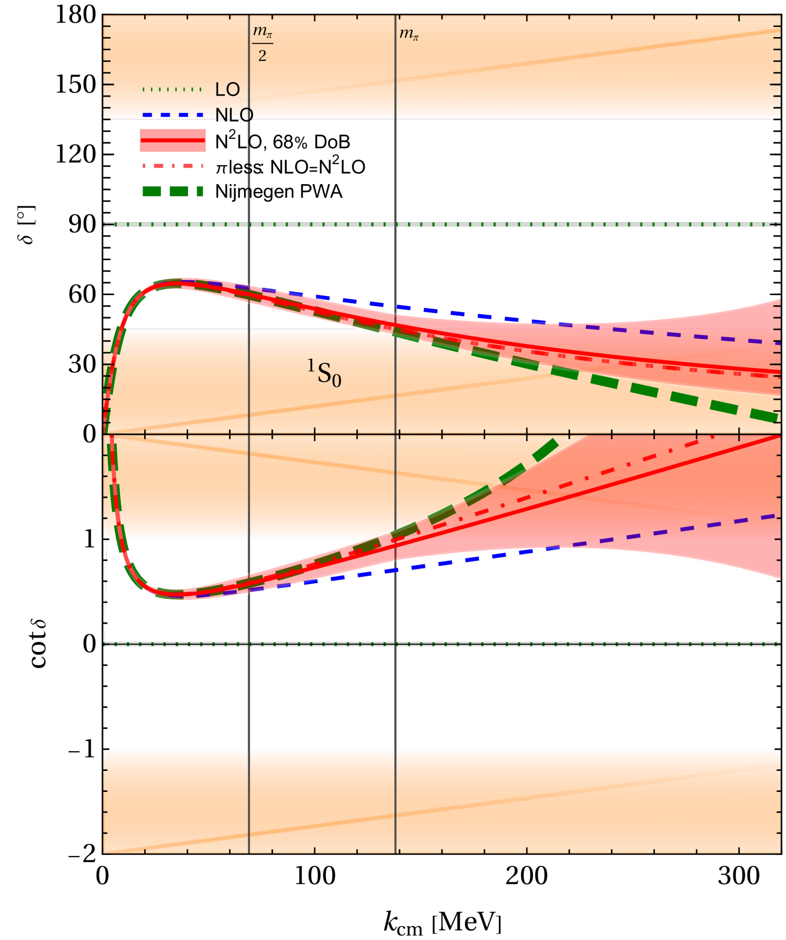

Figure 3: (Colour on-line) Phase shift (top) and $\cot\delta(k)$ (bottom) in the ^{1}S$_0$ channel as a function of k, compared to the Nijmegen PWA [21] (thick green dashed). Green dotted: LO; blue dashed: NLO; red solid: N^{2}LO with 68% degree-of-belief (DoB) interval based on the Bayesian truncation uncertainty under the assumptions of sect. B.1.4; red dash-dotted: NLO=N^{2}LO in EFT($\not\pi$). Shaded areas indicate the "Born Corridors" of fig. 1, *i.e.* regions in which the Unitarity Expansion can *a priori* not be expected to hold. Marked is also the scale of the first and second non-analyticity in $k\cot\delta(k)$, from the first two branch points $k = \pm i\frac{m_\pi}{2}, \pm i m_\pi$ of OPE.

$\cot\delta$ since the Introduction identified the "physical part" of the amplitude, $\cot\delta$ in eq. (1.3), as the primary variable in the Unitarity Expansion. Included in both figures are the N^{2}LO intervals in which higher-order corrections should lie with 68% DoB, based on a Bayesian order-by-order convergence analysis under assumptions detailed in sect. B.1.4. Section 3.5 will argue that this provides also a reasonable estimate of the smallest reasonable range of theory uncertainties combining several assessments.

The excellent agreement between PWA, EFT($\not\pi$) and χEFT(pπ)$_{\rm UE}$ at low k is a result

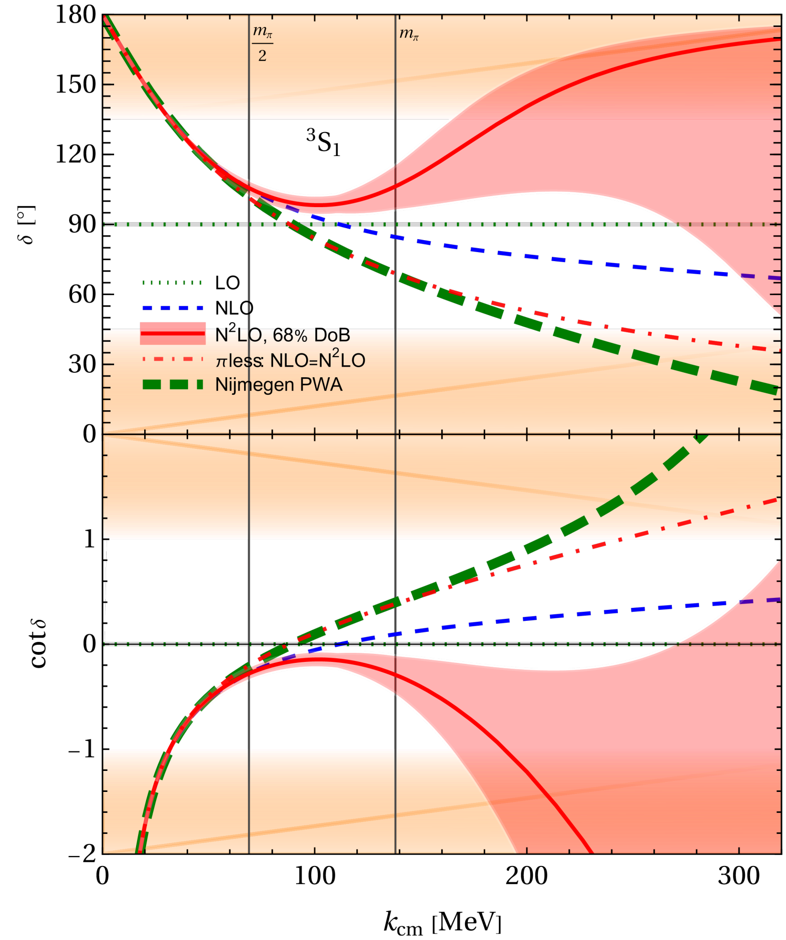

Figure 4: (Colour on-line) Phase shift (top) and $\cot\delta(k)$ (bottom) in the $^3S_1$ channel, compared to the Nijmegen PWA [21] (thick green dashed). Details as in fig. 3.

of our fit to the ERE parameters. At high momenta, differences to the original results by RS, and by FMS [68, 76] are small. While our N^{2}LO is above the PWA, theirs lies a bit below. We attribute this to two aspects: KSW fit at low k to the PWA, while we use the ERE parameters; and we find phase shifts via k$\cot\delta$, while they determine δ directly using eqs. (A.3-A.5); see apps. B.1.5 and A.1. That we expand about Unitarity while they use a finite a at LO, has little impact since $\frac{1}{ka} \ll 1$ for large k.

In this channel, χEFT$(\mathrm{p}\pi)_{\mathrm{UE}}$ appears to accomplish the goal of a self-consistent theory with pions in all of the Unitarity Window, up to its breakdown scale $\overline{\Lambda}_{\mathrm{NN}}$.

3.3 The Spin Triplet, Isospin Singlet: $^3S_1$ Phase Shifts

The result with Wigner-breaking OPE pieces at $\mathcal{O}(Q^1)$ (N^{2}LO) in fig. 4 is catastrophic, as FMS already noticed [68]. While NLO is by eye reasonable, N^{2}LO deviates dramatically from the PWA just above the OPE branch-point scale of $\frac{m_\pi}{2}$. This is the more puzzling as

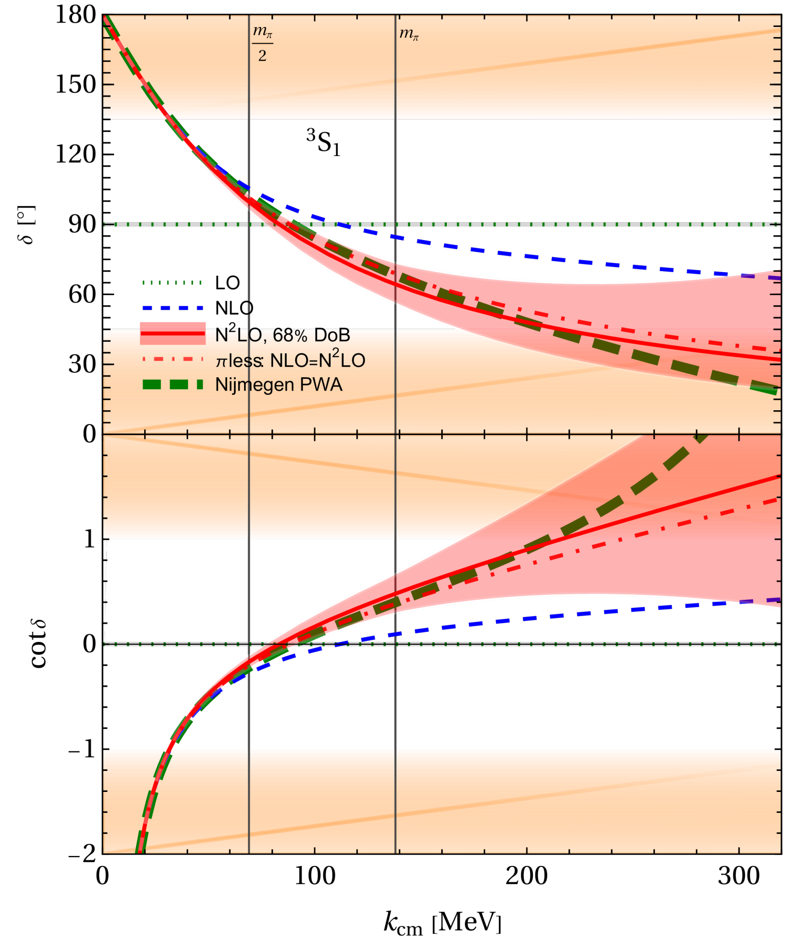

Figure 5: (Colour on-line) Phase shift (top) and $\cot\delta(k)$ (bottom) in the Wigner-symmetric $^3S_1$ channel, compared to the Nijmegen PWA [21] (thick green dashed). Details as in fig. 3.

EFT($\not\pi$) agrees well with the PWA even at $k \gtrsim 100$ MeV. With pions, the difference between NLO and N^{2}LO becomes around $k \approx m_\pi$ as large as between LO and NLO, and larger than the deviation from the PWA. Not even the sign of $\cot\delta$ is correct. The breakdown is hardly gradual but sudden, with no hint at NLO of the unnaturally large N^{2}LO curvature around 100 MeV. This is the more concerning as phase shifts are there nearly at the centre of the Unitarity Window. N^{2}LO pions have an outsized and wrong impact for $k \gtrsim 100$ MeV.

That most of the Unitarity Window is outside the radius of convergence and hardly extends beyond the scale $\frac{m_\pi}{2}$, is unsatisfactory for a "pionful theory".

What is the origin of the stark discrepancy of both convergence and reasonable range of applicability between the $^1S_0$ and $^3S_1$ channels? The former is exclusively Wigner-SU(4) invariant; the latter has a symmetry-breaking component which according to sect. 2.3.2 comes exclusively from the tensor (S $\to$ D $\to$ S) part of once-iterated OPE. Mindful of the importance of this symmetry around Unitarity discussed in the Introduction, fig. 5 shows the $^3S_1$ channel without the Wigner-SU(4) symmetry-breaking term of eq. (2.12).

The qualitative and quantitative improvement is obvious. Similar to $^1S_0$, the phase shift converges now order-by-order even as $k \to \overline{\Lambda}_{NN} \approx 300$ MeV just outside the Unitarity Window. The difference between N^{2}LO and PWA is wholly within the Bayesian 68% DoB band of app. B.1.4, even better than in the $^1S_0$ channel and quite a bit smaller than the shift from NLO to N^{2}LO. Since χEFT(pπ)$_{UE}$ at N^{2}LO and EFT($\not\pi$) at NLO=N^{2}LO are nearly indistinguishable, pionic degrees of freedom have again a minuscule impact beyond $k \gtrsim \frac{m_\pi}{2}$. Even before the much more robust discussion in sect. 3.5, one can thus place the empirical breakdown scale of χEFT(pπ)$_{UE}$ soundly around $k \gtrsim 250 \dots 300$ MeV, which aligns with the formal breakdown scale $\overline{\Lambda}_{NN}$ at which OPE needs to be iterated fully.

We conclude that the Wigner-SU(4) invariant version of χEFT(pπ)$_{UE}$ appears well-suited to overcome the formal inapplicability of EFT($\not\pi$) above the scale of the first branch point. In both the $^1S_0$ and $^3S_1$ channels, it is a self-consistent, convergent theory with pions in all of the Unitarity Window – and potentially somewhat beyond – with a common breakdown scale of $k \gtrsim 250$ MeV $\approx \overline{\Lambda}_{NN}$, plus good agreement with PWAs even at high momenta.

3.4 Wigner-SU(4) Symmetric vs. Breaking Amplitude in $^3S_1$

Why do versions with and without Wigner-SU(4) symmetry-breaking terms lead to such different results? We are unable to cast blame on any combination of terms in $A^{(S)}_{1\text{break}}(k)$, eq. (2.12) and thus turn to a low-energy expansion for further insight. In contradistinction to EFT($\not\pi$), the pionic contributions to all amplitudes in χEFT with Perturbative Pions lead to nonzero coefficients of the ERE, and hence to predictions of all shape parameters v_n in eq. (2.1); see eqs. (A.25), (A.26) and (A.27) in app. A.3. Cohen and Hansen [104–106] argued that PWA and FMS results are incompatible due to a "pattern of gross violation": The coefficients v_n in χEFT(pπ) follow the pattern of the naïve $v_n \sim m_\pi^{-2n+1} \sim r^{2n+1}$ *a-priori* estimate in χEFT and EFT($\not\pi$) but are by a factor of 5 to 10 larger than the PWA values, even after updates [24] to the latter. Their scales seem in the real world rather set by $\overline{\Lambda}_{NN}$ or an even higher scale. Interestingly, Thim recently showed that this issue does not exist when pions are included nonperturbatively and found instead very good agreement with phenomenology within respective uncertainties [107].

In χEFT(pπ)$_{UE}$, the phase shifts at NLO and N^{2}LO as well as EFT($\not\pi$) all describe the PWA analyses of both the $^1S_0$ and $^3S_1$ channel very well for $k \lesssim 70$ MeV, albeit $v_n \equiv 0$ in N^{2}LO EFT($\not\pi$); see figs. 3 to 5. We find a generic scaling as $v_n \sim \frac{1}{\overline{\Lambda}_{NN}^m}$ with $m-1$ the number of OPE iterations (entering at N^{m+1}LO), times combinations of powers of m_π, a, r obscured by both quite large and quite small numerical coefficients; see *e.g.* eqs. (A.25-A.27) in app. A.3. This suggests that the *string* of v_n predictions which is individually too large in χEFT, is highly correlated and produces *in toto* large cancellations between different v_n. Indeed, FMS [68] already saw that all pion contributions at N^{2}LO are for $k \to 0$ *non-analytic* in the quark mass (m_π^2) and can hence *never* be fully absorbed into higher-order χEFT LECs[6]; see app. A.3. Cancellations may be forced in some momentum window but will fail overall.

[6] We thank U. van Kolck to bring this to our attention.

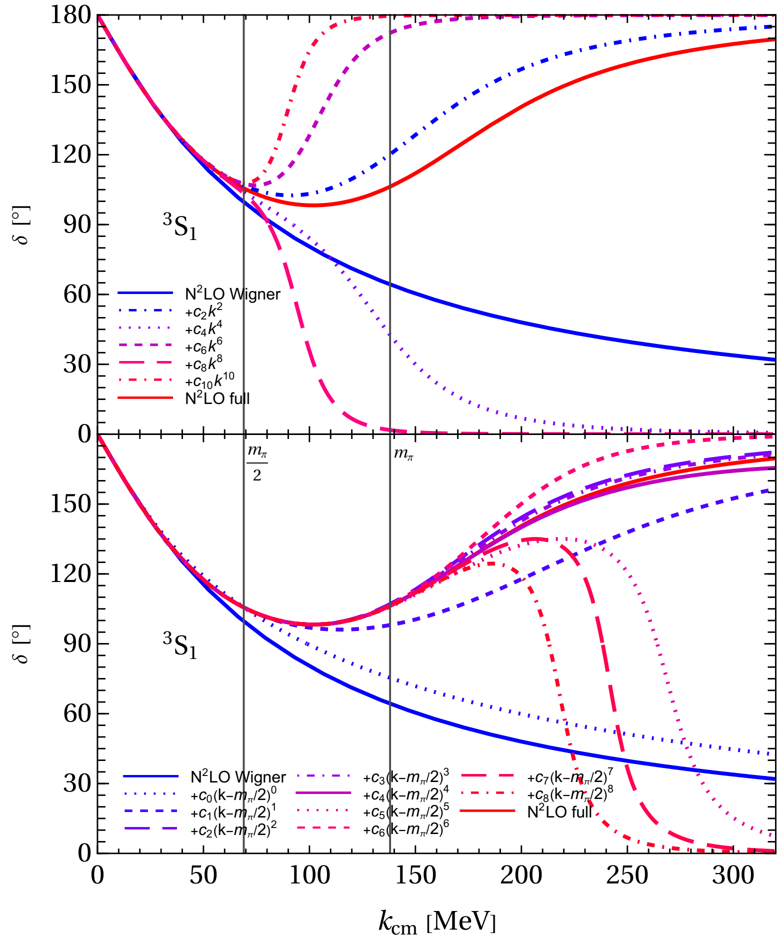

Figure 6: (Colour on-line) Interpolation between the Wigner-symmetric and full $^3\mathrm{S}_1$ phase shift as expansion in powers of k about $k = 0$ (top) and $\frac{m_\pi}{2}$ (bottom); see text for details.

This generalises easily: The low-momentum limit of χEFT with Perturbative Pions leads at odd orders Q^{2n-1} (N^{2n}LO) to non-analyticities because no contact term determined by an effective-range enters. This observation does not necessarily conflict with the χEFT power counting since, as discussed above, the contributions to *all* v_n are nonzero separately at *each* order of Q. The v_n may be vastly changing between orders, but their combined effect on the low-momentum phase shifts (observables) does not. Eventually, a CT at $\mathcal{O}(Q^{2n-2})$ (N^{2n-1}LO) can be used to exactly match v_n to the empirical value, eliminating the issue up to that order and ERE coefficient altogether. Still, the non-analyticities in m_π^2 will persist.

This can explain that the $^1\mathrm{S}_0$ and Wigner-symmetric $^3\mathrm{S}_1$ results agree with PWA despite discrepant predictions for the v_n, but is it also key to the breakdown of the Wigner-breaking version? When one expands the once-iterated, symmetry-breaking OPE of eq. (2.12) for $k \to 0$, the dominant part is $\propto k^4$ with a purely numerical coefficient of $0.2827\ldots$; eq. (A.27). That is about a factor 7 bigger than the corresponding symmetric coefficient $0.0408\ldots$ from eq. 2.9; see eq. (A.26). The next terms, $\propto k^6$ *etc.*, show a similar pattern. This could lead to subtle cancellations at low momenta which are overwhelmed at high k.

The top graph of fig. 6 compares therefore the full amplitude to one in which one adds an expansion of $A^{(\mathrm{S})}_{1\mathrm{break}}(k)$ up to $\mathcal{O}(k^{10})$ to the symmetric part, $A^{(\mathrm{S})}_{1\mathrm{sym}}(k)$. [The series proceeds in powers of k^2 since the ERE is analytic [83–86].] If this converges, then it should smoothly interpolate between the Wigner-symmetric and full result as powers of k^2 are added.

However, large coefficients are clearly not the issue. Just as before, the symmetry-breaking portion is very small for $k \lesssim \frac{m_\pi}{2}$, the scale of the OPE branch point. Above it, the expansion does not converge at all. Each new term is bigger and alternates sign.

We also expanded also around $\frac{m_\pi}{2}$, where all non-negative integer powers of k contribute. As discussed in sects. 2.3.5 and 2.3.6, contributions from this branch point appear at NLO and in both the symmetric and breaking terms of N^{2}LO. According to the lower plot in fig. 6, this series interpolates well between symmetric and full amplitudes. We find that the region of convergence extends, simply because the distance from the first branch point is increased up to $k \approx \frac{m_\pi}{2} + \frac{m_\pi}{\sqrt{2}} \approx 170$ MeV. Above that, convergence is asymptotic: the best, and indeed very good, approximation uses all terms up to and including k^4. We checked that Wigner-breaking terms with branch point at $k = \pm \mathrm{i}\, m_\pi$ alone do not explain the big differences. Rather, the issue seems in combining all symmetry-breaking terms.

3.5 Consistency, Robustness and Uncertainties

We now summarise detailed studies of robustness, consistency and theory truncation uncertainties which are relegated to the appendix. According to the "democratic principle", different but reasonable choices should agree up to higher-order corrections. In concert, these thus test to which degree various EFT assumptions are consistent with the outcomes. To encourage discussion [65], we disclose our choices and why we believe they are reasonable.

We start with *a-priori* estimates based on the idea that the expansion parameter Q of χEFT(pπ)$_{\mathrm{UE}}$ should be small enough so that OPE is perturbative (app. B.1.1) and one is in the Unitarity Window (app. B.1.2). We find that these are consistent with a "Lepage" analysis [108, chap. 2.3] [109] of *data-driven* convergence to PWA results (app. B.1.3), with *a-posteriori* order-by-order convergence via a simple Bayesian analysis of the convergence pattern (app. B.1.4) [100–102], and with *a-posteriori* comparison of different phase shift extractions, directly or via kcotδ inside the Unitarity Window (app. B.1.5). Since all focus on complementing aspects, their uncertainties should be combined, but it is not clear how, and how uncorrelated these approaches are.

Overall, all 5 findings are consistent with the more qualitative observations discussed with figs. 3 to 5: a breakdown scale of $\overline{\Lambda}_{\mathrm{NN}} \approx 300$ MeV; a lower bound of the Unitarity Window of $k_{\mathrm{low}} \lesssim 8$ MeV in $^1\mathrm{S}_0$ and 35 MeV in $^3\mathrm{S}_1$; and an expansion in Q as in eq. (2.4). The Bayesian uncertainty bands at N^{2}LO appear to be a good estimate of truncation errors at about the 68% degree-of-belief (DoB) level, possibly extending to slightly smaller phase shifts at given k. For these, we followed the BUQEYE collaboration to derive probability distributions and DoB intervals via the "max" criterion [99, sect. 4.4] with a simple choice of priors [100–102]: a uniform (flat) distribution for all known and unknown coefficients of the EFT expansion of an observable up to some (unknown but existing) maximum which follows a log-uniform distribution. Reasonable variations of the priors induce variations by $\lesssim 20\%$ in these posteriors [101]. For these priors, the 95% interval at N^{2}LO is about 2.7 times the 68% DoB, *i.e.* not twice like for a Gaußian distribution. The posteriors fall off much slower, namely with inverse powers. It may be of note that we exploit that it is natural in the Unitarity Expansion to set the scale by the Unitarity-ensuring factor $-\mathrm{i}k$ of the scattering amplitude, eq. (1.1)[7], and that uncertainties are constructed to vanish at the renormalisation point (where quasi-exact PWA values must be reproduced). We use the same Bayesian scheme for the uncertainty estimate of the pole parameters of table 1.

We caution that Bayesian uncertainty estimates of the factual convergence pattern of observables complement, but do not replace, conceptual arguments. If an expansion breaks down, for example because non-analyticities limit its radius of convergence, then an order-by-order assessment may be able to heuristically extend the range of applicability beyond that for some processes. But there is no reason why this should hold in all cases. If an EFT is not self-consistently renormalisable order-by-order, no statistical analysis can validate it.

All tests show a clear failure of the expansion when Wigner-breaking terms enter at N^{2}LO in $^3\mathrm{S}_1$, usually around $k \approx [100\ldots150]$ MeV.

We do not test insensitivity to varying the cutoff scale which probes momenta beyond the EFT's range; see *e.g.* [65, 110]. The amplitudes are analytical in the PDS scheme of dimensional regularisation [66, 67]. That choice eliminates any unphysical quantities.

Another assessment of EFT uncertainties varies the renormalisation point, *i.e.* the input determining LECs. Such alternatives add another "uncertainty band" and test the stability of observables, expansion parameter and breakdown scale: The Callan-Symanzik renormalisation group equation's variation of the renormalisation condition needs to be fulfilled up to higher-orders in the EFT expansion, wherever the EFT converges. In χEFT, a preferred "Goldilocks corridor" $k_{\mathrm{fit}} \sim p_{\mathrm{typ}} \sim m_\pi$ captures the Physics at the scales the EFT is designed for and helps avoid potential fine-tuning of coefficients between different orders.

So far, we used $k_{\mathrm{fit}} = 0$ because that is the natural scale at Unitarity. In app. B.2, we add studies with the parameters determined at points inside the Unitarity Window which are natural in χEFT(pπ)$_{\mathrm{UE}}$: the pole position of the amplitude, or at $k_{\mathrm{fit}} = \frac{m_\pi}{2}$, or at m_π, as the branch-point scales of non- and once-iterated OPE. That $\frac{m_\pi}{2}$ is also in the region where both $^1\mathrm{S}_0$ and $^3\mathrm{S}_1$ are closest to Unitarity ($\delta \approx \frac{\pi}{2}$), makes it conceptually attractive. Remember that χEFT(pπ)$_{\mathrm{UE}}$ is constructed to explore precisely this very region $p_{\mathrm{typ}} \sim m_\pi$ around Unitarity. We find that these reasonable choices of renormalisation points at N^{2}LO do not lead to statistically significant changes of phase shifts or empirical breakdown scales.

3.6 Partial-Wave Mixing

As discussed in sect. 2.3.2, tensor OPE induces $^3\mathrm{SD}_1$ mixing in the original Wigner supermultiplet $^1\mathrm{S}_0$-$^3\mathrm{S}_1$. What is its impact of Unitarity, and to which extent are such Wigner-breaking terms demoted? Both mixing angle ε and $^3\mathrm{D}_1$-wave phase shift δ_2 are small, but

[7]We thank D. R. Phillips for this suggestion.

χEFT has no satisfactory explanation. By imposing Wigner-SU(4) symmetry at N^{2}LO, the mixing angle and D wave are nonzero at most as early as $\mathcal{O}(Q^2)$ (N^{3}LO), so $\varepsilon, \delta_2 = 0 + \mathcal{O}(Q^2)$. With $Q \sim 0.5$ at $k \approx m_\pi$ or so and LO being $\mathcal{O}(Q^{-1})$, their natural magnitude can *a priori* be estimated as $(0.5)^3 \lesssim 10°$. The actual values are $\varepsilon(m_\pi) \approx 2°$ ($\varepsilon(2m_\pi) \approx 3°$), $\delta_2(m_\pi) \approx -5°$ ($-15°$). This is markedly smaller, but not entirely incompatible with what is only intended as a rough estimate. It might therefore indicate that V_T enters only at even higher orders. The Unitarity Expansion might thus naturally explain why both the ^{3}SD$_1$ mixing angle and ^{3}D$_1$ wave phase shift are so small. First results are given in refs. [77, 82], and more are forthcoming [95].

4 Interpretation

While we focused so far to establish facts, we now discuss ideas to which these may lead.

4.1 Inferences and Conjecture

In sects. 3.3 and 3.4, we presented evidence that χEFT(pπ)$_{\text{UE}}$ converges quite well in the ^{1}S$_0$ and ^{3}S$_1$ channels at N^{2}LO both order-by-order and to the PWA only if the tensor/Wigner-breaking effects of once-iterated OPE are demoted to N^{3}LO or higher. Traditional chiral power counting for perturbative pions adds them at N^{2}LO, but such phase shifts fail for $k \gtrsim 100$ MeV. Indeed, it has been argued that the breakdown of χEFT with Perturbative Pions occurs at momenta so low that the tensor interaction is simply irrelevant [30, 31]. This is unsatisfactory since ^{3}S$_1$ is there actually close to Unitarity, $\delta(^3\text{S}_1, k \approx 100\text{ MeV}) \approx 85°$. That would be the failure of a description which wants to merge Unitarity and chiral Physics in all of the Unitarity Window. We therefore propose an alternative idea:

> **Conjecture:** The symmetries of the Unitarity Limit are broken weakly in Nuclear Physics. Their footprint shows *persistence*, *i.e.* their impact dominates observables at momentum scales $p_{\text{typ}} \sim m_\pi$ and beyond, and is there more relevant than chiral symmetry. In particular, the tensor/Wigner-SU(4) symmetry-breaking part of one-pion exchange in the NN ^{3}S$_1$ channel is super-perturbative, *i.e.* does not enter before N^{3}LO.

Our study considered only the Wigner-doublet ^{1}S$_0$-^{3}S$_1$ channels since only their phase shifts are well inside the Unitarity Window. We did not address at which order the tensor/Wigner-SU(4) breaking part of one-pion exchange (OPE) enters – except that it is at least N^{3}LO.

This Conjecture is a first step to convert the emergent phenomena of what appear to be accidental/hidden conformal and Wigner-SU(4) symmetries into manifest but weakly broken symmetries in the χEFT Lagrangean itself. Demoting interactions based on renormalisation-group arguments is less familiar than promoting. However, it is expected when one fails to impose symmetries on an EFT but data fits find symmetry-breaking LECs which appear anomalously small, or even zero if the symmetry is exact. For example, QED with different couplings for left- and right-handed electrons would display what one could call an emergent symmetry because the parity-violating interactions are (nearly) zero – and that becomes manifest by postulating that the QED Lagrangean must be parity-conserving.

The Conjecture provides context to the long list of studies which see Wigner-SU(4) symmetry manifest itself both with and without pionic degrees of freedom in essential nuclear interactions, potentials, binding and matrix elements well into the heavy-element region [38–46, 50–61]. It adds that the symmetry is not isolated or accidental but a natural consequence of its exact and unavoidable realisation at the Unitarity Fixed Point; see next subsection.

If the Conjecture is to be successful, then one must find a systematic expansion guided by Wigner-SU(4) symmetry and Unitarity. Like any ordering scheme, it must, *before* the computation, provide reliable, semi-quantitative assessments which Wigner-breaking pion interactions to include at a given order. Ordinarily, correlated two-pion exchange starts for KSW pions at N^{4}LO and has both Wigner-symmetric and breaking pieces. Are the latter demoted? The power counting should also illuminate at which momenta either Wigner-SU(4) symmetry or chiral symmetry dominates. Preferably, it will also differentiate the Unitarity Window from Born Corridors, *e.g.* by being small in one but large in the other. Before considering two candidates: quantum-mechanical operator entanglement (sect. 4.3), and QCD's large-N_C limit (sect. 4.4), we discuss the neighbourhood of the fixed point.

4.2 Universality and Chiral Symmetry Close to the Fixed Point

Central to the Conjecture is that it breaks chiral symmetry at N^{2}LO, resolving the conflict of symmetries in favour of Unitarity. However, that the pion's central and tensor interactions in few-nucleon systems enter at the same chiral order and with the same strength, is a direct consequence of its derivative coupling to the nucleon spin, rooted in chiral symmetry. The Goldstone mechanism converting global chiral symmetry into local, weakly interacting field excitations may eventually be too strong to overcome and lead to the Conjecture' downfall. Why is this violation not that important?

The renormalisation group around the Unitarity fixed point (FP) in the two- and few-nucleon sector may provide some insight; see fig. 7. The FP is non-Gaußian (LO is nonperturbative) and displays conformal invariance. In Nuclear Physics, its universality class is

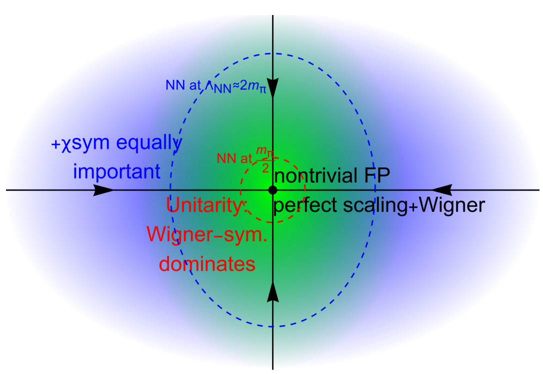

Figure 7: (Colour on-line) Illustration of symmetry-stacking around the Unitarity FP.

defined by adding invariance under Wigner-SU(4) transformations, so all such theories must agree at Unitarity. One of these is EFT($\not\pi$), the EFT to which χEFT reduces very close to the FP (very low momenta). As chiral symmetry is unknown in EFT($\not\pi$), it is subdominant in the immediate vicinity of the FP; Wigner-SU(4) symmetry and its weak breaking dominate. If this were incorrect, then χEFT would belong to a different universality class than EFT($\not\pi$). In this scenario, the Unitarity FP protects Wigner-SU(4) symmetry to be only broken weakly, while chiral symmetry in the few-nucleon sector has no such strong protection, simply because it is not a characteristic symmetry of the FP. This allows for the possibility that chiral symmetry is broken and the Wigner-breaking tensor part V_T is consequently suppressed. That Wigner symmetry (but not chiral symmetry) characterises the FP is now particularly powerful. It virtually guarantees that it survives renormalisation as long as the renormalisation scheme itself respects the FP symmetries. Farther away from the FP, chiral symmetry may then become as important as Wigner-SU(4) symmetry, and eventually dominate for large enough momenta – mandating similar strengths for the OPE's tensor and central pieces. The scale $\overline{\Lambda}_{\rm NN}$ at which OPE becomes nonperturbative is an obvious candidate for this inversion. Since the zero- and one-nucleon sectors of χEFT are perturbative, *i.e.* the projection of the FP onto these is Gaußian, their chiral counting is unaffected. The argument is not implausible but needs to be studied quantitatively.

4.3 Unitarity, Wigner-SU(4) Symmetry and Entanglement

Beane *et al.* (BKKS) [111] pointed to a link between entanglement suppression and Wigner-SU(4) symmetry, which in turn extends to an SU(16) symmetry for three quark flavours that had first been discovered in lattice computations [112]; see also [113–117] for discussions and relations to S-matrix properties[8]. In Quantum Information Theory, entanglement aims to quantify the extent to which a state is "non-classical" at its core. It asks about the a-causal/ethereal influence of measuring quantum numbers of one particle on others at mutually space-like separated points ("QM non-locality"). If the total state of the system is a tensor product of isolated particles, then the system is quasi-classical and its entanglement is zero. If measuring one particle instantaneously and uniquely defines the quantum states of all others ("total collapse of the wave function at a distance"), then entanglement is maximal and the system is fundamentally quantum-mechanical. The most famous example of the latter is given in the Einstein-Podolsky-Rosen Gedankenexperiment [118], inspiring both Bell's inequality [119] and his comparison to Bertlmann's socks [120]. Entanglement (or entangling) power, in turn, is the extent to which an operator is a direct product of single-particle operators. So, entanglement power is the capacity of an operator to create entanglement, namely the average entanglement of final states an operator generates from a set of initial product (un-entangled) states drawn with some given probability distribution [121]. An operator which is a direct product has zero entanglement power. Like entanglement, entanglement power is nonlinear. An operator can map product states into product states (zero entanglement power) and yet itself not contain any direct

[8]We thank one referee and M. Savage for encouraging us to study this point, and N. Klco for pointing out our initial misconceptions.

product (maximal entanglement). The SW_σ operator discussed momentarily is an example. However, a generally-agreed operator-entanglement measure does not yet seem to exist.

In the NN system, the operator of interest is the scattering matrix. As we wish to explore relations between Wigner-SU(4) symmetry and entanglement inside the Unitarity Window, we consider the ${}^1\mathrm{S}_0$-${}^3\mathrm{S}_1$ system only but are aware of Miller's critique that higher partial waves are not negligible at higher momenta [117]. The S matrix is then

$$S = \begin{pmatrix} \mathrm{e}^{2\mathrm{i}\delta[{}^3\mathrm{S}_1]} & 0 \\ 0 & \mathrm{e}^{2\mathrm{i}\delta[{}^1\mathrm{S}_0]} \end{pmatrix} = \mathrm{e}^{2\mathrm{i}\delta[{}^3\mathrm{S}_1]}\; P[{}^3\mathrm{S}_1] + \mathrm{e}^{2\mathrm{i}\delta[{}^1\mathrm{S}_0]}\; P[{}^1\mathrm{S}_0] \;\; . \tag{4.1}$$

The partial-wave projectors P lead to the "SWAP" operator $\mathrm{SW}_\sigma := \frac{1}{2}\,(\mathbb{1}+\vec{\sigma}_1\cdot\vec{\sigma}_2)$ [115, 116]. As it interchanges the spins of nucleon 1 and 2, it has eigenvalue $+1$ for the spin-symmetric (${}^3\mathrm{S}_1$) state, and -1 for the spin-antisymmetric (${}^1\mathrm{S}_0$). Introducing the average and difference of the two phase shifts as $\Sigma := \frac{1}{2}(\delta[{}^3\mathrm{S}_1] + \delta[{}^1\mathrm{S}_0])$ and $\Delta := \delta[{}^3\mathrm{S}_1] - \delta[{}^1\mathrm{S}_0]$, one finds

$$S = \mathrm{e}^{2\mathrm{i}\Sigma}\Big[\mathbb{1}\;\cos\Delta + \mathrm{i}\;\mathrm{SW}_\sigma\;\sin\Delta\Big] \tag{4.2}$$

One can now study the OPE contribution to entanglement. The operator of the central (Wigner-symmetric) term is $(\vec{\sigma}_1\cdot\vec{\sigma}_2)(\vec{\tau}_1\cdot\vec{\tau}_2) = -3\,\mathbb{1}$ in both channels and hence impacts only the $\mathbb{1}$ part of the S matrix. On the other hand, iterations of the Wigner-breaking tensor term $[3\,(\vec{\sigma}_1\cdot\vec{e}_q)\,(\vec{\sigma}_2\cdot\vec{e}_q) - (\vec{\sigma}_1\cdot\vec{\sigma}_2)]\,(\vec{\tau}_1\cdot\vec{\tau}_2)$ are zero in ${}^1\mathrm{S}_0$ but nonzero in ${}^3\mathrm{S}_1$, and hence differentiate between the SW_σ and $\mathbb{1}$ terms, and they mix Wigner super-multiplets of different l. Therefore, they do entangle spins (and isospins) quite differently between ${}^1\mathrm{S}_0$ and ${}^3\mathrm{S}_1$, leading to a phase-shift difference Δ. To quantify that, one needs to find their impact on entanglement.

BKKS defined an operator's entanglement power[9] as a state-independent average over initial direct-product (un-entangled) states which vanishes when out-states remain such a tensor product, using the second Rényi entropy of the one-particle density matrix:

$$\mathcal{E}_{\mathrm{BKKS}}(\Sigma,\Delta) := \frac{\sin^2 2\Delta}{6} \in [0;\frac{1}{6}] \tag{4.3}$$

Based on the binary von Neumann entropy of overlaps to Bell states of spin-$\frac{1}{2}$ particles [113],

$$H[f(\Sigma,\Delta)] := -x\;\ln x - (1-x)\ln(1-x) \in [0;\ln 2] \quad \text{with } x := \frac{1+\sqrt{f(\Sigma,\Delta)}}{2} \quad , \tag{4.4}$$

Miller [117] proposed a different measure[10]:

$$\mathcal{E}_{\mathrm{Miller}}(\Sigma,\Delta) := H[\frac{\cos^2\Delta\,(\cos\Delta - \cos 2\Sigma)^2}{(1-\cos\Delta\;\cos 2\Sigma)^2}] \;\; . \tag{4.5}$$

[9]According to Klco [122], this is strictly speaking the "local purity", related to entanglement power.

[10]We thank G. Miller for pointing out the typographical error that the denominator of eq. (19) in ref. [117] should be squared.

To isolate the effect of SW_σ from that of $\mathbb{1}$, one may also define a third criterion, an *entanglement strength/nonlocality* of the S matrix as magnitude-square of the coefficient of SW_σ, relative to the total S-matrix strength, $\cos^2\Delta + \sin^2\Delta = 1$. This concept is meaningful as S, $\mathbb{1}$ and SW_σ all have eigenvalues of magnitude one. To some degree, it measures the nonlocality of the operator S, and hence its potential to entangle. It thus sits between between the *entanglement* of an operator, *i.e.* the degree to which it can be written as product, and its *entanglement power*, *i.e.* the degree to which it entangles initial product states. The former is zero for $\mathbb{1}$ but maximal for SW_σ, while the latter is zero for both (mapping product states into product states). Only their combination has nonzero entanglement power, *i.e.* maps product states into entangled states, and only because the SW_σ operator is nonlocal as it cannot be written as product state (while $\mathbb{1}$ is obviously not). One then converts that to a binary entanglement entropy using eq. (4.4)[11]:

$$\mathcal{S}(\Delta) := H[\sin^2\Delta] \tag{4.6}$$

This definition does not depend on the mean phase shift, only on the difference. It serves as *relative, simplistic and ad-hoc* measure if one thinks of $\mathbb{1}$ as not adding entanglement to the incident, already fully-entangled ${}^1\mathrm{S}_0$ and ${}^3\mathrm{S}_1$ states. No "additional" entanglement enters in the Wigner-SU(4) symmetric case, $\mathcal{S}(\Delta = 0) = 0$. On the other hand, for a phase-shift difference of 90°, $S(\Delta = \frac{\pi}{2}) = \mathrm{i}\,\mathrm{e}^{2\mathrm{i}\Sigma}\,\mathrm{SW}_\sigma = \pm\mathrm{i}\,\mathrm{e}^{2\mathrm{i}\Sigma} \propto \mathrm{SW}_\sigma$ is maximally nonlocal, with upper (lower) sign for the spin-symmetric (antisymmetric) channel, ${}^3\mathrm{S}_1$ (${}^1\mathrm{S}_0$). The spin wave functions of the final state continue then to be maximally entangled, just like the initial ones. Both become eigenstates to the S matrix, and $\mathcal{S}(\Delta = \frac{\pi}{2}) = \ln 2$ is maximal.

Like $\mathcal{E}_{\mathrm{BKKS}}$ and unlike $\mathcal{E}_{\mathrm{Miller}}$, the relative measure $\mathcal{S}$ does not depend on the mean, Σ. However, it is like $\mathcal{E}_{\mathrm{Miller}}$ maximal for $\Delta = (2n+1)\frac{\pi}{2}$ and zero for $\Delta = n\frac{\pi}{2}$ ($n \in \mathbb{Z}$), while $\mathcal{E}_{\mathrm{BKKS}}$ depends on 2Δ and hence assigns zero where both $\mathcal{E}_{\mathrm{Miller}}$ and $\mathcal{S}$ predict a maximal measure of entanglement. Conversely, $\mathcal{E}_{\mathrm{BKKS}}$ ascribes maximal entanglement power to $\Delta = (2n+1)\frac{\pi}{4}$, where neither $\mathcal{S} \approx 0.41\ldots$ nor $\mathcal{E}_{\mathrm{Miller}}$ are maximal. Miller's and the *ad-hoc* definition agree for $\Sigma = \pm\frac{\pi}{4}$, *i.e.* at the brink of the Unitarity Window.

We do not attempt to resolve the discrepancies between these measures for operator entanglement. Neither do we account for the fact that each initial state ${}^1\mathrm{S}_0$ and ${}^3\mathrm{S}_1$ on which the S matrix acts is separately already maximally entangled and thus not a product state. Hence, the standard ideas described above of measuring entanglement power by applying the operator to product states might not quite apply to the NN states themselves. Rather, we study the degree of entanglement each measure assigns to the S-wave phase shift operator. Each reports zero entanglement for both Unitarity and perfect Wigner-SU(4) symmetry ($\Delta = 0$). If that drives indeed tensor-OPE suppression in the real-world Unitarity Window, some measure of entanglement should be so small there as to serve as an efficient expansion parameter. Ideally, it should be large(r) in the Born Corridors where the Unitarity Expansion fails by design.

Figure 8 uses the Nijmegen PWA for results of each variant (top, normalised to its respective maximum) and the corresponding phase shifts with their average Σ and difference

[11] $\sin^2\Delta$ without eq. (4.4) falls off slightly faster than $\mathcal{S}$, with no marked change of the analysis below.

Δ (bottom). Results for N^{2}LO χEFT(pπ)$_{\rm UE}$ are very similar since the ^{1}S$_0$ and ^{3}S$_1$ phase shifts agree very well with their PWA counterparts. The BKKS entanglement power is maximal well inside the Unitarity Window, namely at $\Delta(k \approx 63.7\text{ MeV}) = \frac{\pi}{4}$, and there always $\gtrsim 0.4$. It drops further in the high-momentum Born Corridor and thus shows no correlation between its size and the Unitarity Window. It does not provide a likely expansion parameter. On the other hand, both Miller's and the *ad-hoc* version are maximal just outside the lower end of the Window, $\Delta(k \approx 19.4\text{ MeV}) = \frac{\pi}{2}$. Both decrease monotonically inside, with $\mathcal{E}_{\rm Miller} \approx 0.4$ ($\mathcal{S} \approx 0.35$) in its centre ($k \approx 100$ MeV) and $\mathcal{E}_{\rm Miller} \approx 0.3$ ($\mathcal{S} \approx 0.17$) at its upper end. Miller's version increases again for $k \geq 200$ MeV, hinting indeed that entanglement thus defined may be characteristic exclusively of the Unitarity Window, and

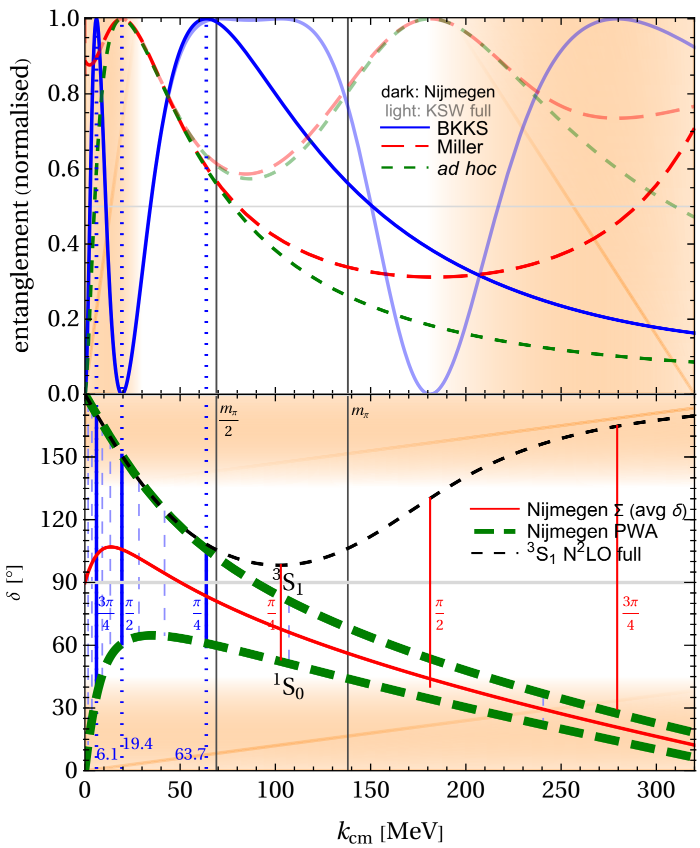

Figure 8: (Colour on-line) Top: Entanglement measures of the phase shifts in the ^{1}S$_0$-^{3}S$_1$ system in the BKKS (blue solid), Miller (red long-dashed) and *ad-hoc* measure (green short-dashed), each normalised to its maximum. Darker lines: Nijmegen PWA; lighter: N^{2}LO with Wigner-breaking terms. Bottom: Nijmegen PWA phase shifts (green thick dashed) and their mean Σ (red solid); the difference Δ is the width of the corridor between the ^{3}S$_1$ and ^{1}S$_0$ phase shifts, with blue lines every $\frac{\pi}{12} = 15°$, and k shown at multiples of $\frac{\pi}{4} = 45°$. Black dashed: ^{3}S$_1$ at N^{2}LO with Wigner-breaking; red vertical lines above $k = m_\pi$: N^{2}LO ^{3}S$_1$-^{1}S$_0$ difference at multiples of $\frac{\pi}{4} = 45°$. Born Corridors and Unitarity Window as before.

not of the Born Corridors. The *ad-hoc* measure may provide a smaller, and hence better-converging, expansion parameter, but it simply continues to decrease in the Born Corridor, potentially indicating little correlation with the Unitarity Window.

The top panel also contains in lighter colours the entanglement measures for χEFT(pπ)$_{\mathrm{UE}}$ at N^{2}LO when the Wigner-breaking terms in ^{3}S$_1$ are added, and on the bottom its ^{3}S$_1$ phase shift with markers where its difference to N^{2}LO ^{1}S$_0$ is a multiple of 45°. All entanglement measures follow in that case that of the Nijmegen PWA up to about 70 MeV, where PWA and N^{2}LO phase shifts start to disagree. The BKKS variant is then near-constant and saturated in the centre of the Unitarity Window, with a rapid dip to zero entanglement at its upper border, followed by another rapid rise inside the Born Corridor to the maximum. Miller's and the *ad-hoc* version are ≥ 0.6 everywhere and rapidly rise at the boundary. All variants agree that the Wigner-breaking part of OPE causes large entanglement inside the Unitarity Window. This may indicate that V_T lifts indeed the entanglement suppression of the Unitarity Limit and its Wigner-SU(4) symmetry.

In conclusion, while there is a clear link between entanglement, Wigner-SU(4) symmetry and the Unitarity Limit itself, the situation is rather muddy in the real world where symmetries are not exact, phase-shift differences not tiny, and measures of entanglement (power) not that small inside the Unitarity Window. None of the definitions provides a clear path to quantifying Wigner-symmetry and its breaking inside the Unitarity Window. It is also a major deficiency that we found each entanglement measure only by actually computing the phase shifts both with and without tensor-OPE. Without an *a-priori* assessment of the relative entanglement measure of the V_C and V_T operators, entanglement as a concept is useless for power-counting – at least for now. These findings clearly need further study.

4.4 Unitarity, Wigner-SU(4) Symmetry and Large-N_c

In contradistinction and returning to a point raised in the Introduction, the typical sizes of contributions can be estimated in the large-N_C expansion of QCD. Recently, Richardson *et al.* studied the relation between large-N_C, Unitarity and entanglement in two-baryon systems with $\Delta(1232)$ and strangeness [123]. The Unitarity Expansion may actually resolve apparent conflict between large-N_C and Wigner symmetry. In large-N_C, the leading non-tensor part of the NN interaction is automatically Wigner-SU(4) symmetric in partial waves with even orbital angular momentum [43, 44]. However, this only holds if the tensor/Wigner-breaking interaction is neglected altogether, and does not apply to odd partial waves (to which the Unitarity Expansion does not apply). And yet, that Wigner symmetry is only weakly broken contradicts the large-N_C finding that tensor (Wigner-breaking) NN interactions should be leading contributions. Calle Cordón and Ruiz Arriola concisely summarised this quandary and proposed as solution that Wigner symmetry is largely intact in intermediate- and long-range tensor OPE, but strongly broken at short distances [45].

We, too, see evidence for such a splitting. Recall from sect. 2.3.5 that the "pion contribution" is actually only the pionic long-distance (non-analytic) part in the chosen renormalisation scheme and condition. By fitting to a and r, Wigner-breaking at low momenta is locked into the short-distance Counter Terms. At very low momenta, that guarantees vanishing pion contributions and thus good agreement with EFT($\not\pi$) and PWAs. By the Uncertainty Principle $\Delta x \Delta p \geq \frac{\hbar}{2}$, this is associated with very large distance scales (very poor resolution) over which the potential is averaged. As resolution increases, more detailed structures in the potential are probed. While we found that the Wigner-breaking (tensor) interaction is insignificant at low momenta (long range/averaged over large distance scales), it becomes strong in $^3\mathrm{S}_1$ as $k \gtrsim 80$ MeV, namely when structures $\delta x \sim 2$ fm are resolved which should be classified as "short" in a theory with perturbative pions. We saw that this leads to unacceptable convergence problems. We hence discard again the offending term by invoking that the Unitarity Expansion's Wigner symmetry is broken weakly.

In this interpretation, the large-N_C argument of dominant tensor interaction only holds if its leading coefficient is of natural size. We propose that an additional symmetry not accounted for by only applying large-N_C is imposed, namely Wigner-SU(4) close to the Unitarity FP. This forces the coefficient to be zero, resolving the apparent conflict. By the argument of sect. 4.2, this exact zero survives renormalisation because Wigner's is a FP symmetry. Clearly, this mechanism is as of yet mere speculation.

In our approach, imposing Wigner symmetry as principle is only legitimate when phase shifts are close to the Unitarity FP, *i.e.* for S waves only. Therefore, no contradiction exists between Wigner symmetry and large-N_C for any higher partial waves, simply because a Wigner symmetry borne out of the Unitarity Limit does not apply there. This also cures the problem that this symmetry is realised at best extremely poorly for $l \geq 1$ [45].

5 Conclusions

5.1 Summary

We formulated an EFT with pionic degrees of freedom and a natural expansion scheme about Unitarity in the $^1\mathrm{S}_0$ and $^3\mathrm{SD}_1$ channels of the NN system: Chiral Effective Field Theory with Perturbative/"KSW" Pions in the Unitarity Expansion (χEFT(pπ)$_{\mathrm{UE}}$). Its analytic next-to-next-to leading order (N^{2}LO) amplitudes are given in sect. 2.3. We interpreted and contextualised the results of sect. 3 in sect. 4, leading to the Conjecture of the Introduction. It resolves for $k \gtrsim m_\pi$ the apparent conflict of conformal and Wigner-SU(4) symmetries around Unitarity with χEFT's chiral symmetry dictated by the Goldstone mechanism, in favour of the symmetries of the nontrivial fixed point. We reiterate that in the NN system, it only applies to the S waves as only their phase shifts are close to Unitarity.

In this formulation, LO is Unitarity itself, *i.e.* the nontrivial fixed point (FP) of the renormalisation group flow. Its only scale is the relative momentum k, and its natural renormalisation scale/fit point for Low-Energy Coefficients (LECs) is the momentum $k_{\mathrm{fit}} = 0$ at which no scale exists. Around Unitarity (kcot$\delta = 0$, $\delta = \frac{\pi}{2}$) lies the Unitarity Window of momenta roughly in the régime 35 MeV $\lesssim k \lesssim$ 200 MeV with phase shifts $45^\circ \lesssim \delta(k) \lesssim 135^\circ$ ($|\cot\delta| \lesssim 1$). In the NN system, it is only relevant for S-waves, but these dominate many low-energy properties of nuclei. Unitarity implies Universality: Details of the interactions are less important than that their impact is so big as to saturate the bounds set by probability conservation. What separates different universality classes is the symmetries imposed at

Unitarity. Besides nonrelativistic conformal invariance (which is automatic at the FP), that is Wigner's combined SU(4) spin-isospin transformations acting on nucleons. Indeed, we find in sects. 3.2 and 3.3 that χEFT(pπ)$_{\text{UE}}$ is in this window very close to "pionless" EFT – explicit pionic degrees of freedom appear to be of little consequence.

This observation nicely aligns with the viewpoint of Information Theory; *cf.* the Introduction: The high degree of symmetry at Unitarity implies that an anomalously large scattering length is important, but not its precise value. In χEFT(pπ)$_{\text{UE}}$, that value is indeed demoted: Its impact is only comparable to that of interaction details parametrised by the effective range and non-iterated OPE. These enter at NLO and are suppressed by $Q \approx 0.5$ relative to LO. The once-iterated central part of OPE is the only information which enters one order in Q higher still, with $\approx 25\%$ relevance, but is completely determined by short-range information (*i.e.* LECs) set already at NLO. Tensor OPE is relegated to higher orders. All this emphasises a central EFT promise to optimally encode the unresolved short-distance information: The high degree of symmetry at Unitarity leads to a better-optimised compression, namely to a reduction of the number and relative importance of independent LECs which encode the information in NN scattering at a given accuracy. Important is that both EFT($\not\pi$) and χEFT(pπ)$_{\text{UE}}$ classify as most relevant the mere existence of anomalously small intrinsic scales, not how their different explicit degrees of freedoms produce them. Unitarity makes their results agree very well – the rest is detail.

In χEFT(pπ)$_{\text{UE}}$, both Wigner-SU(4) and conformal invariance are weakly broken in a systematic expansion in small, dimensionless parameters: $Q \sim \frac{1}{ak} \lesssim 1$ defines the lower bound of the Unitarity Window; and $Q \sim \frac{p_{\text{typ}}}{\overline{\Lambda}_{\text{NN}}} \lesssim 1$ the upper one of a chiral expansion, with $p_{\text{typ}} \sim k, m_\pi$ typical low-momentum scales. We find that χEFT(pπ)$_{\text{UE}}$ at N^{2}LO describes the Physics inside the Unitarity Window which includes pionic degrees of freedom and is both conceptually fully consistent and convergent. Comparison to pole parameters (sect. 3.1) and Partial Wave Analyses (PWAs; sects. 3.2 and 3.3), assessments of theory uncertainties (sect. 3.5) including a Bayesian analysis of order-by-order convergence and variations of extraction methods and of the renormalisation point (app. B.2), all show that the expansion parameter is consistent with the above *a-priori* estimates, and that its empirical breakdown scale is consistent with $\overline{\Lambda}_{\text{NN}} = \frac{16\pi f_\pi^2}{g_A^2 M} \approx 300$ MeV. This is the scale where χEFT with Perturbative Pions is expected to become inapplicable because iterations of OPE are not suppressed. Thus, χEFT(pπ)$_{\text{UE}}$ appears to also apply somewhat into the Born Corridor $|\cot\delta| \gtrsim 1$. That is not surprising as the perturbative (Born) approximation for $\cot\delta \gtrsim 1$ and χEFT(pπ)$_{\text{UE}}$ for $\cot\delta \lesssim 1$ must match in the transition region, $\cot\delta \approx 1$. In contradistinction to the Unitarity Expansion in EFT($\not\pi$), χEFT(pπ)$_{\text{UE}}$ naturally embeds the scales $\frac{m_\pi}{2}$ and m_π associated with the branch points of non- and once-iterated OPE.

Thus, the following picture at nuclear scales might emerge. The NN S waves are treated in perturbation about Unitarity with suppressed tensor-OPE in χEFT– and for some processes even in EFT($\not\pi$). Either version considerably reduces computational complexity without loss of information in the momentum region most relevant for low-energy nuclear systems. The S waves set the dominant patterns of nuclear systems, while the other partial waves are of course relevant for more detailed and complex phenomena. High partial waves are treated in Born approximation (with perturbative OPE) [28–31]; and intermediate partial waves (likely some P and possibly D waves) may need resumming an infinite number of interactions at LO, including potentially all of OPE, but not about Unitarity [25–27, 30, 31]. Such a three-pronged approach is computationally much less intensive than the traditional one of a nonperturbative LO OPE potential with a high number of partial waves.

5.2 Outlook

Further studies are clearly warranted. If the Conjecture of sect. 4.1 is to be successful, then a systematic expansion guided by Wigner-SU(4) symmetry and Unitarity must be found. Such an ordering scheme must provide an *a-priori* classification of the relative importance of Wigner-symmetric and breaking contributions induced by chiral symmetry. It might also differentiate between Unitarity Window and Born Corridors, and illuminate at which distances from the FP Wigner and chiral symmetry dominate, respectively (sect. 4.2). We discussed two candidates, both somewhat problematic: quantum-mechanical operator entanglement (sect. 4.3), and QCD's large-N_C limit (sect. 4.4).

The Conjecture should also be tested in systems with at least 3 nucleons and with external probes. The extant NLO work in χEFT with Perturbative Pions in 2N and 3N systems with external probes of *e.g.* [92, 96, 124–127] can be expanded about Unitarity and extended by at least one order. While we see that EFT($\not\pi$) and χEFT$(\mathrm{p}\pi)_{\mathrm{UE}}$ agree in scattering even at higher momenta, external probes most likely differentiate the two even at quite low energies, *e.g.* in Compton scattering [99, sect. 5.4.1]. Because of the issues with chiral symmetry, pion photoproduction and pion scattering may be of particular interest. All these are well-known to reveal the considerable strength of pion-exchange currents. Fortunately, computations become actually simpler in the Unitarity Expansion, as seen by comparing our N^{2}LO amplitudes to those for $\frac{1}{a} \neq 0$ at the same order [68, 69, 76].

Finally, the Unitarity Expansion for NN S-waves system should also be explored in the χEFT version in which pions are nonperturbative. First LO results are in preparation [128] and reported in [80–82, 129, 130]. Both for perturbative and nonperturbative pions, further clarifications are needed. Can imposing a preference for Unitarity as a highly symmetric state about which to expand provide a quantitative answer to the questions of the Introduction: Why is fine-tuning preferred? How does varying m_π affect it?

We see our Conjecture merely as a first step to merge two highly successful but at first glance incompatible concepts of Nuclear Theory, namely the expansion about Unitarity and χEFT, for mutual benefit and a better understanding of why fine-tuning emerges in low-energy Nuclear Physics.

Author Contributions

The authors shared equally in the tasks related to amplitudes and results described in sects. 2 and 3, which are based on Teng's MSc thesis [77] supervised by Grießhammer. Grießhammer took the lead in the interpretations at the core of sect. 4.

Data Availability Statement

All data underlying this work is available in full from the corresponding author upon request.

Code Availability Statement

MATHEMATICA notebooks are available in full from the corresponding author upon request.

Declarations of Competing Interests

The authors have no financial or non-financial competing interests deriving from personal or financial relationships with people or organisations which may cause them embarrassment.

Acknowledgements

This project was conceived in 2019 with the warm hospitality and financial support of Beihang University (Beijing, China) and of the workshop EFFECTIVE FIELD THEORIES AND AB INITIO CALCULATIONS OF NUCLEI in Nanjing (China). We gratefully acknowledge the organisers and participants of the ECT* workshops THE NUCLEAR INTERACTION: POST-MODERN DEVELOPMENTS and UNIVERSALITY IN STRONGLY INTERACTING SYSTEMS: FROM QCD TO ATOMS, the 11TH INTERNATIONAL WORKSHOP ON CHIRAL DYNAMICS (CD2024), the programme and workshop INT-24-3 QUANTUM FEW- AND MANY-BODY SYSTEMS IN UNIVERSAL REGIMES and the workshop INT-25-92W CHIRAL EFT: NEW PERSPECTIVES at the Institute for Nuclear Theory of the University of Washington (INT-PUB-24-052 and INT-PUB-25-012) for critically evaluating these ideas, and for highly stimulating discussions, especially with Bingwei Long and Dean Lee. We are indebted to Ubirajara van Kolck for encouragement early on and extensive discussions in the final stages. Mario Sánchez Sánchez contributed initially. Ian Stewart clarified typographical errors in the KSW and FMS publications [67–69]. Some are fortunately not in the arXiv versions. Daniel R. Phillips' and Roxanne P. Springer's suggestions and pointers to pertinent publications about the large-N_C limit as well as Mike Birse's concise comments dramatically improved the first arXiv version. Martin J. Savage and Gerald A. Miller pointed out links to quantum entanglement and discussed its use; Silas R. Beane clarified fine points; Natalie M. Klco eradicated a number of misconceptions. We owe a debt of gratitude to the two anonymous referees, Daniel R. Phillips and Martin J. Savage for strenuously insisting on more clarity and conciseness, and to the editors for generous deadline extensions to help with that goal. This work was supported in part by the US Department of Energy under contract DE-SC0015393, by the Fondazione Bruno Kessler via the ECT*, by a travel stipend of the Europe-U.S. Theory Institute for Physics with Exotic Nuclei (EUSTIPEN), by the Istituto Nazionale di Fisica Nucleare (INFN, Italy), by EUROLABS, by the Università degli Studi di Milano (Italy), and by George Washington University: by the Office of the

Vice President for Research and the Dean of the Columbian College of Arts and Sciences; and by an Enhanced Faculty Travel Award of the Columbian College of Arts and Sciences. HWG's research was conducted in part in GW's Campus in the Closet.

A Appendix to Section 2

A.1 From Amplitudes to Phase Shifts

In a perturbative calculation, converting an amplitude into observables is dictated by the theorems of Mathematical Perturbation Theory [88–91]. Only an order-by-order expansion in both amplitude and observable is guaranteed to preserve the symmetries (including S-matrix unitarity) at each order independently. Different paths to observables must at a given order agree within uncertainties set by higher orders. Therefore, we will in app. B.1.5 use different extractions to estimate truncation uncertainties and order-by-order convergence.

We first follow the original KSW/FMS prescription which starts from the S matrix in the Stapp-Ypsilanti-Metropolis (SYM/"bar") parametrisation of the coupled ${}^3\mathrm{SD}_1$ channel [87]:

$$S = \mathbb{1} + \frac{\mathrm{i}kM}{2\pi}\begin{pmatrix} A^{(\mathrm{SS})} & A^{(\mathrm{SD})} \\ A^{(\mathrm{SD})} & A^{(\mathrm{DD})}\end{pmatrix} = \begin{pmatrix} \mathrm{e}^{2\mathrm{i}\delta_0}\cos 2\varepsilon & \mathrm{i}\mathrm{e}^{\mathrm{i}(\delta_0+\delta_2)}\sin 2\varepsilon \\ \mathrm{i}\mathrm{e}^{\mathrm{i}(\delta_0+\delta_2)}\sin 2\varepsilon & \mathrm{e}^{2\mathrm{i}\delta_2}\cos 2\varepsilon \end{pmatrix} \quad . \tag{A.1}$$

Throughout, the ${}^1\mathrm{S}_0$ case is retrieved by setting $\delta_2 = \varepsilon = 0$, $A^{(\mathrm{SD})} = A^{(\mathrm{DD})} = 0$.

Like the amplitudes $A = A_{-1} + A_0 + A_1 + A_2 \ldots$, each phase shift and the mixing angle ε is expanded in powers of the small, dimensionless parameter:

$$\delta_0 = \delta_{0,-1} + \delta_{0,0} + \delta_{0,1} + \delta_{0,2} + \ldots \text{ and likewise for } \delta_2, \varepsilon_1 \quad , \tag{A.2}$$

where $\delta_{0,-1} \gg \delta_{0,0} \gg \delta_{0,1} \gg \delta_{0,2} \ldots$ and the second subscript denotes again the order in Q. In χEFT with Perturbative Pions, only the S wave phase shift is nonzero at LO, while $\delta_{2,-1} = \varepsilon_{2,-1} = 0$ vanish. Expanding and matching order-by-order, we quote the result from KSW/FMS [66–69]. The only nonzero LO contribution is

$$\delta_{0,-1} = -\frac{\mathrm{i}}{2}\ln\left[1 + \frac{\mathrm{i}kM}{2\pi}A^{(\mathrm{SS})}_{-1}\right] \quad . \tag{A.3}$$

At NLO and N^{2}LO, one adds for the S wave phase shifts

$$\delta_{0,0} = \frac{kM}{4\pi}\,\frac{A^{(\mathrm{SS})}_0}{1 + \frac{\mathrm{i}kM}{2\pi}A^{(\mathrm{SS})}_{-1}} \quad , \tag{A.4}$$

$$\delta_{0,1} = \frac{kM}{4\pi}\,\frac{A^{(\mathrm{SS})}_1 - \mathrm{i}\,\frac{kM}{4\pi}[A^{(\mathrm{SD})}_0]^2}{1 + \frac{\mathrm{i}kM}{2\pi}A^{(\mathrm{SS})}_{-1}} - \mathrm{i}\,(\delta_{0,0})^2 \quad . \tag{A.5}$$

While the SD-mixing NLO amplitude $A^{(\mathrm{SD})}_0$ enters at N^{2}LO, sect. 2.3.6 shows that it cancels in the ${}^3\mathrm{S}_1$ channel against terms in $A^{(\mathrm{SS})}_1$. Formulae for δ_2 and ε can be found in [67–69, 77].

In the Unitarity limit, the term in the denominators simplifies to $1 + \frac{ikM}{2\pi} A_{-1}^{(\mathrm{SS})}|_{\mathrm{Uni}} = -1$ and the LO phase shift is in both S waves as expected identically

$$\delta_{0,-1} \equiv \frac{\pi}{2} = 90^\circ \quad . \tag{A.6}$$

However, from the pionless amplitudes of eq. (2.3), the NLO correction,

$$\delta_{0,0} = \frac{1}{ka} - \frac{kr}{2} \quad , \tag{A.7}$$

suffers an apparent divergence for $1 \gg ka \to 0$. The same holds for χEFT(pπ)$_{\mathrm{UE}}$. Strictly speaking, this is not an issue since such a limit is outside the window $\frac{1}{ka} \lesssim 1$ in which the Unitarity Expansion converges. Still, the divergence may obscure features close to $k = 0$ which can be of interest. Ultimately, its origin is a mismatch between defining the low-energy parameters in the ERE of $\mathrm{kcot}\delta$, eq. (2.1), and the constraint that $\delta(k \to 0) \to 0$ or 180° at NLO and in physical systems, while the value is 90° at Unitarity.

We therefore use another definition which expands not the phase shifts but the "physical" part of the amplitude, *i.e.* $\mathrm{kcot}\delta$ as in eq. (1.3), extending the approach by RS [76] to the coupled $^3\mathrm{SD}_1$ system. Replace phase shifts ($l = 0, 2$) by

$$\mathrm{e}^{2\mathrm{i}\delta_l} = 1 + \frac{2\mathrm{i}k}{\mathrm{kcot}\delta(k) - \mathrm{i}k} \text{ with } \mathrm{kcot}\delta = \mathrm{kcot}\delta_{l,-1} + \mathrm{kcot}\delta_{l,0} + \mathrm{kcot}\delta_{l,1} + \mathrm{kcot}\delta_{l,2} + \dots , \tag{A.8}$$

expand the mixing parameter ε as before, use that $\mathrm{kcot}\delta_{2,-1} = 0$ vanishes at LO to find

$$\mathrm{kcot}\delta_{0,-1} = \mathrm{i}k + \frac{4\pi}{M} \frac{1}{A_{-1}^{(\mathrm{SS})}} \tag{A.9}$$

$$\mathrm{kcot}\delta_{0,0} = -\frac{4\pi}{M} \frac{A_0^{(\mathrm{SS})}}{[A_{-1}^{(\mathrm{SS})}]^2} \tag{A.10}$$

$$\mathrm{kcot}\delta_{0,1} = -\frac{4\pi}{M} \left(\frac{A_1^{(\mathrm{SS})}}{[A_{-1}^{(\mathrm{SS})}]^2} - \frac{[A_0^{(\mathrm{SS})}]^2}{[A_{-1}^{(\mathrm{SS})}]^3} \right) + \mathrm{i}k \frac{[A_0^{(\mathrm{SD})}]^2}{[A_{-1}^{(\mathrm{SS})}]^2} \tag{A.11}$$

Deriving the corresponding formulae for $\mathrm{kcot}\delta_2$ and ε is again straightforward [77].

The phase shifts are then simply found by inverting $\mathrm{kcot}\delta_0$ at the appropriate order. In the Unitarity limit, the LO expression is as expected

$$\mathrm{kcot}\delta_{0,-1}\big|_{\mathrm{Uni}} = 0 \quad , \tag{A.12}$$

i.e. $\delta_{0,-1}(k) = \mathrm{arccot}[\frac{0}{k}] \equiv \frac{\pi}{2} = 90^\circ$. Now, one finds at NLO in pionless EFT from eq. (2.3) by construction the effective-range result:

$$\mathrm{kcot}\delta_{0,0}\big|_{\mathrm{Uni}} = -\frac{1}{a} + \frac{r}{2}k^2 \implies \delta_0 = \mathrm{arccot}[\frac{0 - \frac{1}{a} + \frac{r}{2}k^2}{k}] \overset{k\to 0}{=} \arctan 0 \quad . \tag{A.13}$$

This is finite (0° for $a < 0$, 180° for $a > 0$) and reproduces at NLO the first two terms of ERE and EFT($\not\pi$) (2.1). The $\mathcal{O}(Q^n)$ (N^{n+1}LO) terms are (also beyond Unitarity Expansion)

$$\mathrm{kcot}\delta_{0,n} = \begin{cases} v_{\frac{n+2}{2}} k^{n+2} & \text{for } n \geq 2 \text{ even} \\ 0 & \text{for } n \geq 1 \text{ odd} \end{cases} \quad . \tag{A.14}$$

Since the N^2LO contribution vanishes, we refer to such results as "EFT($\not\pi$) NLO=N^2LO".

In the following, we will mostly use the kcotδ form, cognisant of the fact that phase shifts at $\frac{1}{ka} \gtrsim 1$ are outside the Unitarity Window. In both variants to extract phase shifts, as in all expansions which are consistent within Mathematical Perturbation Theory, all phase shifts $\delta_0, \delta_2, \varepsilon$ as well as kcotδ are at each order real below the pion-production threshold, *i.e.* S-matrix unitarity is manifest at each order. In sect. 3.5 and app. B.1, we will compare both versions to assess truncation uncertainties and radius of convergence.

A.2 From Amplitudes to Pole Positions

Poles of the S matrix, and hence of the amplitudes, at complex momentum $\mathrm{i}\gamma$ correspond to real bound states for $\mathrm{Re}[\gamma] > 0, \mathrm{Im}[\gamma] = 0$; to virtual states for $\mathrm{Re}[\gamma] < 0, \mathrm{Im}[\gamma] = 0$, and to resonances for $\mathrm{Re}[\gamma] < 0, \mathrm{Im}[\gamma] \neq 0$. Unitarity is at $\gamma = 0$. Nonrelativistically, the corresponding (real or virtual) binding energies are $B = \frac{\gamma^2}{M} > 0$ when bound.

Extracting bound state properties from amplitudes follows again Mathematical Perturbation Theory [88–91]; see also [76, 92] and [93]. Poles are zeroes of the inverse S matrix (or amplitude) and appear in all coupled waves concurrently. It suffices to find the zeroes of the denominator in eq. (A.8). Expand both kcot$\delta(k)$ and the pole position, *i.e.* its argument:

$$k_{\text{pole}} = \mathrm{i}(\gamma_{-1} + \gamma_0 + \gamma_1 + \dots) \ . \tag{A.15}$$

Likewise, the (rescaled) residue at the pole is found by expanding

$$Z^{-1} = \frac{4\pi\mathrm{i}}{M}\,\frac{\mathrm{d}}{\mathrm{d}k}\frac{1}{A(k)}\bigg|_{k=\mathrm{i}\gamma} = \mathrm{i}\,\frac{\mathrm{d}}{\mathrm{d}k}\left(\mathrm{kcot}\delta_0(k) - \mathrm{i}k\right)\bigg|_{k=\mathrm{i}\gamma} \quad . \tag{A.16}$$

For ease of notation, we also define the mth derivative of the nth ($\mathcal{O}(Q^n)$, N^{n+1}LO) contribution to kcotδ_0 at $k = \mathrm{i}\gamma_{-1}$ as $\mathrm{kcot}\delta^{(m)}_{0,n}(\mathrm{i}\gamma_{-1}) := \frac{\mathrm{d}^m \mathrm{kcot}\delta_{0,n}(k)}{\mathrm{d}k^m}|_{k=\mathrm{i}\gamma_{-1}}$. The leading-order pole position is determined implicitly, and the residue is fixed by the Unitarity part, $\mathrm{i}k$:

$$\mathrm{kcot}\delta_{0,-1}(\mathrm{i}\gamma_{-1}) + \gamma_{-1} \stackrel{!}{=} 0 \ \ , \ \ (Z_{-1})^{-1} = 1 + \mathrm{i}\ \mathrm{kcot}\delta^{(1)}_{0,-1}(\mathrm{i}\gamma_{-1}) \ . \tag{A.17}$$

The other orders are again solved by iteration:

$$\mathrm{i}\gamma_0 = \frac{\mathrm{kcot}\delta_{0,0}(\mathrm{i}\gamma_{-1})}{\mathrm{i} - \mathrm{kcot}\delta^{(1)}_{0,-1}(\mathrm{i}\gamma_{-1})} \tag{A.18}$$

$$\mathrm{i}\gamma_1 = \frac{\mathrm{i}\gamma_0}{\mathrm{kcot}\delta_{0,0}(\mathrm{i}\gamma_{-1})}\left(\mathrm{kcot}\delta_{0,1}(\mathrm{i}\gamma_{-1}) + \mathrm{i}\gamma_0\ \mathrm{kcot}\delta^{(1)}_{0,0}(\mathrm{i}\gamma_{-1}) + \frac{(\mathrm{i}\gamma_0)^2}{2}\ \mathrm{kcot}\delta^{(2)}_{0,-1}(\mathrm{i}\gamma_{-1})\right) \tag{A.19}$$

For expressions via amplitudes, one starts from $[A_{-1}(k_{\text{pole}})+A_0(k_{\text{pole}})+\dots]^{-1}\stackrel{!}{=}0$ or inserts eqs. (A.9) to (A.11). Usually, $\mathrm{k}\cot\delta$ is analytic in k^2 around γ_{-1}, so that $\mathrm{kcot}\delta_{0,n}^{(m)}(\mathrm{i}\gamma_{-1})=0$ for odd $n\geq 1$ from eq. (A.14). In the Unitarity Expansion ($\gamma_{-1}=0$), $\mathrm{kcot}\delta_{0,-1}\equiv 0\equiv \mathrm{kcot}\delta_{-1\mathrm{p}}^{(m)}$ vanishes with all its derivatives, and the last term in parenthesis is zero.

Expanding the residue is straightforward; we only quote the next nontrivial term:

$$Z_0=-\mathrm{i}(Z_{-1})^2\left(\mathrm{kcot}\delta_{0,0}^{(1)}(\mathrm{i}\gamma_{-1})+\mathrm{i}\gamma_0\;\mathrm{kcot}\delta_{0,-1}^{(2)}(\mathrm{i}\gamma_{-1})\right)\quad . \tag{A.20}$$

That both the Unitarity limit and ERE/EFT($\not\pi$) expand about the same point $k=0$ has a curious consequence which we present in some detail as sect. 3.1 demonstrates that the same postdiction emerges in χEFT(pπ)$_{\text{UE}}$ at renormalisation point $k=0$. Since $\mathrm{k}\cot\delta$ is there analytic in k^2, one can use directly eq. (2.1). All odd orders of γ_n and all even orders of Z_n are zero. The first nonzero terms are:

$$\mathrm{i}\gamma_0=\frac{\mathrm{i}}{a}\;\;,\;\;\mathrm{i}\gamma_2=\frac{\mathrm{i}r}{2a^2}\;\;,\;\;\mathrm{i}\gamma_4=\frac{\mathrm{i}r^2}{2a^3}\;\;,\;\;\mathrm{i}\gamma_6=\frac{\mathrm{i}}{2a^4}\left(\frac{5r^3}{4}-2v_2\right) \tag{A.21}$$

$$Z_{-1}=1\;\;,\;\;Z_1=\frac{r}{a}\;\;,\;\;Z_3=\frac{3r^2}{2a^2}\;\;,\;\;Z_5=\frac{1}{2a^3}\left(5r^3-8v_2\right) \tag{A.22}$$

[The first term in each line and $\mathrm{i}\gamma_1=0=Z_0$ also follow from inserting the pionless amplitudes of eq. (2.3) into eqs. (A.18) and (A.19).] These series converge since $\frac{r}{a}\ll 1$ inside the Unitarity Window and we assume $v_n\sim m_\pi^{-2n+1}$ are natural as well.

While the shape parameter v_2 enters at $\mathcal{O}(Q^2)$ (N^{3}LO) in ERE/EFT($\not\pi$), it shifts the pole only at a very high $\mathcal{O}(Q^6)$ (N^{7}LO) when the parameters of the Unitarity Expansion are determined at $k=0$. The reason is that $\mathrm{kcot}\delta_{0,n}(k\to 0)\propto k^{2n+2}$ beyond NLO, so that at zero momentum $\mathrm{kcot}\delta_{0,n}^{(m)}(0)=0$ – unless $m=2n+2$ so that $\mathrm{kcot}\delta_{0,n}^{(2n+2)}(0)=(2n+2)!\;v_{\frac{n+2}{2}}$. This is inconsequential as long as all derivatives and functions in the pole expansion must be taken at a LO pole position $\gamma_{-1}\neq 0$. But Unitarity mandates $\mathrm{i}\gamma_{-1}=0$, so nearly all contributions to the pole momentum disappear. As a consequence, the binding momentum and residue can be determined to quite high order in the Unitarity Expansion, even if the ERE is given only to N^{2}LO (expanding in $\sqrt{\frac{r}{a}}$ would induce non-analyticities in r,a):

$$\mathrm{i}\gamma=\frac{\mathrm{i}}{a}\left(1+\frac{r}{2a}+\frac{r^2}{2a^2}+\mathcal{O}(\frac{r^3}{a^3})\right) \tag{A.23}$$

$$Z=1+\frac{r}{a}+\frac{3r^2}{2a^2}+\mathcal{O}(\frac{r^3}{a^3}) \tag{A.24}$$

This result is accurate only up to and including N^{2}LO in $\frac{r}{a}$. It coincides with the outcome of ERE/EFT($\not\pi$) without Unitarity Expansion at N^{2}LO. When the scattering length is included at LO (instead of NLO as in the Unitarity Expansion), terms with n powers of $\frac{1}{a}\sim Q^{-1}$ are merely reshuffled to n orders earlier, leading to $\mathrm{i}\gamma_{-1}^{\text{trad}}=\mathrm{i}\gamma_0$, $\mathrm{i}\gamma_0^{\text{trad}}=\mathrm{i}\gamma_2$, $Z_0^{\text{trad}}=Z_1$ *etc.*

A.3 The Zero-Momentum Limit

Reporting the $k \to 0$ limit of the χEFT(pπ)$_{\mathrm{UE}}$ amplitudes serves a dual purpose. It confirms that the amplitudes reduce to those of EFT($\not\pi$); and it allows further insight into the stark discrepancy between Wigner-SU(4) symmetric and breaking pion contributions.

At NLO, the impact of $A_0^{(\mathrm{S})}(k)$ reduces for low momenta to contributions analytic in m_π^2, and hence in the quark mass, which are eventually absorbed into higher-order χEFT LECs:

$$\lim_{k\to 0} \mathrm{k}\cot\delta_{0,0}(k) = \left(-\frac{1}{a} + \frac{r}{2}k^2\right) - \frac{2}{m_\pi^2\,\overline{\Lambda}_{\mathrm{NN}}}k^4\left(1 + \mathcal{O}(\frac{k^2}{m_\pi^2})\right) \quad . \tag{A.25}$$

The Wigner-SU(4) symmetric N^{2}LO amplitude $A_1^{(^1\mathrm{S}_0)}(k) = A_{1\mathrm{sym}}^{(\mathrm{S})}(k)$ reduces to

$$\lim_{k\to 0} \mathrm{k}\cot\delta_{1,0}(k)|_{\mathrm{sym}} = \\ \frac{4}{m_\pi\,\overline{\Lambda}_{\mathrm{NN}}}\left[\left(\frac{8}{5am_\pi^2} + \frac{r}{3}\right) - \frac{4}{m_\pi\,\overline{\Lambda}_{\mathrm{NN}}}\overbrace{\frac{(384\ln 2 - 227)}{960}}^{=0.040800...}m_\pi\right]k^4\left(1 + \mathcal{O}(\frac{k^2}{m_\pi^2})\right) \tag{A.26}$$

Finally, the symmetry-breaking N^{2}LO amplitude $A_{1\mathrm{break}}^{(\mathrm{S})}(k)$ reduces at low momenta to[12]

$$\lim_{k\to 0} \mathrm{k}\cot\delta_{1,0}(k)|_{\mathrm{break}} = -\left(\frac{4}{m_\pi\,\overline{\Lambda}_{\mathrm{NN}}}\right)^2\overbrace{\frac{384\ln 2 - 187}{280}}^{=0.28274...}m_\pi k^4\left(1 + \mathcal{O}(\frac{k^2}{m_\pi^2})\right) \quad . \tag{A.27}$$

Each OPE iteration adds one power of $\frac{4}{\overline{\Lambda}_{\mathrm{NN}} m_\pi}$. Neither N^{2}LO contribution is analytic in the quark mass (m_π^2). That is relevant for sect. 3.4.

B Appendix to Section 3

B.1 Assessing Uncertainties

To quantify the observations of sects. 3.2 and 3.3, we estimate theory uncertainties: *a-priori* order-by-order convergence; *a-priori* estimates from the assumption to be inside the Unitarity Window; *data-driven* convergence to PWAs; *a-posteriori* order-by-order convergence via Bayesian statistics; and *a-posteriori* comparison of different ways to extract phase shifts.

B.1.1 *A-Priori*: Order-By-Order Estimates

The typical low-momentum scales are $\frac{1}{a} \to 0$ in the Unitarity Expansion, $r \sim \frac{1}{m_\pi}$, k and m_π. As discussed in sects. 2.3.5 and 2.3.6, n inverse powers of the *a-priori* breakdown scale $\overline{\Lambda}_{\mathrm{NN}} \approx 300$ MeV parametrise the relative strength by which $(n-1)$-times-iterated OPE is suppressed against LO (no OPE). Therefore, $\frac{m_\pi}{\overline{\Lambda}_{\mathrm{NN}}} \approx 0.5$ and for $Q \lesssim 1$ from eq. (2.4), the upper limit of χEFT with Perturbative Pions is expected to be $k \lesssim \overline{\Lambda}_{\mathrm{NN}} \approx 300$ MeV.

[12]Since $A_0^{(\mathrm{S})}$ has no Wigner-SU(4) breaking contribution, $A_0^{(\mathrm{SS})} = 0$ in eq. (A.11).

Since $Q \approx 0.5$ at $k \approx m_\pi$ and N^{2}LO is complete, corrections in $\delta(k \sim m_\pi)$ should be of order $Q^3 \approx \frac{1}{8} \approx 10\%$ relative to $\delta_{0,-1} = \frac{\pi}{2}$, if coefficients follow the Naturalness Assumption [5, 94, 131–137]. As $k \to \overline{\Lambda}_{\text{NN}}$, NLO and N^{2}LO corrections should become comparable to LO. That happens at a slightly lower $k \approx 150$ MeV in the ^{1}S$_0$ channel (*cf.* fig. 3). In the Wigner-symmetrised ^{3}S$_1$ wave, N^{2}LO corrections are consistently somewhat larger than NLO, as allowed by Naturalness, but they exceed thrice NLO at $k \approx 170$ MeV; fig. 5.

B.1.2 *A-Priori*: Inside the Unitarity Window

According to eq. (2.4), the Unitarity Window $\frac{1}{ka} < 1$ with upper limit $|\cot\delta| < 1$ imposes 8 MeV $\lesssim k \lesssim$ 160 MeV in ^{1}S$_0$, and 35 MeV $\lesssim k \lesssim$ 230 MeV in ^{3}S$_1$. In both, ratios of small scales are not inconsistent with Naturalness: $|\frac{1}{am_\pi}| < 0.1$ in ^{1}S$_0$ and ≈ 0.25 in ^{3}S$_1$ about Unitarity; $\frac{rm_\pi}{2} \approx 0.9$ in ^{1}S$_0$ and ≈ 0.6 in ^{3}S$_1$. Therefore, changes from N^{3}LO may at $k \approx m_\pi$ be $0.6^3 \approx 0.2$ in ^{3}S$_1$, and $0.9^3 \approx 0.7$ in ^{1}S$_0$ – assuming again Naturalness. That appears large, but actual NLO-to-N^{2}LO corrections are much smaller.

B.1.3 *Data-Driven*: Convergence to the PWA

Comparison to an empirical PWA as next-best approximation to data can quantify how accurately the EFT reproduces experimental information [108, chap. 2.3] [109]. The double-logarithmic plots of fig. 9 contain information about expansion parameter and breakdown scale. First, deviations between calculation and data should be of order 1 for all orders when $Q \approx 1$. That determines the empirical breakdown scale $\overline{\Lambda}_{\text{emp}}$. Second, since each new order adds one power of $Q = \frac{k, m_\pi}{\overline{\Lambda}_{\text{emp}}}$ in the expansion of observables, slopes should increase by one power of Q from one order to the next for $k \gg m_\pi$ where the momentum scale dominates. Furthermore, the plots help quantify the assertions in sects. 3.2 and 3.3 that the Wigner-symmetric forms agree well with PWAs.

Excellent agreement at small k is no surprise since the low-k phase shifts are fitted to the ERE which is determined from a PWA. For the ^{1}S$_0$ channel, NLO, N^{2}LO and pionless corrections all approach unity around $\overline{\Lambda}_{\text{emp}}(^1\text{S}_0) \approx 270$ MeV which is close to the expected breakdown scale $\overline{\Lambda}_{\text{NN}} \approx 300$ MeV. We believe that is still sufficiently far away to be unaffected by the point $k \approx 350$ MeV where the χEFT(pπ)$_{\text{UE}}$ result is nonzero but the Nijmegen PWA crosses zero; *cf.* [74]. That induces an artificial divergence which cannot be remedied by plotting $\cot\delta$ instead. Slopes seem indeed to increase by roughly one from LO to NLO, and from NLO to N^{2}LO, and N^{2}LO is consistently more aligned with data than NLO. The EFT($\not\pi$) result might have an even better slope, but it suffers from an artificial zero since it crosses the empirical phase shift at an already relatively high $k \approx 100$ MeV. We estimate an empirical expansion parameter from scaling at momenta where reproducing the ERE has worn off: $Q(k \approx 200 \text{ MeV}) \approx 0.6$ at NLO, and $Q^2(k \approx 200 \text{ MeV}) \approx 0.25$ at N^{2}LO. That is not inconsistent with the *a-priori* estimate $Q = \frac{k \approx 200 \text{ MeV}}{\overline{\Lambda}_{\text{NN}}} \approx 0.7$.

In the ^{3}S$_1$ channel, the failure of the N^{2}LO result including Wigner-breaking terms (red solid line) is obvious: It breaks down at $k \approx 150$ MeV, and N^{2}LO corrections are already significantly larger than NLO ones for $k \gtrsim 100$ MeV. In contradistinction, the Wigner-symmetric version at N^2LO (black long-dashed line) has the expected slope increase. For $k \gtrsim 170$ MeV, it demonstrates consistent improvement over NLO, towards the PWA, and, most remarkably, over EFT($\not\pi$). This adds to the evidence that χEFT(pπ)$_{\mathrm{UE}}$ has a radius of convergence which is not only formally larger than that of a pionless version, but also empirically. The extractions of an empirical breakdown scale at NLO (≈ 250 MeV) and N^2LO (≈ 350 MeV) differ but are both well compatible with the expected breakdown scale $\overline{\Lambda}_{\mathrm{NN}} \approx 300$ MeV. The issue may be that N^2LO and PWA happen to agree at $k = 200$ MeV, inducing an artificial zero. That also makes it difficult to read off estimates of the expansion parameter for $k \gg m_\pi$. We find instead $Q(k \approx 120\text{ MeV}) \approx 0.2$ from NLO, and $Q^2(k \approx 120\text{ MeV}) \approx 0.06$ from N^2LO, which is quite a bit smaller than an *a-priori* estimate $Q = \frac{(k\approx 120\text{ MeV}+m_\pi)/2}{\overline{\Lambda}_{\mathrm{NN}}} \approx 0.4$ in which m_π cannot be neglected as typical low scale.

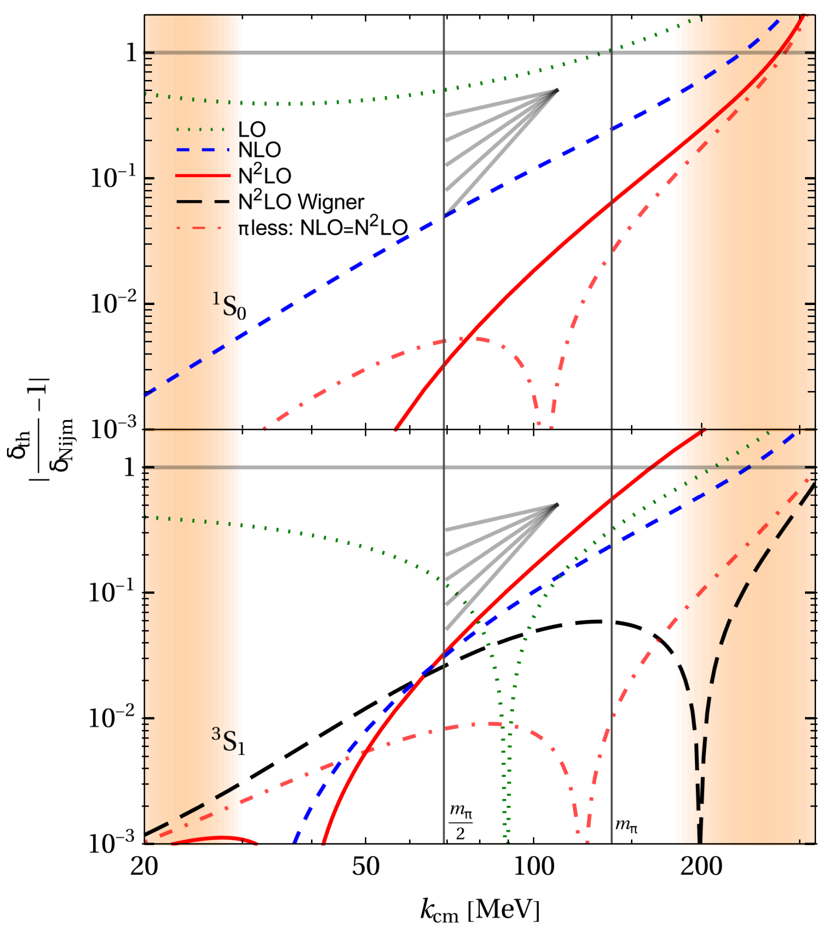

Figure 9: (Colour on-line) Double-logarithmic plots of the relative deviation between our results and the Nijmegen PWA in the $^1S_0$ (top) and $^3S_1$ (bottom) channels. The gray lines represent slopes of $k^{1,2,3,4,5}$. Colour-coding as in fig. 3; shaded: Born Corridors.

B.1.4 *A-Posteriori*: Bayesian Order-By-Order Convergence

The *a-priori* estimates of apps. B.1.1 and B.1.2 can account only qualitatively for the Naturalness of coefficients [5, 94, 131–137]. Factors of 2 or 3 can change $\overline{\Lambda}_{\mathrm{NN}}$ and order-by-order convergence substantially. A statistical interpretation via Bayesian analysis of the information on Naturalness that is available from the known orders quantifies theory uncertainties from truncation at a given order; see *e.g.* [138–140] and references therein.

We first analyse truncation uncertainties for the pole position, eqs. (A.23) and table 1, following the simple approach of refs. [100–102]. Expand

$$\mathrm{i}\gamma = \mathrm{i}\left[\gamma_{-1} + \gamma_0 + \sum_{n=1} \gamma_n\right] = \mathrm{i}\gamma_0 \left[1 + \sum_{m=1} c_m \epsilon^n\right] \tag{B.1}$$

to define dimensionless coefficients c_m assumed to be of natural size with expansion parameter ϵ. Truncated after n known coefficients, $|c_{\max,n+1}| \approx \max\limits_{m\leq n}\{|c_m|\}$ reasonably estimates higher orders and $\pm|c_{\max,n+1}|\,\epsilon^{n+1}$ is a reasonable truncation uncertainty [99, sect. 4.4].

The EFT($\not\pi$) and χEFT(pπ)$_{\mathrm{UE}}$ expressions for the pole parameters agree, and eq. (A.23) suggests $\epsilon = \frac{r}{a}$ with $c_1 = c_2 = \frac{1}{2}$ for γ. Since $\mathrm{i}\gamma_{-1} = 0$, only $\mathrm{i}\gamma_0 = \frac{\mathrm{i}}{a}$ sets a scale. If one would likewise choose $\epsilon = \frac{r}{a}$ for the residue, eq. (A.24), coefficients $c_1 = \frac{1}{2}, c_2 = \frac{3}{2}, c_3 = \frac{5}{2}, c_4 = \frac{35}{8} \approx 4.4, \ldots$ quickly outgrow the Naturalness Assumption $c_n \lesssim \frac{1}{\epsilon}$. The reason, well-explored in EFT($\not\pi$), is its high sensitivity to the pole position [141]. From eq. (A.22) or the ERE residue with no expansion in $\frac{r}{a}$ and $v_n = 0$, $Z^{-1} = \sqrt{1 - \frac{2r}{a}}$ proceeds in powers of $\epsilon = \frac{2r}{a}$ and $c_1 = \frac{1}{2}, c_2 = \frac{3}{8}, c_3 = \frac{5}{16}, c_4 = \frac{35}{128} \approx 0.3, \ldots$ are indeed natural. Thus, the expansion parameter for Z is twice that of $\mathrm{i}\gamma$. Ignoring such additional information in a Bayesian prior leads to inconsistent and wildly under-estimated uncertainties in particular in $^3\mathrm{S}_1$ where $\frac{2r}{a} \approx 0.6$ is not so small and dominates against corrections from higher ERE parameters. In $^1\mathrm{S}_0$, corrections from $\frac{2r}{a} \approx -0.2$ are similar in size to ERE corrections.

The BUQEYE collaboration derived probability distributions and degree-of-belief (DoB) intervals to statistically interpret $\pm|c_{n+1}|\,\epsilon^{n+1}$ [101]. A simple choice of priors is a uniform (flat) distribution for all known and unknown $|c_m|$ up to some (unknown but existing) maximum $\bar{c}$ which follows a log-uniform distribution. With $n = 2$ known terms, $\pm|c_{\max,3}|\,\epsilon^3$ encompasses roughly a 68% DoB interval. With only $n = 1$ term known, $\pm|c_{\max,2}|\,\epsilon^2$ sets a 50% DoB interval since fewer information leads to greater uncertainty. For these priors, the 68% DoB for $n = 1$ known term is actually at about $\pm 1.6\,|c_{\max,2}|\,\epsilon^2$, and the 95% interval for $n = 2$ known terms at about $\pm 2.7\,|c_{\max,3}|\,\epsilon^3$. This is not simply a factor 2 from the 68% DoB width for a Gaußian distribution because the posteriors fall off much slower, namely with inverse powers. Reasonable variations of the priors lead for $n \geq 2$ known drawings to variations by $\lesssim 20\%$ in these posteriors. Thus, we set the 68% DoB intervals as $\pm\frac{\mathrm{i}}{a}\frac{r^3}{2a^3}$ for the pole position and $\pm\frac{4r^3}{a^3}$ for its residue, each multiplied by about 2.7 for 95% DoBs.

We apply the same method to $\mathrm{k}\cot\delta(k)$ at each k and extract the corresponding uncertainties for phase shifts. This assumes that uncertainties at different k are very strongly correlated, which appears reasonable given that $\cot\delta(k)$ is near-linear for $k \gtrsim 100$ MeV; *cf.* figs. 3 and 5. The LO coefficient is again zero, $\mathrm{k}\cot\delta_{0,-1} = 0$. Around Unitarity, the

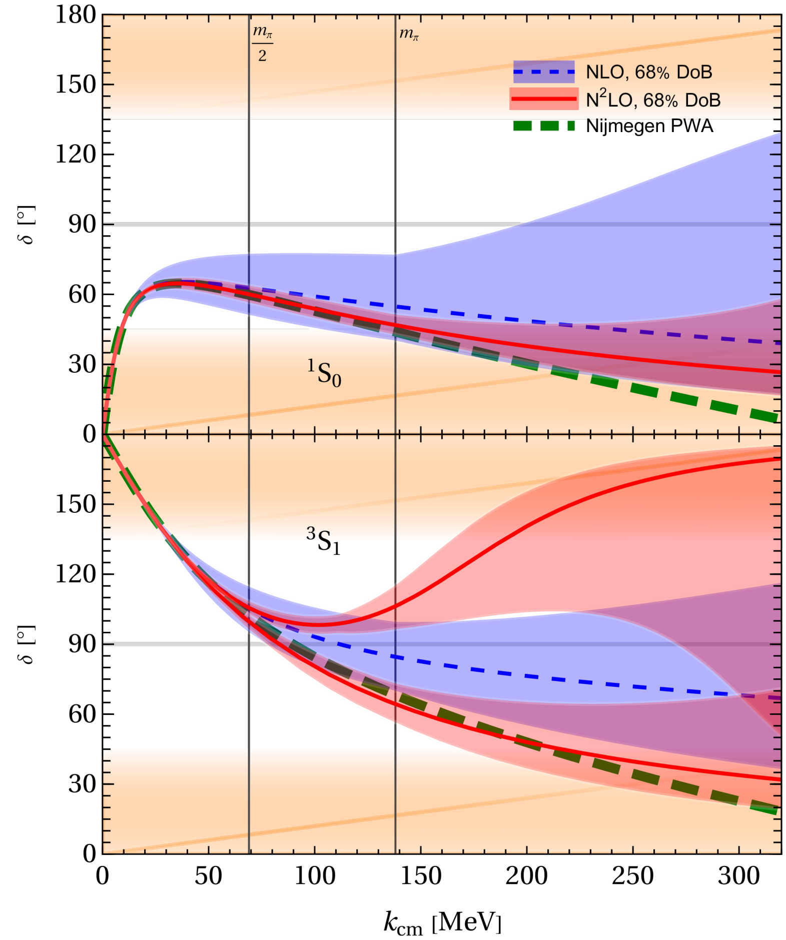

Figure 10: (Colour on-line) The 68% DoB uncertainties of phase shifts at N^{2}LO (red) and NLO (blue, using the rescaling factor from 50% described in the text) in the ^{1}S$_0$ channel (top), and in the ^{3}S$_1$ channel with and without Wigner-breaking terms (bottom), under the assumptions of priors described in the text. Details as in fig. 3.

Unitarity-ensuring factor $-ik$ of eq. (1.1) sets a natural scale. Since the theory is renormalised at $k = 0$ to the ERE, we ensure that uncertainty bands vanish as $k \to 0$ by setting

$$c_0 = \frac{\mathrm{kcot}\delta_{0,0}(k) - \mathrm{kcot}\delta_{0,0}(0)}{k\ Q} \ \ , \ \ c_1 = \frac{\mathrm{kcot}\delta_{0,1}(k)}{k\ Q^2} \ \ . \tag{B.2}$$

This choice is aligned with cotδ as prime variable. We simply accommodate the various scales which make up the numerator of the expansion parameter in eq. (2.4) as

$$Q \approx \frac{\max\{k; m_\pi\}}{\overline{\Lambda}_{\rm NN}} \ \ , \tag{B.3}$$

noting that this choice of breakdown scale is consistent with the numbers in app. B.1.3.

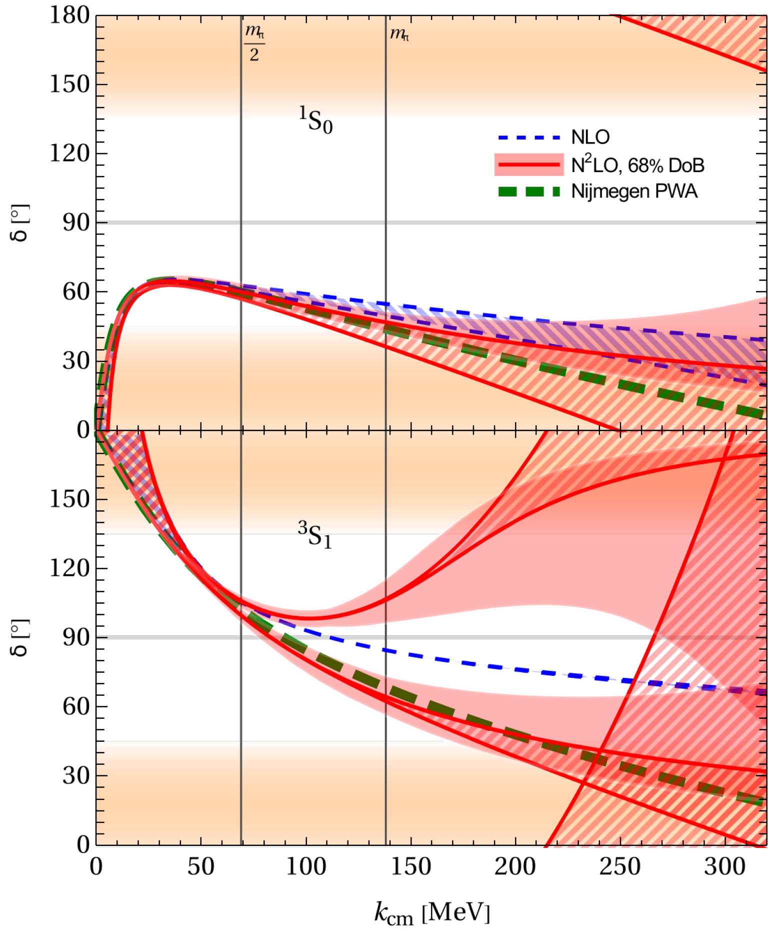

Figure 11: (Colour on-line) Phase shifts for the two variants to extract the $^1S_0$ (top) and $^3S_1$ (bottom) phase shifts of app. A.1: directly (pure lines), and via kcotδ (lines with Bayesian uncertainty bands), at N^{2}LO (red) and NLO (blue). The differences are marked by the hatched areas (blue: NLO; red: N^{2}LO). Details as in fig. 3.

The N^{2}LO uncertainties are shown in figs. 3 to 5. Figure 10 includes the NLO bands (rescaled as above to 68% DoBs). They overlap very well in the $^1S_0$ channel and reasonably in the Wigner-symmetric $^3S_1$ version. For both, the N^{2}LO band is throughout smaller than the NLO one. In the $^3S_1$ wave with Wigner-breaking terms, NLO and N^{2}LO uncertainties still overlap. However, the width of the N^{2}LO band approaches rapidly that of NLO and exceeds it for $k \gtrsim 200$ MeV, which is further proof that this version does not converge well.

B.1.5 *A-Posteriori*: Different Ways to Extract Phase Shifts

In app. A.1, we discuss two variants to extract phase shifts from amplitudes: directly, or via kcotδ. As noted there, when both are preformed at the same order in Q, these two must agree up to higher-order corrections where their convergence ranges overlap. If the results differ vastly, the expansion breaks down. This is a particularly interesting tool to measure the size of the Unitarity Window. When one expands about it centre at $\cot\delta = 0$,

$$\cot\delta(k) = \left(\frac{\pi}{2} - \delta(k)\right) + \frac{1}{3}\left(\frac{\pi}{2} - \delta(k)\right)^3 + \mathcal{O}(\left(\frac{\pi}{2} - \delta(k)\right)^5) \tag{B.4}$$

proceeds in odd powers of $90° - \delta(k)$. The first correction is smaller than $\frac{1}{4}$ of the leading term for approximately $\delta \in [40°; 140°]$, *i.e.* close to the points $\delta = 45°, 135°$ at which the Unitarity Expansion of eq. (1.3) is expected to fail because $|\cot\delta| = 1$.

The very good agreement of extractions both at NLO and N^{2}LO in all χEFT(pπ)$_{\text{UE}}$ variants, fig. 11, is therefore no surprise. At the low end of the Unitarity Window, they diverge starkly for the reason discussed in app. A.1: According to eq. (A.13), using $k\cot\delta(k \to 0)$ leads to $\delta(k \to 0) = 0, 180°$ at Unitarity from NLO on, while the phase-shift extraction encounters a divergence, $\delta(k \to 0) \to \frac{1}{ka} \to \infty$, eq. (A.7). Thus, discrepancies are expected for $k \lesssim \frac{1}{|a|} = 8$ MeV in ^{1}S$_0$ and $\lesssim 35$ MeV in ^{3}S$_1$. Interestingly, for higher momenta pushing into the Born Corridors, the induced bands are smaller than the Bayesian estimates, and phase shifts from the direct methods tend to lie slightly below the $k\cot\delta$ variant.

B.2 Varying the Renormalisation Point

So far, we used the ERE around $k = 0$ because that is the natural scale at Unitarity. Now, we treat the symbols a and r as if they were not scattering length and effective range but (finite pieces of) LECs whose values reproduce the Nijmegen values of $k\cot\delta$ and its derivative at a particular k_{fit}. Any choice is legitimate, as long as $k_{\text{fit}} \ll \overline{\Lambda}_{\text{NN}}$ [65].

RS and FMS used the pole position of the amplitude as input [68, 76]. This natural choice for bound-state properties avoids universal (and thus trivial) correlations between

	^{1}S$_0$			^{3}S$_1$		
k_{fit}	a [fm]	r [fm]	(γ [MeV], Z)	a [fm]	r [fm]	(γ [MeV], Z)
empirical	$-23.735(6)*$	$2.673(9)*$	$(-7.892, 0.9034)$	$5.435(2)*$	$1.852(2)*$	$(+47.7023\ , 1.689)*$
pole	-23.7104	2.7783		5.6128	2.3682	
$\frac{m_\pi}{2}$ NLO	-38.988	3.3270	$(-4.86\ , 0.925)$	4.9310	2.4966	$(+55.\ , 1.9)$
$\frac{m_\pi}{2}$ N^{2}LO	-25.428	2.7281	$(-7.38\ , 0.910(5))$	4.7768	2.4492	$(+57(3).\ , 1.9(5))$
$\frac{m_\pi}{2}$ sym.				5.4625	1.6124	$(+43.0(5)\ , 1.4(1))$
m_π NLO	$+\ 9.2856$	4.2285	$(+28.\ , 1.8)$	3.3442↯	3.1886↯	$(+114.\ , 3.)$↯
m_π N^{2}LO	$+34.3335$	2.8956	$(+6.01\ , 1.10)$	1.8376↯	3.3741↯	$(+387(330)., 8(25).)$↯
m_π sym.				4.5344	1.7006	$(+55(1).\ , 1.6(2))$

Table 2: Values of a, r interpreted as LECs to reproduce $k\cot\delta$ and its derivative at a certain k_{fit}. The empirical values are found from the Granada values [24] as described in app. A.2. An asterisk $*$ is input; a lightning bolt ↯ indicates the result cannot converge because $r \gtrsim a$. For a, r, spurious precision is used because of some fine-tuning. N^{2}LO uncertainties for pole position γ and residue Z are based on the uncertainty estimate of app. A.2. If none is given, it is smaller than the last quoted significant figure.

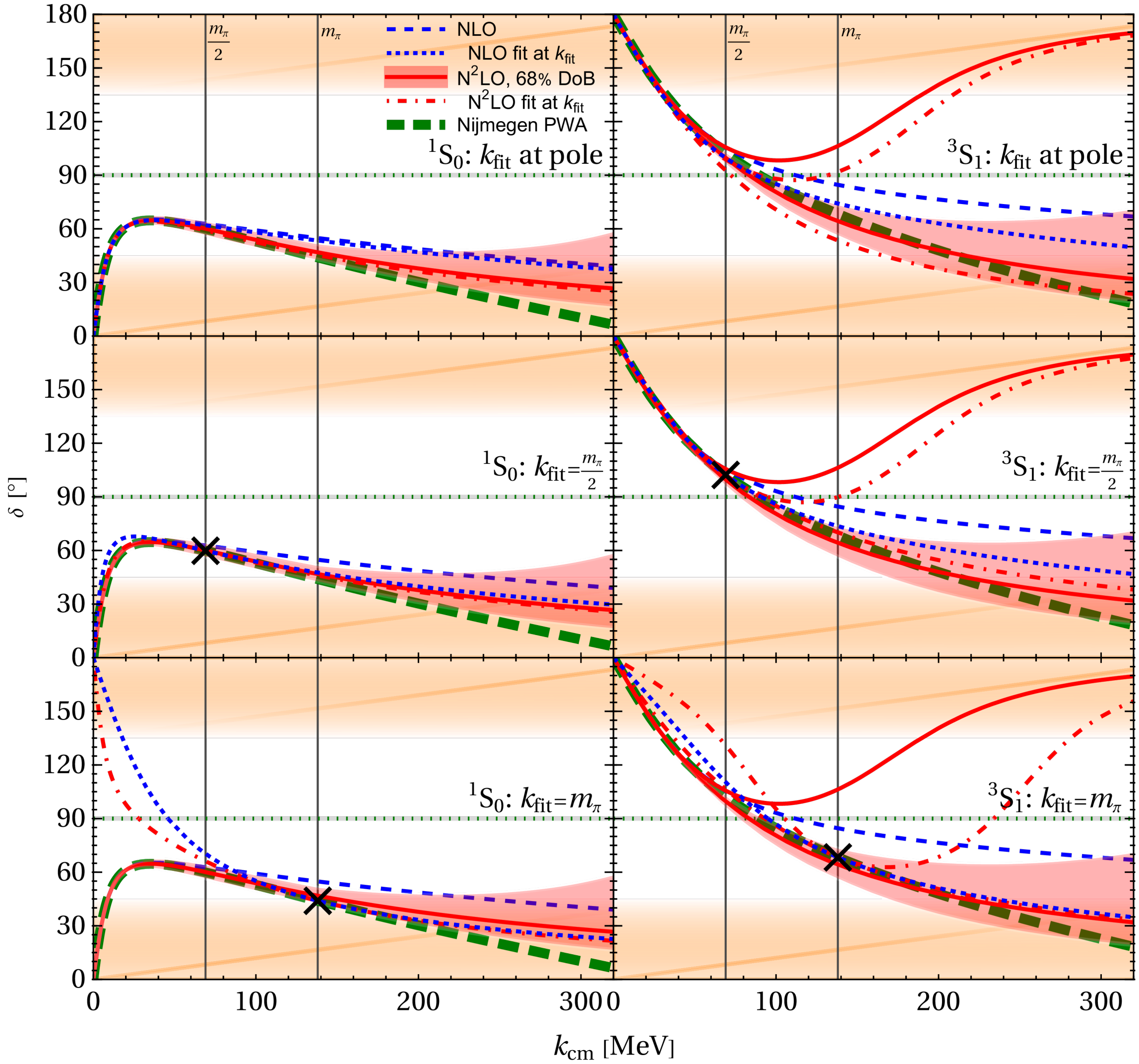

Figure 12: (Colour on-line) Phase shifts in the $^1S_0$ (left) and $^3S_1$ (right) channels, fitted to the pole (top), $k_{fit} = \frac{m_\pi}{2}$ (centre) and m_π (bottom). NLO: blue short-dashed. N^2LO and Wigner-invariant N^2LO are both red dot-dashed but simple to differentiate. Crosses mark fit points. The results for $k_{fit} = 0$ with Bayesian N^2LO (in $^3S_1$ for the symmetric form only) bands are colour-coded as in fig. 3.

binding energies and observables like the charge radius. One can find such a and r from the empirical pole position and residue of table 1 up to $\mathcal{O}(\frac{r^3}{a^3})$ by inverting eqs. (A.23/A.24). No pion contributions enter. The results in table 2 differ only slightly from the Granada group's best values for physical scattering length and effective range at $k = 0$. On the other hand, since the leading nonzero contribution (NLO) is $i\gamma_0 = \frac{i}{a}$ from eq. (A.18), $k_{fit}a = \gamma a \approx 1$ lies by design just at the brink of the Unitarity Window. That is dangerous.

We thus also explore two natural renormalisation points of $\chi EFT(p\pi)_{UE}$ inside the Unit-

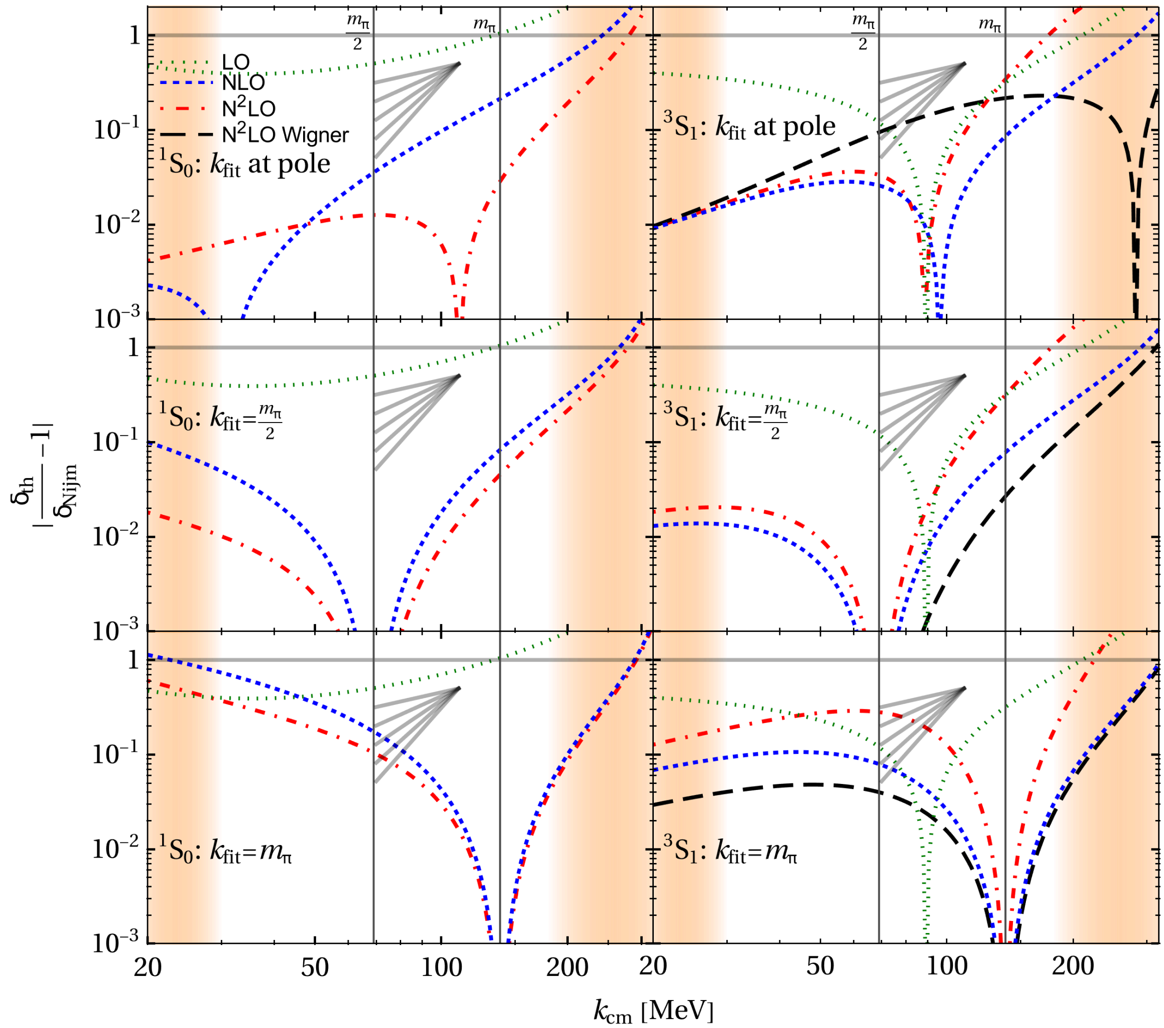

Figure 13: (Colour on-line) Double-logarithmic plots in the ${}^1\mathrm{S}_0$ (left) and ${}^3\mathrm{S}_1$ (right) channels of the relative deviation of results fitted to the pole (top), $k_{\text{fit}} = \frac{m_\pi}{2}$ (centre) and m_π (bottom), to the Nijmegen PWA. LO: green dotted; NLO: blue short-dashed; N^2LO: red dot-dashed; Wigner-symmetric N^2LO: black dashed; see also fig. 9.

arity Window: the branch-point scales $k_{\text{fit}} = \frac{m_\pi}{2}$ and m_π of non- and once-iterated OPE.

Figure 12 shows the phase shifts for the three choices, and fig. 13 the double-logarithmic plots of convergence to the PWA. The results of both fits to the pole and $\frac{m_\pi}{2}$ are well within the N^2LO bands of 68% DoB uncertainties from Bayesian truncation uncertainties with $k_{\text{fit}} = 0$. According to table 2, the pole position and residue is still captured adequately, though discrepancies increase and order-by-order convergence gets poorer for $k_{\text{fit}} = \frac{m_\pi}{2}$. The nominal ${}^1\mathrm{S}_0$ scattering length changes sign for $k_{\text{fit}} = m_\pi$ (bottom panels), and the extracted pole parameters and their uncertainties are meaningless since the phase shifts clearly diverge from the PWA well inside the Unitarity Window for $k \lesssim 60$ MeV. The ${}^3\mathrm{S}_1$ results at NLO and Wigner-symmetric N^{2}LO have $\frac{r}{a} \gtrsim 1$ (marked by lightning bolts ↯). This does not only violate the expansion of pole and residue in powers of $\frac{r}{a}$ (eqs. (A.23/A.24)), but also the Unitarity-Window constraint $\frac{r}{2a} \ll 1$. Apparently, the "leverage arm" from the fit point to the lower bound of the Unitarity Window is too large.

Interestingly, NLO is for all fit points at least as good, and sometimes even better, than the $k_{\text{fit}} = 0$ answers. Some of this may be because the phase shift is simply required to go through the PWA result. However, the N^{2}LO curves with Wigner-SU(4) symmetry do not show such a uniform trend. The convergence plots of fig. 13 are very similar to the $k_{\text{fit}} = 0$ case for the pole fit. Except for the pole fit, they are dominated by the enforced identity with the phase shifts and derivatives of the PWA at the fit points. This makes the slopes seem steeper. However, the empirical breakdown scale of all fits is unchanged and in the same range of around 300 MeV as before. We therefore consider this to be a robust result.

The only exception is, of course, the ${}^3\mathrm{S}_1$ channel with Wigner-SU(4) breaking interactions (red dot-dashed lines). Even when the fit forces matching at $k_{\text{fit}} = m_\pi$, does it diverge quickly at higher k. We see no scenario in which these amplitudes can be made to reasonably agree with the PWA, or with the pole position and residue (table 2).

Different but reasonable choices of the renormalisation point at N^{2}LO do therefore not change phase shifts or empirical breakdown scales in a statistically significant way.

References

[1] E. Epelbaum, U. G. Meißner and W. Glöckle, Nucl. Phys. A **714** (2003), 535-574 doi:10.1016/S0375-9474(02)01393-3 [arXiv:nucl-th/0207089 [nucl-th]].

[2] E. Braaten and H.-W. Hammer, Phys. Rev. Lett. **91** (2003), 102002 doi:10.1103/PhysRevLett.91.102002 [arXiv:nucl-th/0303038 [nucl-th]].

[3] S. R. Beane, K. Orginos and M. J. Savage, Int. J. Mod. Phys. E **17** (2008), 1157-1218 doi:10.1142/S0218301308010404 [arXiv:0805.4629 [hep-lat]].

[4] J. Bulava *et al.* [BaSc], [arXiv:2505.05547 [hep-lat]].

[5] H.-W. Hammer, S. König and U. van Kolck, Rev. Mod. Phys. **92** (2020), no. 2, 025004 doi:10.1103/RevModPhys.92.025004 [arXiv:1906.12122 [nucl-th]].

[6] R. Machleidt and F. Sammarruca, Prog. Part. Nucl. Phys. **137** (2024), 104117 doi:10.1016/j.ppnp.2024.104117 [arXiv:2402.14032 [nucl-th]].

[7] A. Kievsky and M. Gattobigio, Few Body Syst. **57** (2016), 217 doi:10.1007/s00601-016-1049-5 [arXiv:1511.09184 [nucl-th]].

[8] S. König, H. W. Grießhammer, H.-W. Hammer and U. van Kolck, Phys. Rev. Lett. **118** (2017), no. 20, 202501 doi:10.1103/PhysRevLett.118.202501 [arXiv:1607.04623 [nucl-th]].

[9] U. van Kolck, Few Body Syst. **58** (2017), no. 3, 112 doi:10.1007/s00601-017-1271-9.

[10] A. Kievsky, M. Viviani, D. Logoteta, I. Bombaci and L. Girlanda, Phys. Rev. Lett. **121** (2018), no. 7, 072701 doi:10.1103/PhysRevLett.121.072701 [arXiv:1806.02636 [nucl-th]].

[11] U. van Kolck, Nuovo Cim. C **42** (2019), no. 2-3-3, 52 doi:10.1393/ncc/i2019-19052-7.

[12] S. König, Eur. Phys. J. A **56** (2020), no. 4, 113 doi:10.1140/epja/s10050-020-00098-9 [arXiv:1910.12627 [nucl-th]].

[13] I. Tews, J. M. Lattimer, A. Ohnishi and E. E. Kolomeitsev, Astrophys. J. **848** (2017), no. 2, 105 doi:10.3847/1538-4357/aa8db9 [arXiv:1611.07133 [nucl-th]].

[14] M. Gattobigio, A. Kievsky and M. Viviani, Phys. Rev. C **100** (2019), no. 3, 034004 doi:10.1103/PhysRevC.100.034004 [arXiv:1903.08900 [nucl-th]].

[15] A. Kievsky, A. Polls, B. Juliá-Díaz, N. K. Timofeyuk and M. Gattobigio, Phys. Rev. A **102** (2020), no. 6, 063320 doi:10.1103/PhysRevA.102.063320 [arXiv:2006.09758 [cond-mat.quant-gas]].

[16] P. E. Georgoudis, Nucl. Phys. A **1015** (2021), 122297 doi:10.1016/j.nuclphysa.2021.122297 [arXiv:2006.15508 [nucl-th]].

[17] P. E. Georgoudis, Adv. Nucl. Phys. **28** (2022), 167-172 doi:10.12681/hnps.3600.

[18] L. Contessi, J. Kirscher and M. Pavon Valderrama, Phys. Rev. A **109** (2024) no.3, 032217 doi:10.1103/PhysRevA.109.032217 [arXiv:2303.01312 [cond-mat.quant-gas]].

[19] U. van Kolck, Eur. Phys. J. A **56** (2020), no. 3, 97 doi:10.1140/epja/s10050-020-00092-1 [arXiv:2003.09974 [nucl-th]].

[20] A. Kievsky, L. Girlanda, M. Gattobigio and M. Viviani, Ann. Rev. Nucl. Part. Sci. **71** (2021), 465-490 doi:10.1146/annurev-nucl-102419-032845 [arXiv:2102.13504 [nucl-th]].

[21] V. G. J. Stoks, R. A. M. Klomp, M. C. M. Rentmeester and J. J. de Swart, Phys. Rev. C **48** (1993), 792-815 doi:10.1103/PhysRevC.48.792, nn-online.org accessed August 2024.

[22] R. Navarro Pérez, J. E. Amaro and E. Ruiz Arriola, Phys. Rev. C **88** (2013), 024002 [erratum: Phys. Rev. C **88** (2013), no. 6, 069902] doi:10.1103/PhysRevC.88.024002 [arXiv:1304.0895 [nucl-th]].

[23] R. Navarro Pérez, J. E. Amaro and E. Ruiz Arriola, Phys. Rev. C **88** (2013), no. 6, 064002 [erratum: Phys. Rev. C **91** (2015), no. 2, 029901] doi:10.1103/PhysRevC.88.064002 [arXiv:1310.2536 [nucl-th]].

[24] E. Ruiz Arriola, J. E. Amaro and R. Navarro Pérez, Front. in Phys. **8** (2020), 1 doi:10.3389/fphy.2020.00001 [arXiv:1911.09637 [nucl-th]].

[25] S. Wu and B. Long, Phys. Rev. C **99** (2019) no.2, 024003 doi:10.1103/PhysRevC.99.024003 [arXiv:1807.04407 [nucl-th]].

[26] D. B. Kaplan, Phys. Rev. C **102** (2020) no. 3, 034004 doi:10.1103/PhysRevC.102.034004 [arXiv:1905.07485 [nucl-th]].

[27] R. Peng, S. Lyu and B. Long, Commun. Theor. Phys. **72** (2020) no.9, 095301 doi:10.1088/1572-9494/aba251 [arXiv:2011.13186 [nucl-th]].

[28] N. Kaiser, R. Brockmann and W. Weise, Nucl. Phys. A **625** (1997), 758-788 doi:10.1016/S0375-9474(97)00586-1 [arXiv:nucl-th/9706045 [nucl-th]].

[29] S. R. Beane, P. F. Bedaque, M. J. Savage and U. van Kolck, Nucl. Phys. A **700** (2002), 377-402 doi:10.1016/S0375-9474(01)01324-0 [arXiv:nucl-th/0104030 [nucl-th]].

[30] M. C. Birse, Phys. Rev. C **74** (2006), 014003 doi:10.1103/PhysRevC.74.014003 [nucl-th/0507077].

[31] M. C. Birse, PoS CD **09** (2009), 078 doi:10.22323/1.086.0078 [arXiv:0909.4641 [nucl-th]].

[32] T. Mehen, I. W. Stewart and M. B. Wise, Phys. Lett. B **474** (2000), 145-152 doi:10.1016/S0370-2693(00)00006-X [arXiv:hep-th/9910025 [hep-th]].

[33] Y. Nishida and D. T. Son, Phys. Rev. D **76** (2007), 086004 doi:10.1103/PhysRevD.76.086004 [arXiv:0706.3746 [hep-th]].

[34] H. W. Hammer and D. T. Son, Proc. Nat. Acad. Sci. **118** (2021), e2108716118 doi:10.1073/pnas.2108716118 [arXiv:2103.12610 [nucl-th]].

[35] E. Wigner, Phys. Rev. **51** (1937), 106; *ibid.* **56** (1939), 519.

[36] F. Hund, Zeitschrift für Physik **105** (1937), 202.

[37] T. Mehen, I. W. Stewart and M. B. Wise, Phys. Rev. Lett. **83** (1999), 931-934 doi:10.1103/PhysRevLett.83.931 [arXiv:hep-ph/9902370 [hep-ph]].

[38] E. Epelbaum, U. G. Meißner, W. Gloeckle and C. Elster, Phys. Rev. C **65** (2002), 044001 doi:10.1103/PhysRevC.65.044001 [arXiv:nucl-th/0106007 [nucl-th]].

[39] D. O. Riska, Nucl. Phys. A **710** (2002), 55-82 doi:10.1016/S0375-9474(02)01091-6 [arXiv:nucl-th/0204016 [nucl-th]].

[40] V. S. Timoteo, S. Szpigel and E. Ruiz Arriola, Phys. Rev. C **86** (2012), 034002 doi:10.1103/PhysRevC.86.034002 [arXiv:1108.1162 [nucl-th]].

[41] E. Ruiz Arriola, V. S. Timoteo and S. Szpigel, PoS **CD12** (2013), 106 doi:10.22323/1.172.0106 [arXiv:1302.3978 [nucl-th]].

[42] S. S. Li Muli, T. R. Djärv, C. Forssén and D. R. Phillips, [arXiv:2503.16372 [nucl-th]].

[43] D. B. Kaplan and M. J. Savage, Phys. Lett. B **365** (1996), 244-251 doi:10.1016/0370-2693(95)01277-X [arXiv:hep-ph/9509371 [hep-ph]].

[44] D. B. Kaplan and A. V. Manohar, Phys. Rev. C **56** (1997), 76-83 doi:10.1103/PhysRevC.56.76 [arXiv:nucl-th/9612021 [nucl-th]].

[45] A. Calle Cordón and E. Ruiz Arriola, Phys. Rev. C **78** (2008), 054002 doi:10.1103/PhysRevC.78.054002 [arXiv:0807.2918 [nucl-th]].

[46] E. Ruiz Arriola, Symmetry **8** (2016) no.6, 42 doi:10.3390/sym8060042.

[47] E. Noether, Nachrichten von der Gesellschaft der Wissenschaften zu Göttingen, Mathematisch-Physikalische Klasse 1918 (1918), 235, online at eudml.org/doc/59024.

[48] M. C. Birse, J. A. McGovern and K. G. Richardson, Phys. Lett. B **464** (1999), 169-176 doi:10.1016/S0370-2693(99)00991-0 [arXiv:hep-ph/9807302 [hep-ph]].

[49] T. Barford and M. C. Birse, Phys. Rev. C **67** (2003), 064006 doi:10.1103/PhysRevC.67.064006 [arXiv:hep-ph/0206146 [hep-ph]].

[50] P. F. Bedaque, H.-W. Hammer and U. van Kolck, Nucl. Phys. A **676** (2000), 357-370 doi:10.1016/S0375-9474(00)00205-0 [arXiv:nucl-th/9906032 [nucl-th]].

[51] H. W. Grießhammer and M. R. Schindler, Eur. Phys. J. A **46** (2010), 73-83 doi:10.1140/epja/i2010-11017-x [arXiv:1007.0734 [nucl-th]].

[52] J. Vanasse, Phys. Rev. C **86** (2012), 014001 doi:10.1103/PhysRevC.86.014001 [arXiv:1110.1039 [nucl-th]].

[53] X. Lin, H. Singh, R. P. Springer and J. Vanasse, Phys. Rev. C **108** (2023), no. 4, 044001 doi:10.1103/PhysRevC.108.044001 [arXiv:2210.15650 [nucl-th]].

[54] X. Lin and J. Vanasse, Phys. Rev. C **112** (2025) no.2, 024001 doi:10.1103/qgcx-r63r [arXiv:2408.14602 [nucl-th]].

[55] M. C. Birse, B. Krippa and N. R. Walet, Phys. Rev. C **87** (2013), 054001 doi:10.1103/PhysRevC.87.054001 [arXiv:1207.5735 [nucl-th]].

[56] B. N. Lu, N. Li, S. Elhatisari, D. Lee, E. Epelbaum and U. G. Meißner, Phys. Lett. B **797** (2019), 134863 doi:10.1016/j.physletb.2019.134863 [arXiv:1812.10928 [nucl-th]].

[57] D. Lee, S. Bogner, B. A. Brown, S. Elhatisari, E. Epelbaum, H. Hergert, M. Hjorth-Jensen, H. Krebs, N. Li and B. N. Lu, *et al.* Phys. Rev. Lett. **127** (2021), no. 6, 062501 doi:10.1103/PhysRevLett.127.062501 [arXiv:2010.09420 [nucl-th]].

[58] I. N. Izosimov, doi:10.1142/9789811209451_0009.

[59] J. Liu, T. Wang and B. N. Lu, Eur. Phys. J. A **61** (2025) no.4, 85 doi:10.1140/epja/s10050-025-01568-8 [arXiv:2502.13565 [nucl-th]].

[60] Z. W. Niu and B. N. Lu, [arXiv:2506.12874 [nucl-th]].

[61] S. Shen, T. A. Lähde, D. Lee and U. G. Meißner, Eur. Phys. J. A **57** (2021), no. 9, 276 doi:10.1140/epja/s10050-021-00586-6 [arXiv:2106.04834 [nucl-th]].

[62] A. Ekström and L. Platter, Phys. Lett. B **860** (2025), 139207 doi:10.1016/j.physletb.2024.139207 [arXiv:2409.08197 [nucl-th]].

[63] A. Ekström and L. Platter, [arXiv:2507.08700 [nucl-th]].

[64] H. W. Grießhammer, S. König, D. R. Phillips, U. van Kolck, in: *Nuclear Forces for Precision Nuclear Physics – a collection of perspectives*, I. Tews, Z. Davoudi, A. Ekström, J. D. Holt (eds.), Few-Body Syst. **63** (2022) 67 doi:10.1007/s00601-022-01749-x [arXiv:2202.01105 [nucl-th]].

[65] H. W. Grießhammer, Few Body Syst. **63** (2022), no. 2, 44 doi:10.1007/s00601-022-01739-z [arXiv:2111.00930 [nucl-th]].

[66] D. B. Kaplan, M. J. Savage and M. B. Wise, Phys. Lett. B **424** (1998), 390-396 doi:10.1016/S0370-2693(98)00210-X [arXiv:nucl-th/9801034 [nucl-th]].

[67] D. B. Kaplan, M. J. Savage and M. B. Wise, Nucl. Phys. B **534** (1998), 329-355 doi:10.1016/S0550-3213(98)00440-4 [arXiv:nucl-th/9802075 [nucl-th]].

[68] S. Fleming, T. Mehen and I. W. Stewart, Nucl. Phys. A **677** (2000), 313-366 doi:10.1016/S0375-9474(00)00221-9 [arXiv:nucl-th/9911001 [nucl-th]].

[69] S. Fleming, T. Mehen and I. W. Stewart, Phys. Rev. C **61** (2000), 044005 doi:10.1103/PhysRevC.61.044005 [arXiv:nucl-th/9906056 [nucl-th]].

[70] F. Oosterhof, B. Long, J. de Vries, R. G. E. Timmermans and U. van Kolck, Phys. Rev. Lett. **122** (2019) no.17, 172501 doi:10.1103/PhysRevLett.122.172501 [arXiv:1902.05342 [hep-ph]].

[71] F. Oosterhof, J. de Vries, R. G. E. Timmermans and U. van Kolck, Phys. Lett. B **820** (2021), 136525 doi:10.1016/j.physletb.2021.136525 [arXiv:2105.05715 [nucl-th]].

[72] F. Oosterhof, *Baryon-Number Violation in Chiral Effective Field Theory*, PhD thesis, University of Groningen 2022.

[73] D. B. Kaplan and J. V. Steele, Phys. Rev. C **60** (1999), 064002 doi:10.1103/PhysRevC.60.064002 [arXiv:nucl-th/9905027 [nucl-th]].

[74] M. Sánchez Sánchez, C. J. Yang, B. Long and U. van Kolck, Phys. Rev. C **97** (2018) no.2, 024001 doi:10.1103/PhysRevC.97.024001 [arXiv:1704.08524 [nucl-th]].

[75] S. R. Beane, D. B. Kaplan and A. Vuorinen, Phys. Rev. C **80** (2009), 011001 doi:10.1103/PhysRevC.80.011001 [arXiv:0812.3938 [nucl-th]].

[76] G. Rupak and N. Shoresh, Phys. Rev. C **60** (1999), 054004 doi:10.1103/PhysRevC.60.054004 [arXiv:nucl-th/9902077 [nucl-th]].

[77] Y. P. Teng, *The Unitarity Limit of NN Scatering With Perturbative Pions to N2LO*, MS thesis, George Washington University 2023.

[78] H. W. Grießhammer, *What Can Possibly Go Wrong?*, ECT* workshop The Nuclear Interaction: Post-Modern Developments, Trento (Italy), 19 August 2024.

[79] H. W. Grießhammer, *The Unitarity Limit of the NN System with Perturbative Pions*, Chiral Dynamics 2024, Bochum (Germany), 26 August 2024.

[80] H. W. Grießhammer, *Two Nucleons Near Unitarity with Perturbative Pions: Persistence vs Chiral Symmetry*, INT-24-3 Quantum Few- and Many-Body Systems in Universal Regimes, Seattle (USA), 17 October 2024.

[81] H. W. Grießhammer, *Towards the Unitarity Limit in EFTs with Pions*, INT Program INT-25-29W Chiral EFT: New Perspectives, Seattle (USA), 17 March 2025.

[82] H. W. Grießhammer, PoS **(CD2024)** 085 doi:10.22323/1.479.0085 [arXiv:2504.13353 [nucl-th]].

[83] J. Schwinger, hectographed notes on nuclear physics, Harvard University 1947.

[84] G. F. Chew and M. L. Goldberger, Phys. Rev. **75** (1949) 1637.

[85] F. C. Barker and R. E. Peierls, Phys. Rev. **75** (1949), 3122.

[86] H. A. Bethe, Phys. Rev. **76** (1949), 38.

[87] H. P. Stapp, T. J. Ypsilantis, and N. Metropolis, *Phys. Rev.* **105** (1957), 302.

[88] R. Bellman, *Perturbation Techniques in Mathematics, Physics and Engineering*, Holt, Rinehart and Winston 1964.

[89] C. M. Bender and S. A. Orszag, *Advanced Mathematical Methods for Scientists and Engineers*, McGraw Hill 1978.

[90] J. A. Murdock, *Perturbations – Theory and Methods*, John Wiley & Sons 1991.

[91] M. H. Holmes, *Introduction to Perturbation Methods*, 2nd ed., Springer 2013.

[92] P. F. Bedaque and H. W. Grießhammer, Nucl. Phys. A **671** (2000), 357-379 doi:10.1016/S0375-9474(99)00691-0 [arXiv:nucl-th/9907077 [nucl-th]].

[93] H. W. Grießhammer, *Technical Note: Strict Perturbation Theory for Nonperturbative Algorithms*, distributed in response to the ECT* workshop NEW IDEAS IN CONSTRAINING NUCLEAR FORCES 2018, updated April 2021, available from the author.

[94] H. W. Grießhammer, Eur. Phys. J. A **56** (2020), no. 4, 118 doi:10.1140/epja/s10050-020-00129-5 [arXiv:2004.00411 [nucl-th]].

[95] Y. P. Teng and H. W. Grießhammer, *The Unitarity Expansion in χEFT with Perturbative Pions in the Mixed* ^{3}SD$_1$ *and Higher* NN *Partial Waves*, in preparation.

[96] D. B. Kaplan, M. J. Savage and M. B. Wise, Phys. Rev. C **59** (1999), 617-629 doi:10.1103/PhysRevC.59.617 [arXiv:nucl-th/9804032 [nucl-th]].

[97] J. J. de Swart, C. P. F. Terheggen and V. G. J. Stoks, [arXiv:nucl-th/9509032 [nucl-th]].

[98] F. W. Olver, D. W. Lozier, R. Boisvert and C. W. Clark (eds.), *The NIST Handbook of Mathematical Functions*, Cambridge University Press 2010.

[99] H. W. Grießhammer, J. A. McGovern, D. R. Phillips and G. Feldman, Prog. Part. Nucl. Phys. **67** (2012), 841-897 doi:10.1016/j.ppnp.2012.04.003 [arXiv:1203.6834 [nucl-th]].

[100] M. Cacciari and N. Houdeau, JHEP **1109** (2011), 039 [arXiv:1105.5152 [hep-ph]].

[101] R. J. Furnstahl, N. Klco, D. R. Phillips and S. Wesolowski, Phys. Rev. C **92** (2015), 024005 [arXiv:1506.01343 [nucl-th]].

[102] H. W. Grießhammer, J. A. McGovern and D. R. Phillips, Eur. Phys. J. A **52** (2016), no. 5, 139 doi:10.1140/epja/i2016-16139-5 [arXiv:1511.01952 [nucl-th]].

[103] H. W. Grießhammer, Nucl. Phys. A **744** (2004), 192-226 doi:10.1016/j.nuclphysa.2004.08.012 [arXiv:nucl-th/0404073 [nucl-th]].

[104] T. D. Cohen and J. M. Hansen, Phys. Rev. C **59** (1999), 13-20 doi:10.1103/PhysRevC.59.13 [arXiv:nucl-th/9808038 [nucl-th]].

[105] T. D. Cohen and J. M. Hansen, Phys. Rev. C **59** (1999), 3047-3051 doi:10.1103/PhysRevC.59.3047 [arXiv:nucl-th/9901065 [nucl-th]].

[106] T. D. Cohen and J. M. Hansen, [arXiv:nucl-th/9908049 [nucl-th]].

[107] O. Thim, Few Body Syst. **65** (2024), no. 3, 69 doi:10.1007/s00601-024-01938-w [arXiv:2403.10292 [nucl-th]].

[108] R. Landau, J. Páez and C. Bordeianu, *A Survey of Computational Physics: Introductory Computational Science*, Princeton University Press 2008.

[109] G. P. Lepage, [nucl-th/9706029].

[110] H. W. Grießhammer, PoS **CD15** (2016), 104 doi:10.22323/1.253.0104 [arXiv:1511.00490 [nucl-th]].

[111] S. R. Beane, D. B. Kaplan, N. Klco and M. J. Savage, Phys. Rev. Lett. **122** (2019) no.10, 102001 doi:10.1103/PhysRevLett.122.102001 [arXiv:1812.03138 [nucl-th]].

[112] M. L. Wagman, F. Winter, E. Chang, Z. Davoudi, W. Detmold, K. Orginos, M. J. Savage and P. E. Shanahan, Phys. Rev. D **96** (2017) no.11, 114510 doi:10.1103/PhysRevD.96.114510 [arXiv:1706.06550 [hep-lat]].

[113] C. H. Bennett, D. P. DiVincenzo, J. A. Smolin and W. K. Wootters, Phys. Rev. A **54** (1996), 3824-3851 doi:10.1103/PhysRevA.54.3824 [arXiv:quant-ph/9604024 [quant-ph]].

[114] S. R. Beane and R. C. Farrell, Annals Phys. **433** (2021), 168581 doi:10.1016/j.aop.2021.168581 [arXiv:2011.01278 [hep-th]].

[115] I. Low and T. Mehen, Phys. Rev. D **104** (2021) no.7, 074014 doi:10.1103/PhysRevD.104.074014 [arXiv:2104.10835 [hep-th]].

[116] Q. Liu, I. Low and T. Mehen, Phys. Rev. C **107** (2023) no.2, 025204 doi:10.1103/PhysRevC.107.025204 [arXiv:2210.12085 [quant-ph]].

[117] G. A. Miller, Phys. Rev. C **108** (2023) no.3, L031002 doi:10.1103/PhysRevC.108.L031002 [arXiv:2306.03239 [nucl-th]].

[118] A. Einstein, B. Podolsky and N. Rosen, Phys. Rev. **47** (1935), 777-780 doi:10.1103/PhysRev.47.777.

[119] J. S. Bell, Physics Physique Fizika **1** (1964), 195.

[120] J. S. Bell, J. Phys. Colloq. **42** (1981), 41-62 doi:10.1051/jphyscol:1981202

[121] P. Zanardi, Phys. Rev. A **63** (2001), 040304 doi:10.1103/PhysRevA.63.040304 [arXiv:quant-ph/0010074 [quant-ph]].

[122] N. Klco, private communication.

[123] T. R. Richardson, M. R. Schindler and R. P. Springer, [arXiv:2411.01715 [nucl-th]].

[124] J. W. Chen, H. W. Grießhammer, M. J. Savage and R. P. Springer, Nucl. Phys. A **644** (1998), 221-234 doi:10.1016/S0375-9474(98)80012-2 [arXiv:nucl-th/9806080 [nucl-th]].

[125] J. W. Chen, H. W. Grießhammer, M. J. Savage and R. P. Springer, Nucl. Phys. A **644** (1998), 245-259 doi:10.1016/S0375-9474(98)00591-0 [arXiv:nucl-th/9809023 [nucl-th]].

[126] M. J. Savage and R. P. Springer, Nucl. Phys. A **686** (2001), 413-428 doi:10.1016/S0375-9474(00)00568-6 [arXiv:nucl-th/9907069 [nucl-th]].

[127] B. Borasoy and H. W. Grießhammer, Int. J. Mod. Phys. E **12** (2003), 65-80 doi:10.1142/S0218301303001156 [arXiv:nucl-th/0105048 [nucl-th]].

[128] H. W. Grießhammer, in preparation.

[129] H. W. Grießhammer, *Unitarity for Two Nucleons with Pions*, 2019 Fall Meeting of the Division of Nuclear Physics of the American Physical Society, Washington DC (USA), 15 October 2019.

[130] H. W. Grießhammer, *Are Nucleon-Nucleon Interactions As Important As We Think?*, Maier-Leibnitz-Colloquium, Physics Departments of TU München and München University, 8 July 2021.

[131] G. 't Hooft, NATO Sci. Ser. B **59** (1980), 135 doi:10.1007/978-1-4684-7571-5_9.

[132] A. Manohar and H. Georgi, Nucl. Phys. B **234** (1984), 189 [n.b. Acknowledgement] doi:10.1016/0550-3213(84)90231-1.

[133] H. Georgi and L. Randall, Nucl. Phys. B **276** (1986), 241 doi:10.1016/0550-3213(86)90022-2.

[134] S. Weinberg, Phys. Rev. Lett. **63** (1989), 2333 doi:10.1103/PhysRevLett.63.2333.

[135] H. Georgi, Phys. Lett. B **298** (1993), 187 doi:10.1016/0370-2693(93)91728-6 [hep-ph/9207278].

[136] H. W. Grießhammer, Nucl. Phys. A **760** (2005), 110 doi:10.1016/j.nuclphysa.2005.05.202 [nucl-th/0502039].

[137] U. van Kolck, *Tower of Effective Field Theories: Status and Perspectives*, workshop The Tower of Effective (Field), Theories and the Emergence of Nuclear Phenomena (EFT and Philosophy of Science), CEA/SPhN Saclay (France), 17 January 2017.

[138] *Enhancing the Interaction between Nuclear Experiment and Theory Through Information and Statistics*, special issue J. Phys. G **42** (2015), no. 3.

[139] *Further Enhancing the Interaction between Nuclear Experiment and Theory through Information and Statistics (ISNET 2.0)*, special issue J. Phys. G **46** (2019), no. 10.

[140] D. R. Phillips, R. J. Furnstahl, U. Heinz, T. Maiti, W. Nazarewicz, F. M. Nunes, M. Plumlee, M. T. Pratola, S. Pratt and F. G. Viens, *et al.* J. Phys. G **48** (2021), no. 7, 072001 doi:10.1088/1361-6471/abf1df [arXiv:2012.07704 [nucl-th]].

[141] D. R. Phillips, G. Rupak and M. J. Savage, Phys. Lett. B **473** (2000), 209-218 doi:10.1016/S0370-2693(99)01496-3 [arXiv:nucl-th/9908054 [nucl-th]].